AFRL-RH-WP-TR-2020-0058

Characterization of Chemical Contaminants in A-10 Pilot Breathing Air and Toxicokinetic Simulation to Predict Impact on Pilot Performance

Daniel Reilly, Ryan McNeilly, Daniel Cowan,
Converse Griffith, Jr, Danielle McKenzie-Smith
UES

Tammie Covington, Jeffery Gearhart,

Henry M. Jackson Foundation

Matthew W. Linakis, Heather Pangburn, Christin Duran, John Frazey,

711 HPW/RHB

JULY 2020
Final Report

AIR FORCE RESEARCH LABORATORY
711TH HUMAN PERFORMANCE WING,
AIRMAN SYSTEMS DIRECTORATE,
WRIGHT-PATTERSON AIR FORCE BASE, OH 45433
AIR FORCE MATERIEL COMMAND
UNITED STATES AIR FORCE

NOTICE AND SIGNATURE PAGE

Using Government drawings, specifications, or other data included in this document for any purpose other than Government procurement does not in any way obligate the U.S. Government. The fact that the Government formulated or supplied the drawings, specifications, or other data does not license the holder or any other person or corporation or convey any rights or permission to manufacture, use, or sell any patented invention that may relate to them.

Qualified requestors may obtain copies of this report from the Defense Technical Information Center (DTIC) (http://www.dtic.mil).

AFRL-RH-WP-TR-2020-0058 HAS BEEN REVIEWED AND IS APPROVED FOR PUBLICATION IN ACCORDANCE WITH ASSIGNED DISTRIBUTION STATEMENT.

//signature//

CHRISTIN M. DURAN, PhD, CIH

Site lead, Research Chemical Engineer
Performance Optimization Branch
Airman Biosciences Division

//signature//

LOGAN A. WILLIAMS, PhD

Airman Readiness Optimization Performance
Core Research Area Lead
Airman Biosciences Division

This report is published in the interest of scientific and technical information exchange, and its publication does not constitute the Government's approval or disapproval of its ideas or findings.

REPORT DOCUMENTATION PAGE

Form Approved
OMB No. 0704-0188

1. REPORT DATE *(DD-MM-YY)*	2. REPORT TYPE	3. DATES COVERED *(From - To)*
07-07-20	Final	12/2017 – 12/2018

4. TITLE AND SUBTITLE
Characterization of Chemical Contaminants in A-10 Pilot Breathing Air and Toxicokinetic Simulation to Predict Impact on Pilot Performance

5a. CONTRACT NUMBER
FA8650-17-C-6834

5b. GRANT NUMBER

5c. PROGRAM ELEMENT NUMBER
00000F

6. AUTHOR(S)
*Daniel Reilly, Ryan McNeilly, Daniel Cowan, Converse Griffith, Danielle McKenzie-Smith
**Tammie Covington, MS, Jeffery Gearhart
***Matthew W. Linakis, Christin Duran, , Heather Pangburn,, John Frazey

5d. PROJECT NUMBER
18-091

5e. TASK NUMBER
00

5f. WORK UNIT NUMBER
Legacy RHM

7. PERFORMING ORGANIZATION NAME(S) AND ADDRESS(ES)
*UES, Inc.
4401 Dayton Xenia Road
Dayton, OH 45432

**Henry M. Jackson Foundation
6720A Rockledge Dr
Bethesda, MD 20817

8. PERFORMING ORGANIZATION REPORT NUMBER

9. SPONSORING/MONITORING AGENCY NAME(S) AND ADDRESS(ES)
***Air Force Materiel Command
Air Force Research Laboratory
711th Human Performance Wing
Airman Systems Directorate
Airman Biosciences Division
Performance Optimization Branch
Wright-Patterson AFB, OH 45433

10. SPONSORING/MONITORING AGENCY ACRONYM(S)
711 HPW/RHBC

11. SPONSORING/MONITORING AGENCY REPORT NUMBER(S)
AFRL-RH-WP-TR-2020-0058

12. DISTRIBUTION/AVAILABILITY STATEMENT
Distribution A. Approved for public release.

13. SUPPLEMENTARY NOTES
MSC/PA-2020-0195 88ABW-2020-2608, cleared 18 August 2020

14. ABSTRACT
A-10 pilots have experienced physiological events (PEs) which result in diminished mission effectiveness. A potential explanation for PEs in pilots is improper functioning of the breathing air delivery system. Physiological complications may occur due to insufficient oxygen control or the introduction of chemical contamination through engine bleed air or degrading materials in the life support system. Two studies were completed to measure chemical contamination and investigate the potential role in cognitive outcomes. In the first study, partial combustion gases, volatile organic compounds and ultrafine particles were measured in A-10 cockpit and pilot breathing air during ground engine runs. In the second study, a toxicokinetic simulation was completed to determine the potential effects of low levels of carbon monoxide (CO) on cognitive health. The measurements made during ground engine runs found that most constituents measured in pilot breathing air rarely exceeded their respective exposure limits, with the exception of nitrogen oxides (NO_x). The toxicokinetic simulation focused on CO exposure during ground operations and revealed that at exposures of $\leq$ 50 ppm, it is unlikely that CO exposure alone would lead to any subtle cognitive effects. Therefore, CO at the concentrations observed during ground runs were unlikely to result in cognitive effects.

15. SUBJECT TERMS
On-Board Oxygen Generation System, OBOGS, Liquid Oxygen System, LOX, Physiological Events, Carbon monoxide, Nitrogen oxides, pharmacokinetic modeling

16. SECURITY CLASSIFICATION OF:			17. LIMITATION OF ABSTRACT:	18. NUMBER OF PAGES	19a. NAME OF RESPONSIBLE PERSON (Monitor)
a. REPORT	b. ABSTRACT	c. THIS PAGE			Dr. Christin Duran
Unclassified	Unclassified	Unclassified	SAR	88	19b. TELEPHONE NUMBER *(Include Area Code)* N/A

TABLE OF CONTENTS

LIST OF FIGURES

LIST OF TABLES

ACKNOWLEDGEMENTS

We would like to thank the maintenance team at Davis-Monthan Air Force Base for performing engine runs. We also want to thank Darrin Ott, PhD, Core Competency Lead in the Warfighter Medical Optimization Division of the 711th Human Performance Wing (711 HPW) for leadership and guidance, as well as the A-10 Support Program Office for organizational support. Dr. Jennifer Martin's group in the Airman Systems Directorate carried out the gas chromatography-mass spectroscopy needed to detect specific volatile organic compounds on thermal desorption tubes.

1.0 EXECUTIVE SUMMARY

United States Air Force (USAF) A-10 pilots have experienced unexplained physiological events (PEs) which can result in degraded mission effectiveness. Symptoms that can be experienced during PEs include lightheadedness, headaches, fatigue, nausea, and shortness of breath (Lt. Col. Elliott, 2019). A potential explanation for PEs is improper functioning of the breathing air delivery system. The accidental admittance of chemical and particulate contamination into pilot breathing air through engine bleed air or degrading materials in the life support system as well as insufficient oxygen (O_2) control are theories for how improper breathing air delivery system function could lead to PEs.

There were two studies completed to investigate the potential impact of chemical contaminants on PEs in A-10 aircraft. In the first study, levels of chemical contaminants were measured in cockpit and pilot breathing air during ground engine runs in both non-incident and incident aircraft. The motivation was that an inherent issue with incident aircraft may cause chemical contaminants to be introduced into the environmental control system when the engines are running. In the second study, a toxicokinetic simulation was used to predict the potential impact of carbon monoxide (CO) exposure during ground operations on pilot cognition.

In the first study, we measured gas-phase and particulate components of A-10 cockpit and pilot breathing air during twelve ground engine runs, each carried out on a different aircraft, at Davis-Monthan Air Force Base (AFB) between December 13, 2017 and December 15, 2017. Two of the twelve aircraft were equipped with a Liquid Oxygen (LOX) system and the remainder with On-Board Oxygen Generation systems (OBOGS). In three of the twelve aircraft tested, a PE had occurred (referred to as 'incident aircraft').

To sample pilot breathing air, an OBOGS Air Ground (OAGr) sampling system was designed and built. The OAGr system samples simultaneously from two sources: the cockpit and pilot breathing air system. Each flow path incorporated an identical suite of sampling instruments and methods. Measurements were made in real-time for volumetric flow rate, temperature, relative humidity (RH), O_2, partial combustion gases, total volatile organic compounds (VOCs), and ultrafine particles (UFPs) measured as Lung Deposited Surface Area (LDSA). Samples were also collected in thermal desorption (TD) tubes for offline characterization of VOCs using gas chromatography-mass spectroscopy (GC/MS). Engine runs were divided into four test phases, during which the engine throttle, breathing air pressure, and breathing air O_2 settings were varied to observe the effect on the constituents of cockpit and pilot breathing air.

Across all twelve engine runs, the volumetric flow rate of air pulled from the pilot breathing air averaged 4.7 liters per minute ($L*min^{-1}$) and ranged from 0.4 to 7.2 $L*min^{-1}$. In the pilot breathing air, carbon dioxide (CO_2) concentrations averaged 300.5 parts per million (ppm) and ranged from 276 to 324 ppm. CO concentrations in the pilot breathing air averaged 0 ppm and ranged from 0 to 0.8 ppm. Nitrogen dioxide (NO_2) concentrations averaged 0.1 ppm and ranged from 0.0 to 0.5 ppm. Nitric oxide (NO) concentrations averaged 0 ppm and ranged from 0 to 10.1 ppm. NO readings showed positive sensor creep with increases in temperature in some engine runs, so the upper end of the concentration range may be artificially high. Total VOC concentrations averaged 0.49 ppm and ranged from 0.06 to 1.01 ppm. Fifty-one specific VOCs were tested for in the TD tubes, of which fifteen were detected. The five most commonly detected compounds were acetone (found 60 times, maximum value 47.9 parts per billion (ppb)),

ethanol (46, 54.0 ppb), toluene (34, 19.4 ppb), 1,3-butadiene (29, 8.8 ppb), and methylene chloride (26, 6.9 ppb).

Contaminant exposure concentrations were compared to published Occupational Exposure Limits (OELs). OELs for CO_2, CO, NO_2 and NO were based on maximum allowable concentrations in the MIL-STD 3050 (Department of Defense, 2015). For total VOCs, the OEL was the 1 ppm system control value indicated by the 711th Human Performance Wing (HPW). The OEL used for sulfur oxides (SO_x) was the National Institute of Safety and Health (NIOSH) Time-Weighted Average Recommended Exposure Limit (TWA REL) of 2 ppm for sulfur dioxide (SO_2). In pilot breathing air, 0 percent (%) of the CO_2, 0% of CO, 0% of total VOCs, and 0.1% of SO_x observations exceeded OELs. However, 67.5% NO_2 and 13.0% of NO observations exceeded OELs. The specific VOCs identified in the TD tubes did not exceed the system control value of 1 ppm individually or in combination.

Engine run test phases affected the levels of certain chemicals, including O_2, NO_2, LDSA, and commonly found VOCs. In pilot breathing air, the mean O_2 concentration was 46.4% when regulator O_2 was set to normal and 76.3% when the regulator O_2 was set to 100%. NO_2 concentrations appeared to be highest in pilot breathing air when the throttle was 85%, the O_2 setting was 100%, and the pressure was set to 'Emergency' (test phase 4). LDSA was highest in cockpit air when the throttle was at idle and both the regulator O_2 and pressure settings were at normal (test phase 2). The more commonly found VOCs were higher at idle engine thrust (test phases 1 and 2).

Additional parameters of interest included sampling location (i.e. cockpit versus OBOGS or LOX system) and incident status of the aircraft. Sampling location most strongly affected CO_2 concentrations where levels were higher in the cockpit than in pilot breathing air. The incident status of the aircraft did not play an obvious role in the levels of chemicals measured. Due to the small sample size of twelve aircraft with only three being labelled as incident aircraft, no inferential statistical tests were used to determine whether O_2 or contaminants were statistically different in incident versus non-incident aircraft.

In the second study, a toxicokinetic simulation was completed to predict the potential effects of low levels of CO exposure during ground operations on cognition. Toxicokinetic modeling results revealed that at exposures of less than or equal to 50 ppm, it is exceptionally unlikely that CO would lead to any subtle cognitive effects in pilots. The simulations further suggested that CO concentrations of 150 ppm would be needed to result in 3% carboxyhemoglobin (COHb), a conservative estimate for the level of CO binding at which subtle cognitive deficits may manifest.

Follow-on research will be designed to address limitations in the present studies. First, the present studies were focused on ground-based exposures, which may not be representative of contaminants present during flight. Further, although individual chemical contaminants at the levels observed in this study are unlikely to contribute to performance effects in pilots when exposed on the ground, chemicals can produce toxicity through synergistic and additive effects, and additional stressors experienced during high performance flight can affect the metabolism of chemical contaminants. Therefore, future research will focus on measuring chemical exposures during flight, as well as on developing and applying more advanced toxicokinetic simulations that evaluate the impact of chemical mixtures on pilot performance characteristics using physiological parameters representative of those experienced during high performance flight.

2.0 INTRODUCTION

PEs have been an issue in the USAF since at least 2008, when F-22 pilots began reporting hypoxia-like symptoms (United States Air Force Scientific Advisory Board, 2012). More recently, PEs have been reported in training aircraft, the T-6 Texan II, which resulted in an operational pause as an entire fleet of T-6 aircraft was grounded during November 2017 (Air Education and Training Command, 2018a, 2018b). Many of the aircraft involved in PEs use the OBOGS, a dual-bed molecular sieve, to supply O_2 enriched breathing gas to aircrew at appropriate levels according to the aircraft altitude.

A number of hypothetical causes of PEs have been advanced that postulate in different ways a problem with the pilot breathing air. These hypotheses include but are not limited to insufficient O_2 (hypoxia), insufficient CO_2 (hypocapnia), excessive CO_2 (hypercapnia), cockpit pressure fluctuations, and chemical or particulate contamination of the pilot breathing air. Exposure to contaminants during ground operations prior to take-off could also potentially play a role in cognitive decline associated with PEs.

The current research was completed in response to PEs reported by A-10 pilots at Davis-Monthan AFB in November 2017 (Everstine, 2018). PEs occurred in aircraft equipped with both OBOGS and LOX breathing systems (see APPENDIX A for descriptions of these systems). The incident that occurred in the aircraft equipped with LOX was found to be associated with a malfunction with the cabin pressure and oxygen regulator, but the root cause for PEs in the aircraft equipped with the OBOGS was not clear.

In order to better understand the potential role of chemical contaminants on PEs observed in A-10 aircraft, there were two studies completed. In the first study, levels of chemical contaminants were measured in cockpit and pilot breathing air during ground engine runs in both non-incident and incident aircraft. The motivation was that an inherent issue with incident aircraft may lead to the introduction of chemical contaminants into the environmental control system when the engines are running. In the second study, a toxicokinetic simulation was used to predict the potential impact of hypothetical concentrations of CO exposed to pilots while on the flight line on cognition.

3.0 COCKPIT AND PILOT BREATHING AIR CHARACTERIZATION

3.1 Background

Chemical or particulate contamination of the pilot breathing air is one possible explanation for PEs. One source for contamination is aircraft fluid leakage into the environmental control system. Engines have seals to prevent oil leakage; however, these seals are not 100% effective. Furthermore, changes in operating temperature or in the pressure differentials within the engine can affect oil leakage rates (Michaelis, 2016). Tricresyl phosphates, a component in engine lubricating oils, have been detected in the heat exchangers or coalesce bags of Australian military aircraft (Denola et al., 2011; Hanhela et al., 2005).

The leakage of aircraft fluids into the environmental control system can lead to the presence of combustion gases in breathing air. In laboratory experiments, exposure of engine lubricating oils to high temperatures representative of the environmental control system generated 46-144 ppm CO, while hydraulic fluids exposed to the same high temperatures generated 2-18 ppm CO (National Research Council, 2002). In another study, CO concentrations of 141 ppm were produced by heating engine oils in laboratory experiments (van Netten and Leung, 2000).

Both military and commercial aircraft commonly use engine bleed air to pressurize the environmental control system, so information about potential chemical contaminants in aircraft can be found by reviewing studies in commercial passenger aircraft. Compounds of concern measured in Boeing 767 bleed air have included CO_2, CO, and low concentrations of acetaldehyde and formaldehyde (National Research Council, 2002). Also found in the Boeing 767 bleed air was particulate matter, including particles less than 2.5 μm in diameter (National Research Council, 2002). VOCs from bleed air have also been found to reach the cabin. Rosenberger (2018) found that replacing the regular high-efficiency particulate air (HEPA) filters with charcoal-equipped HEPA filters reduced total VOCs in a commercial aircraft cabin.

Previous studies have been completed to investigate chemical contaminants in pilot breathing air in military aircraft. The USAF Scientific Advisory Board (2012) examined the possibility that CO_2, CO, or one of a number of organic compounds capable of causing central nervous system symptoms accounted for the PEs experienced by F-22 pilots. In these studies, trace levels of VOCs and other chemicals were found to be commonly present in OBOGS breathing air. The origin was traced to their presence in atmospheric air and leaks of small quantities into the environmental control system. The levels were not found to reach concentrations consistent with symptoms reported in incidents.

3.2 Approach

In this study, measurements were made during ground engine runs to characterize chemical contaminants in cockpit and pilot breathing air in the A-10 during four combinations of engine throttle and breathing air regulator settings. Measurements were made using the in-house built OAGr sampling system, which was designed to sample from two air sources simultaneously. In each flow path, temperature, RH, air flow rate, and concentrations of O_2, CO_2, CO, NO_2, NO, SO_x, total VOCs, and UFPs were measured in real-time. The OAGr was also used to collect VOCs onto TD tubes for later laboratory analysis using GC/MS.

Concentrations of chemical contaminants were compared to OELs, which were based on MIL-STD 3050, American Conference of Governmental Industrial Hygienists (ACGIH), NIOSH, and Occupational Safety and Health Administration (OSHA). A table summarizing OELs for chemicals measured can be found in APPENDIX B. Constituents of air in the cockpit and pilot breathing air were characterized using overall summary statistics, boxplots categorized by throttle and regulator settings, and time series plots for each contaminant during each engine run.

3.3 Methods

Ground Engine Runs

During each engine run, the throttle, regulator O_2, and regulator pressure settings were systematically altered following the test protocol in Table 1, starting with phase 1 and ending with phase 4. Each test phase lasted 10-15 minutes.

Table 1. A-10 Test Protocol

Test Phase	Throttle	Regulator O_2	Regulator Pressure
1	Idle	100%	Normal
2	Idle	Normal	Normal
3	85%	Normal	Normal
4	85%	100%	Emergency

Engine runs were conducted on twelve different aircraft from December 13 – 15, 2017 at Davis-Monthan AFB (Table 2). PEs had occurred in three of the aircraft (labelled incident aircraft). In two of the aircraft, the pilot breathing air was supplied by a LOX system rather than the OBOGS. More information about the OBOGS and LOX systems can be found in APPENDIX A. During all engine runs, both cockpit and pilot breathing air were sampled simultaneously.

Table 2. Engine Run and Aircraft Characteristics Summary

Date	Engine Run	Aircraft ID	Incident Status	O_2 System
13 Dec 2017	1	32	Non-incident	OBOGS
13 Dec 2017	2	33	Non-incident	OBOGS
13 Dec 2017	3	34	Non-incident	OBOGS
14 Dec 2017	4	35	Incident	OBOGS
14 Dec 2017	5	36	Incident	OBOGS
14 Dec 2017	6	37	Non-incident	OBOGS
14 Dec 2017	7	38	Non-incident	OBOGS
14 Dec 2017	8	39	Non-incident	OBOGS
15 Dec 2017	9	40	Non-incident	OBOGS
15 Dec 2017	10*	41	Incident	LOX
15 Dec 2017	11	42	Non-incident	OBOGS
15 Dec 2017	12*	43	Non-incident	LOX

*Engine runs were incomplete

As indicated in Table 2, data collection during engine runs 10 and 12 were incomplete. During engine run 10 (aircraft 41), an instrument in the OAGr collecting real-time gas phase data from the pilot breathing air flow path overheated during test phase 2. The engines were stopped and restarted, and data collection resumed for test phases 3 and 4. During engine run 12 (aircraft 43), the same instrument in the OAGr faulted during test phases 1, 2, and 3. Consequently, little cockpit flow path data is available for these test phases. After test phase 3, the A-10 engines were stopped, the battery was replaced, the engines were restarted, and data collection resumed for test phase 4.

For each engine run, the data collection team kept handwritten field notes containing important meta data, such as the tail number, date, and timing of changes in the throttle and regulator settings. The meta data in the field notes was consolidated into an Excel spreadsheet with the chemical measurement data and used to support data analysis.

Sampling Methods

Cockpit and pilot breathing air were characterized using the OAGr system (Fig. 1). The OAGr system was designed for flight line usage and is comprised of a suite of sampling instruments that are fully contained in a Pelican Case with latching mechanisms to contain the sampling equipment and eliminate concerns for Foreign Object Debris. The OAGr system runs completely on battery power and can sample from two independent sources simultaneously. In the A-10, which is a single-seater aircraft, one sampling flow path was left unconnected to pull air samples from the cockpit, while the second sampling flow path was connected to the aircraft using a standard pilot oxygen hose and quick disconnect assembly. Diaphragm sampling pumps (Gilair Plus STP, Sensidyne) pulled air through the respective flow paths. The total flow rate in the pilot breathing air flow path was measured using a mass flow meter (M100SLPN-D, AliCat).

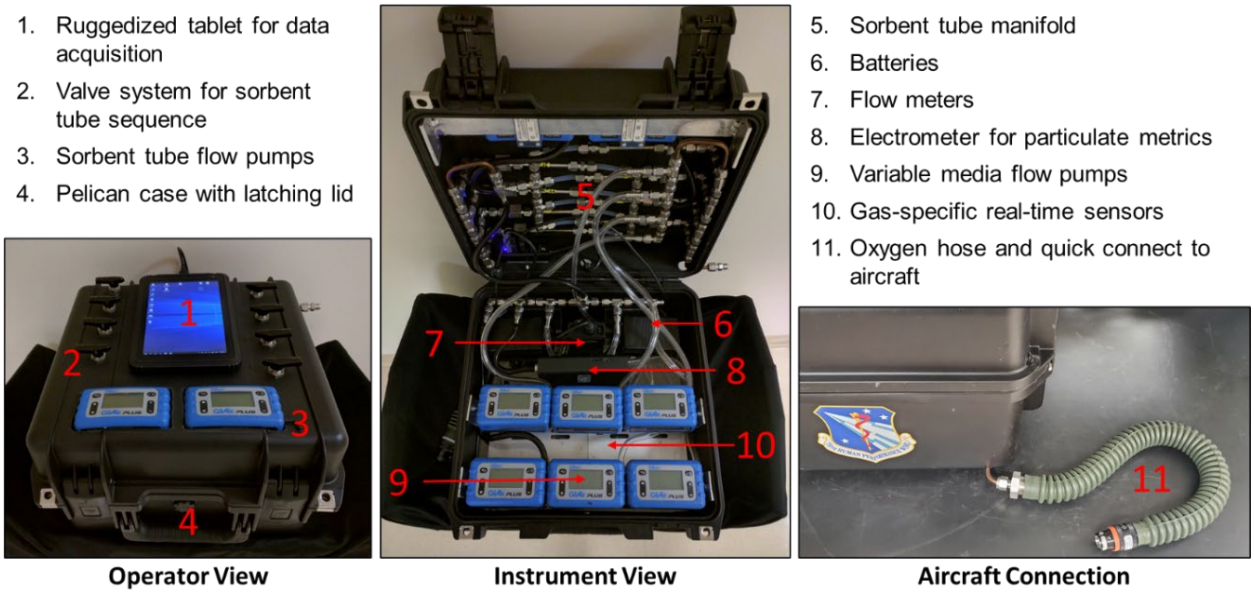

Figure 1. OAGr system used for aircraft sampling

The OAGr system includes a combination of direct reading sensors for real-time measurements and collection media for offline characterization. The direct reading sensors output real-time data to a graphical user interface secured to the front face of the device and consist of thermodynamic sensors (pressure, temperature, RH) and validated gas-specific commercial off-the-shelf sensors (O_2, CO_2, CO, NO_2, NO, SO_x, and total VOCs) using a custom-designed gas monitor module from Makel Engineering, Inc (MEI). Gas sensors were chosen using chemicals known to exist in engine exhaust. The sampling rate of the Makel sensor package was 3 Hertz (Hz) to capture minimal fluctuations in chemical concentrations. The list of sensor technologies and ranges are shown in Table 3.

Table 3. Makel Device Sensors and Specifications

Endpoint	Sensor Type	Manufacturer	Model Number	Range
pressure	differential	MEI	proprietary	7.25 – 15.95 PSIA
temperature	thermocouple	MEI	proprietary	-40°C – 30°C
RH	humidity	MEI	proprietary	0 – 100%
O_2	electrochemical	MEI	proprietary	21 – 96%
CO_2	NDIR	Alphasense	NDIR-IRC-A1	0 – 5000 ppm
CO	electrochemical	Alphasense	CO-AF	0 – 400 ppm
NO	electrochemical	Alphasense	NO-A1	0 – 50 ppm
NO_2	electrochemical	Alphasense	NO_2-A1	0 – 10 ppm
SO_x	electrochemical	Alphasense	SO_2-AF	0 – 10 ppm
total VOCs	PID	Alphasense	PID-AH Rev 2	100 ppb – 10 ppm

Abbreviations: °C = degrees Celsius; ND = not determined; NDIR = Nondispersive Infrared; PID = Photoionization Detector; PSIA = Pounds per Square Inch Absolute

Electrometers were used for measuring UFPs at a sampling rate of 1 Hz (Partector, CH Technologies Naneos Particle Solutions GMBH).

In addition to direct reading sensors, sampling pumps connected to sampling media were used to capture chemical contaminants for offline analysis. TD tubes with tri-bed sorbent (SVI™, Perkin-Elmer) were used to collect VOCs. Filter cassettes with 37 mm mixed cellulose ester filters were used to collect samples for analysis of heavy metals, and solid sorbent tubes with 10% 2-(hydroxymethyl) piperidine on XAD®-2 were used to collect samples for analysis of aldehydes.

TD tubes were collected for each engine run test phase (see Table 1) in each of the two flow paths, which resulted in eight TD tubes collected for each engine run. The serial numbers printed on the tubes were used to track the engine run, test phase and sampling source for which they were used and the sampling time. Filter cassettes and solid sorbent tubes were collected for the duration of each engine run in each of the two flow paths, which resulted in two filter cassettes and two solid sorbent tubes collected for each engine run.

TD tubes were analyzed internally by Dr. Jennifer Martin's group in the Airman Systems Directorate of the 711th HPW in accordance with Environmental Protection Agency (EPA)

Technical Order (TO) 17. Filter cassettes and solid sorbent tubes were sent to ALS Environmental for offline analysis. The filter cassettes were analyzed for heavy metals using modified NIOSH method 7300, and the solid sorbent tubes were analyzed for aldehydes using NIOSH method 2539.

Data Analysis

Summary statistics (minimum, mean, maximum, standard deviation, and number of observations) were calculated for each chemical constituent measured. Boxplots were generated to evaluate O_2 and chemical contaminants as a function of throttle and regulator setting for each aircraft and sample location (cockpit or pilot breathing air). Boxplots were made only for those VOCs detected in more than ten samples. For boxplots, the length of the 'whiskers' used is 1.5 times the interquartile range (i.e. difference between 75th and 25th percentiles or middle 50%). Data points which lie outside the range of the whiskers are denoted by individual points. Time series plots were made for data collected in real-time. Algorithms were developed to plot real-time data automatically using a Python script.

3.4 Results

O_2 and Airflow Conditions

A summary of O_2 concentrations and airflow conditions, including volumetric flow rate (pilot breathing air only), temperature, and RH across all engine runs is shown in Table 4. O_2 concentrations remained near ambient levels (21%) in cockpit air and varied substantially with regulator settings in pilot breathing air. Volumetric air flow was measured only in the pilot breathing air flow path and averaged 4.7 $L*min^{-1}$. Temperature was similar in each flow path. RH was three times lower in pilot breathing air than in cockpit air.

Table 4. Summary of Real-time Data for O_2 Concentration and Airflow Conditions

Endpoint	Air Source	Mean	Standard Deviation	Peak	Observations
O_2 (%)	Cockpit	21.4	0.6	31.1	94690
	OBOGS/LOX	55.8	16.2	92	109046
Flowrate ($L*min^{-1}$)	OBOGS/LOX	4.6	2.1	8.8	88973
Temperature (°C)	Cockpit	28.5	4.7	36.0	95032
	OBOGS/LOX	29.3	4.8	37.2	109357
RH (%)	Cockpit	12.5	4.0	23.0	95032
	OBOGS/LOX	4.0	3.3	17.0	109357

Summary statistics shown in Table 4 were further broken down by engine/regulator settings in APPENDIX C (Table C1). The results show that O_2 concentrations averaged 57%, 47%, 46%, and 76% during test phase Idle/100%/Normal, Idle/Normal/Normal, 85%/Normal/Normal, and 85%/100%/Emergency, respectively. Average values for volumetric flow rate remained relatively consistent across engine run test phases. There was a slight increase in average

temperature over the course of each engine run, resulting in a total change of about 4-5°C in both cockpit and pilot breathing air. The average RH of cockpit air decreased slightly over the course of each engine run by about 3.4%, with the greatest amount of change occurring during the last test phase when RH decreased substantially to an average value of 1.5%.

The data are further visualized below using faceted box plots (Figures 2-5).

O_2 concentrations were consistent in the cockpit air at around 21% (Figure 2, plot labeled Cabin). O_2 concentrations in breathing air varied with regulator setting and across aircraft. Of particular note is during the 100% emergency O_2 setting (test phase 4), during which average readings were below 75% O_2 in the O_2 breathing line of four aircraft (32, 34, 35 and 36). The O_2 concentration in the two aircraft with LOX systems approached the upper limit of the sensor range of 96% during test phase 4.

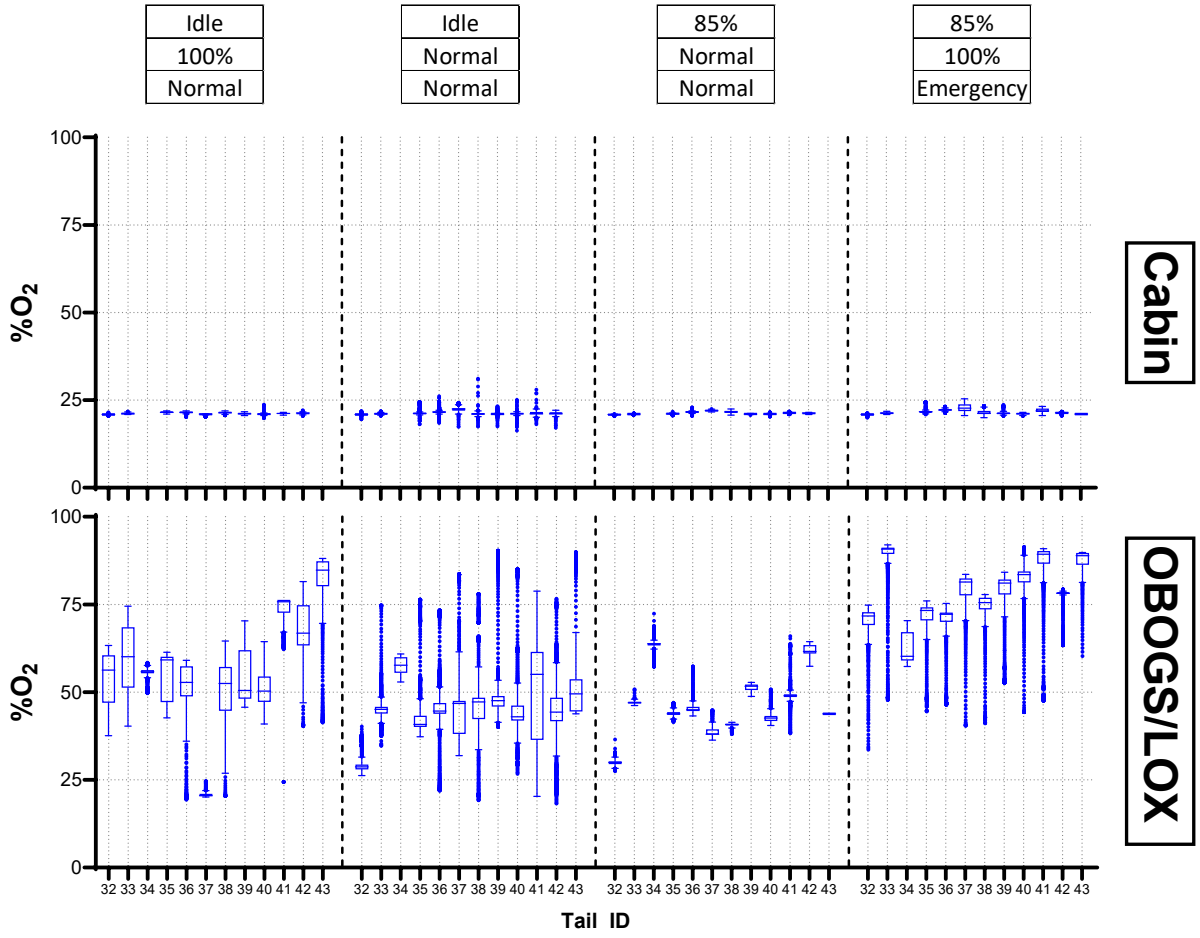

Figure 2. O_2 boxplot by aircraft, sampling location, throttle, regulator O_2, and regulator pressure settings. Aircraft 41 and 43 are LOX aircraft. Aircraft 35, 36 and 41 are incident aircraft.

Volumetric flow rates were only measured in the pilot breathing air flow path (Figure 3). Flow rates were the most variable during the idle engine run test phase with normal O_2 and pressure regulator settings (test phase 2). No values higher than about 8 L/min were recorded during testing. The volumetric flow rate was particularly low during engine runs for aircraft 34, 35 and 39. No data were available for engine runs with Aircraft 32, 33, 41 (test phases 3 and 4) and 42.

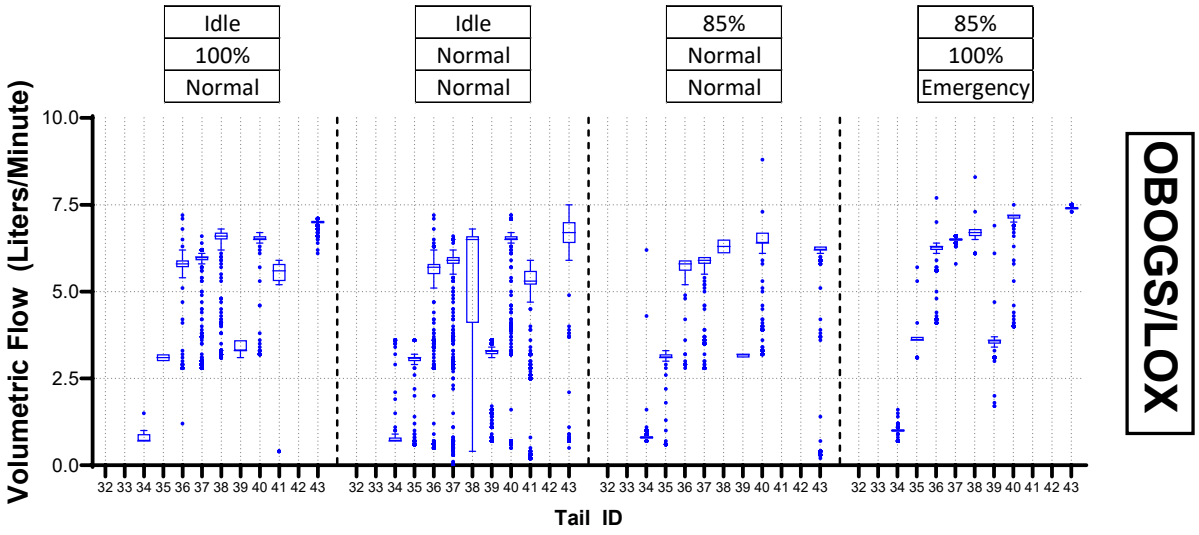

Figure 3. Volumetric flow rate boxplot by aircraft and engine run test phase. Aircraft 41 and 43 are LOX aircraft. Aircraft 35, 36 and 41 are incident aircraft. Volumetric flow data from aircraft 33 omitted due to sensor error.

Temperature readings showed a high degree of variability across aircraft, engine/regulator settings, and cockpit versus breathing air (Figure 4). There appeared to be a slight increase in temperature across the four test phases for individual aircraft, which is more apparent in the time series plots (see APPENDIX D).

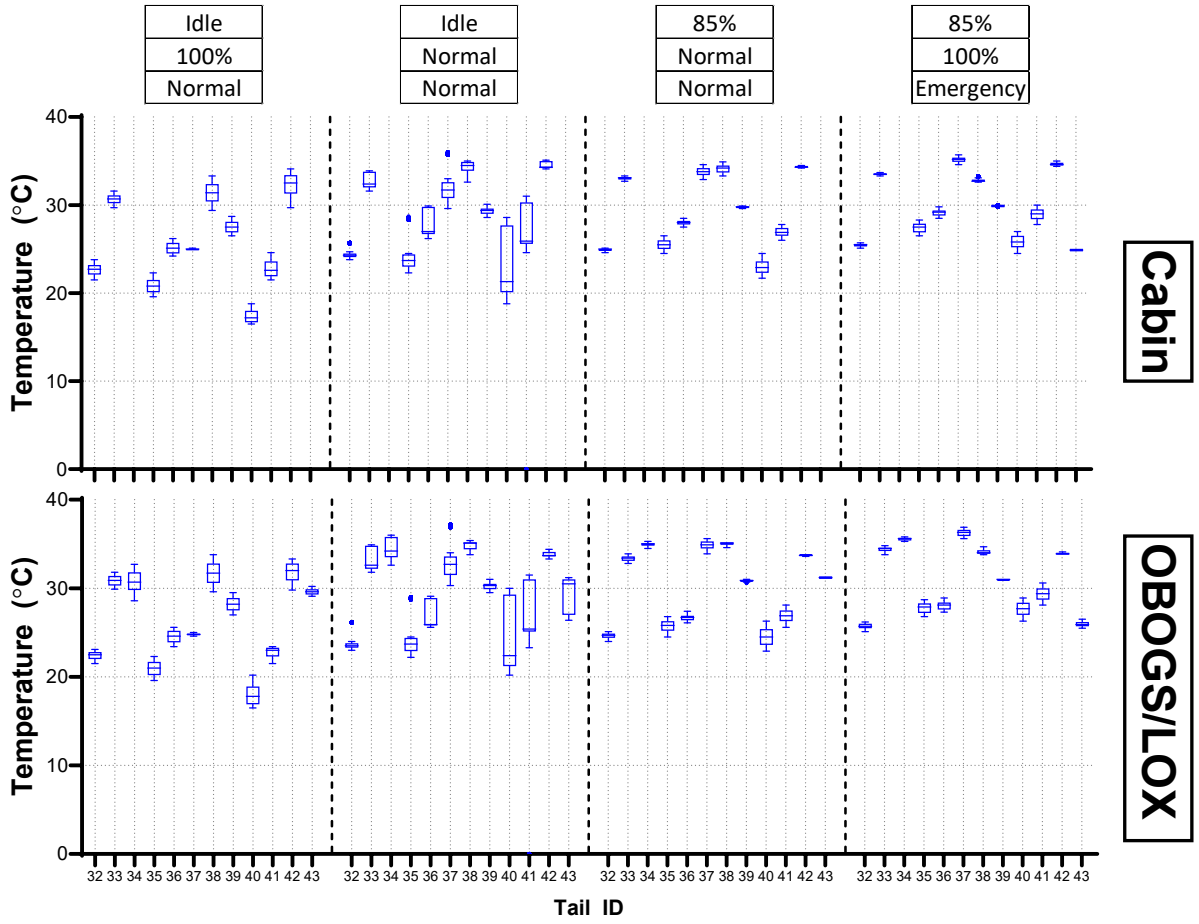

Figure 4. Temperature boxplot by aircraft, sampling location, throttle, regulator O_2, and regulator pressure settings. Aircraft 41 and 43 are LOX aircraft. Aircraft 35, 36 and 41 are incident aircraft.

The RH of pilot breathing air was generally very low compared to ambient air in the cockpit (Figure 5). In pilot breathing air, RH remained primarily <15% with all average RH values below 5% in the 85%/100%/Emergency test phase (test phase 4).

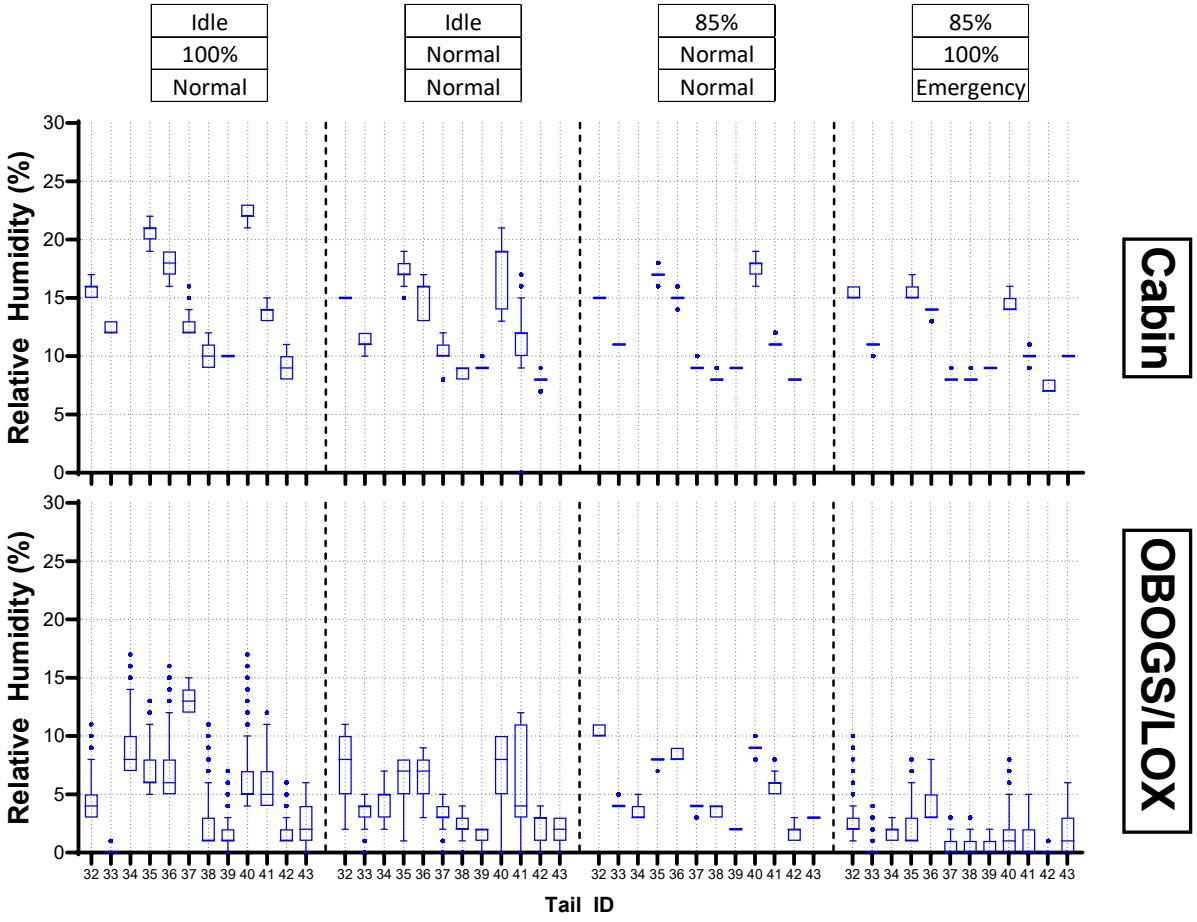

Figure 5. RH boxplot by aircraft, sampling location, throttle, regulator O_2, and regulator pressure settings. Aircraft 41 and 43 are LOX aircraft. Aircraft 35, 36 and 41 are incident aircraft.

Time series plots for each individual engine run further elucidate trends in O_2 and airflow conditions (see APPENDIX D). O_2 concentration climbed to a peak of 75% to 97% during test phases 1 and 4 when the regulator was set to 100% O_2. When recorded, volumetric flow rate remained steady over the course of individual engine runs, but often showed periodic sharp dips in values by 3 or up to 5 $L*min^{-1}$ lasting only a few seconds each time. There was a slight steady increase in temperature in both cockpit and pilot breathing air over the course of each engine run. The RH in pilot breathing air was consistently lower than in cockpit air and was driven to zero in most engine runs during test phase 4 when the regulator was set to 100% O_2 and Emergency pressure, and sometimes also during test phase 2 when the regulator was set to 100% O_2 and normal pressure. RH trended inversely with temperature in cockpit air and inversely with O_2 concentrations in pilot breathing air.

Chemical Contaminants Monitored in Real-Time

A summary table was generated to investigate the mean, standard deviation, range of values, and percent of observations where OELs were exceeded for each chemical contaminant measured in real-time across all engine runs (Table 5). OELs for CO_2, CO, NO_2, and NO were based on MIL-STD-3050 maximum allowable concentrations (Department of Defense, 2015). The maximum allowable concentrations for inlet gas to the OBOGS were used for cockpit air and were 5000 ppm and 50 ppm for CO_2 and CO, respectively and 5 ppm for NO_2 and NO. The maximum allowable concentrations for outlet gas from the OBOGS were used for pilot breathing air and were 500 ppm and 10 ppm for CO_2 and CO, respectively and 0.1 ppm for NO_2 and NO. The OEL used for SO_x (2 ppm) is the NIOSH TWA for SO_2. The 711th HPW established a system control value of 1 ppm for total VOCs, which was used for the OEL. There is no OEL for LDSA. OELs are listed in APPENDIX B, Table B1.

Results show that CO_2, CO, and SO_x exceeded their respective OELs in < 1% of observations. Similarly, total VOCs exceeded the system control value of 1 ppm in less than 1% of the observations. In contrast, NO_2 and NO commonly exceeded their respective OEL of 0.1 ppm. Note that there is no OEL for UFPs.

Table 5. Summary of Real-time Data for Chemical Contaminants

Endpoint	Air Source	Mean	Standard Deviation	Minimum-Maximum	Observations	% > OEL
CO_2 (ppm)	Cockpit	306.0	34.6	292 - 811	94614	0.0
	OBOGS/LOX	300.5	3.8	276 - 324	109331	0.0
CO (ppm)	Cockpit	0.3	0.5	0 - 7.7	95032	0.0
	OBOGS/LOX	0.0	0.0	0 - 0.8	109354	0.0
NO_2 (ppm)	Cockpit	0.0	0.0	0 - 1.3	95032	0.0
	OBOGS/LOX	0.1	0.1	0 - 0.5	109357	67.5
NO (ppm)	Cockpit	0.0	0.1	0 - 0.7	94813	0.0
	OBOGS/LOX	0.0	0.1	0 - 0.6	109160	13.0
SO_x (ppm)	Cockpit	0.0	0.1	0 - 6.8	95032	0.0
	OBOGS/LOX	0.0	0.2	0 - 12.4	109357	0.1
Total VOCs (ppb)	Cockpit	308.1	36.9	0 - 1101.9	95584	0.0
	OBOGS/LOX	491.0	91.6	0 - 1005.6	109000	0.0
LDSA ($\mu m^2/cm^2$)	Cockpit	274.5	706.2	0.12 - 5012.81	41179	NA
	OBOGS/LOX	23.5	76.9	0.01 - 939.84	41402	NA

Summary statistics shown in Table 5 are further broken down by engine/regulator settings in APPENDIX C (Table C2). The results show consistent values for CO and CO_2 across test phases. In pilot breathing air, NO_2 concentrations exceeded the OEL of 0.1 ppm in 60%, 51%, 70%, and 99% of readings during test phase Idle/100%/Normal, Idle/Normal/Normal, 85%/Normal/Normal, and 85%/100%/Emergency, respectively. NO concentrations exceeded the

OEL of 0.1 ppm in 0.4%, 16.7%, 18.1%, and 18.1% of readings during test phase Idle/100%/Normal, Idle/Normal/Normal, 85%/Normal/Normal, and 85%/100%/Emergency, respectively.

The data are further visualized below using faceted box plots (Figures 6-12).

CO_2 remained near ambient (~300 ppm) in pilot breathing air and occasionally exceeded 500 nm in cockpit air (Figure 6). Engine run phase did not seem to influence CO_2 concentrations.

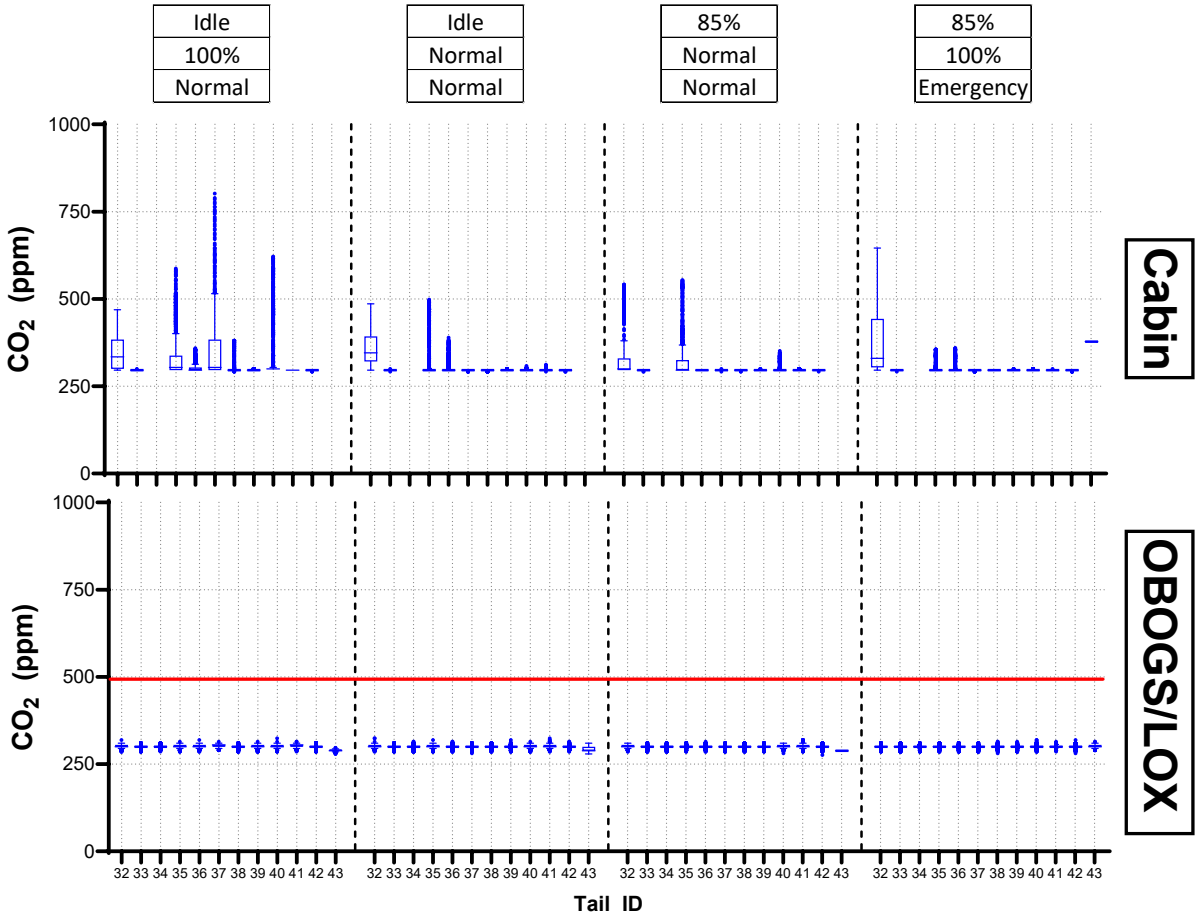

Figure 6. CO_2 boxplot by aircraft, sampling location, throttle, regulator O_2, and regulator pressure settings. The red horizontal line is the MIL-STD 3050 OEL of 500 ppm for CO_2 for the OBOGS/LOX air. The OEL of 5000 ppm for cabin air is not shown on the plot. Aircraft 41 and 43 are LOX aircraft. Aircraft 35, 36 and 41 are incident aircraft.

CO concentrations were higher in cockpit air than pilot breathing air. In cockpit air, average CO concentrations for all aircraft were less than 2 ppm; however, higher peaks of up to 8 ppm were occasionally measured (Figure 7).

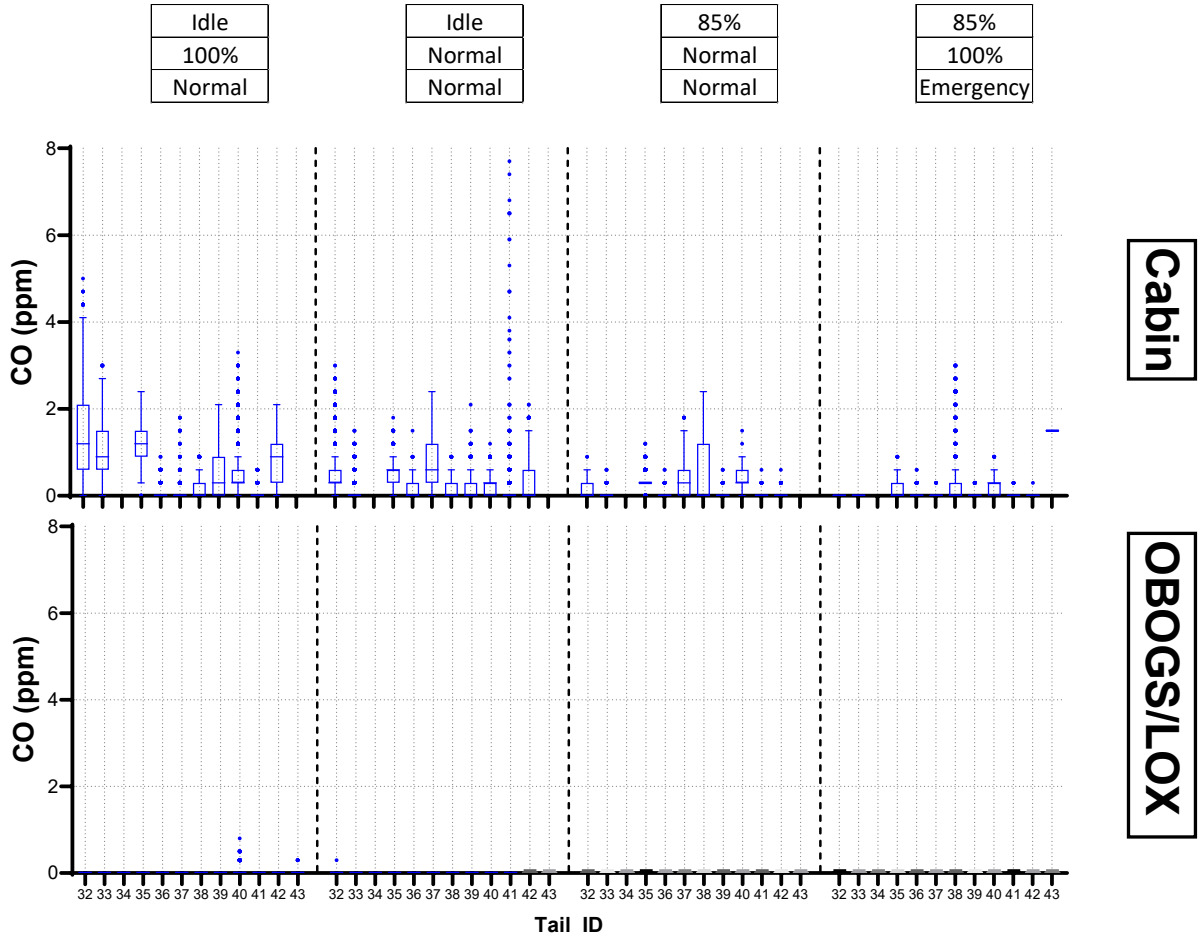

Figure 7. CO boxplot by aircraft, sampling location, throttle, regulator O_2, and regulator pressure settings. The MIL-STD 3050 OEL of CO is 50 ppm for cabin air and 10 ppm for OBOGS/LOX air. Aircraft 41 and 43 are LOX aircraft. Aircraft 35, 36 and 41 are incident aircraft.

NO_2 exceeded its OEL more often than other contaminants and was most commonly present in the air from the pilot breathing air system (Figure 8).

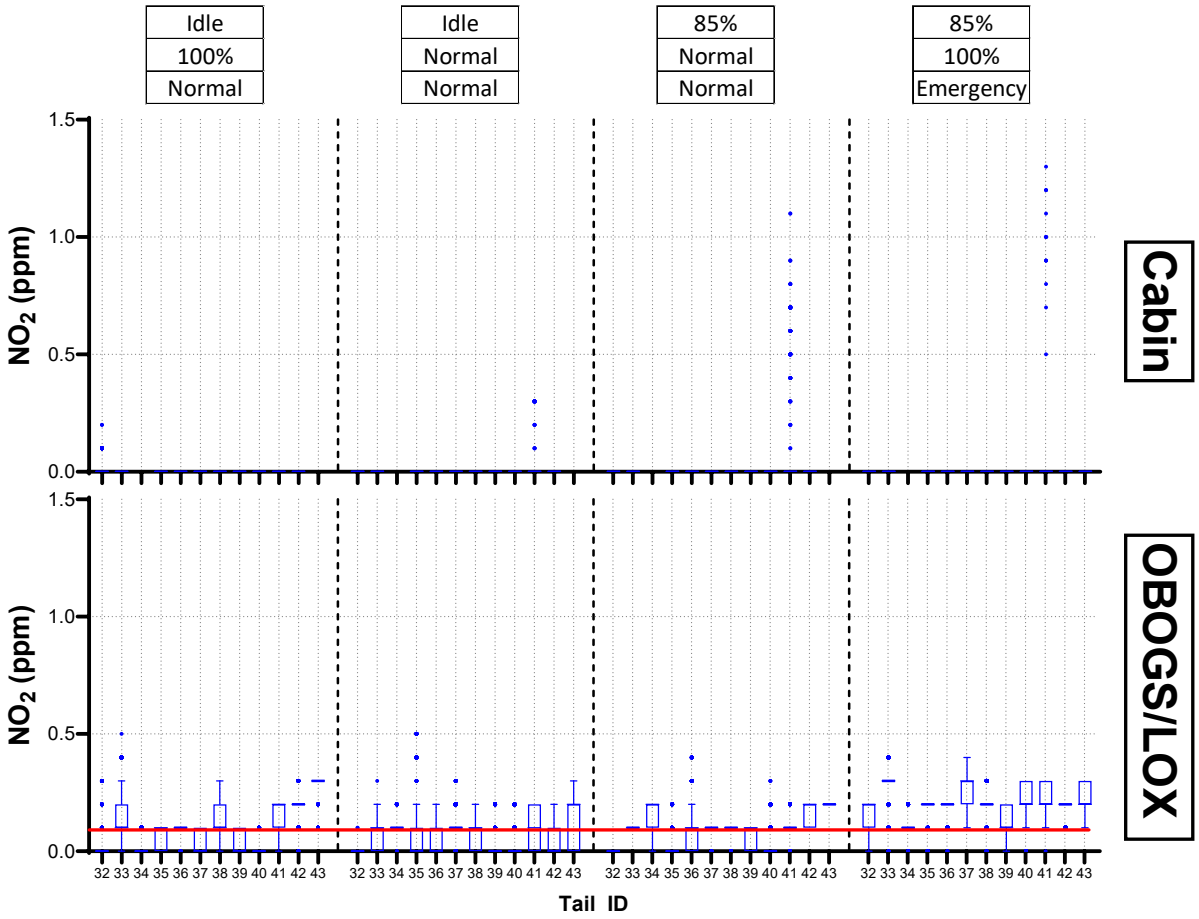

Figure 8. NO_2 boxplot by aircraft, sampling location, throttle, regulator O_2, and regulator pressure settings. The red horizontal line is the MIL-STD 3050 OEL of 0.1 ppm for nitrogen oxides for OBOGS/LOX outlet. The OEL for cabin air is 5 ppm. Aircraft 41 and 43 are LOX aircraft. Aircraft 35, 36 and 41 are incident aircraft.

NO exceeded its OEL in aircraft 33, 34, and 41 in pilot breathing air and 41 in cockpit air (Figure 9). Aircraft 41, a LOX and incident aircraft, showed higher readings than the other aircraft.

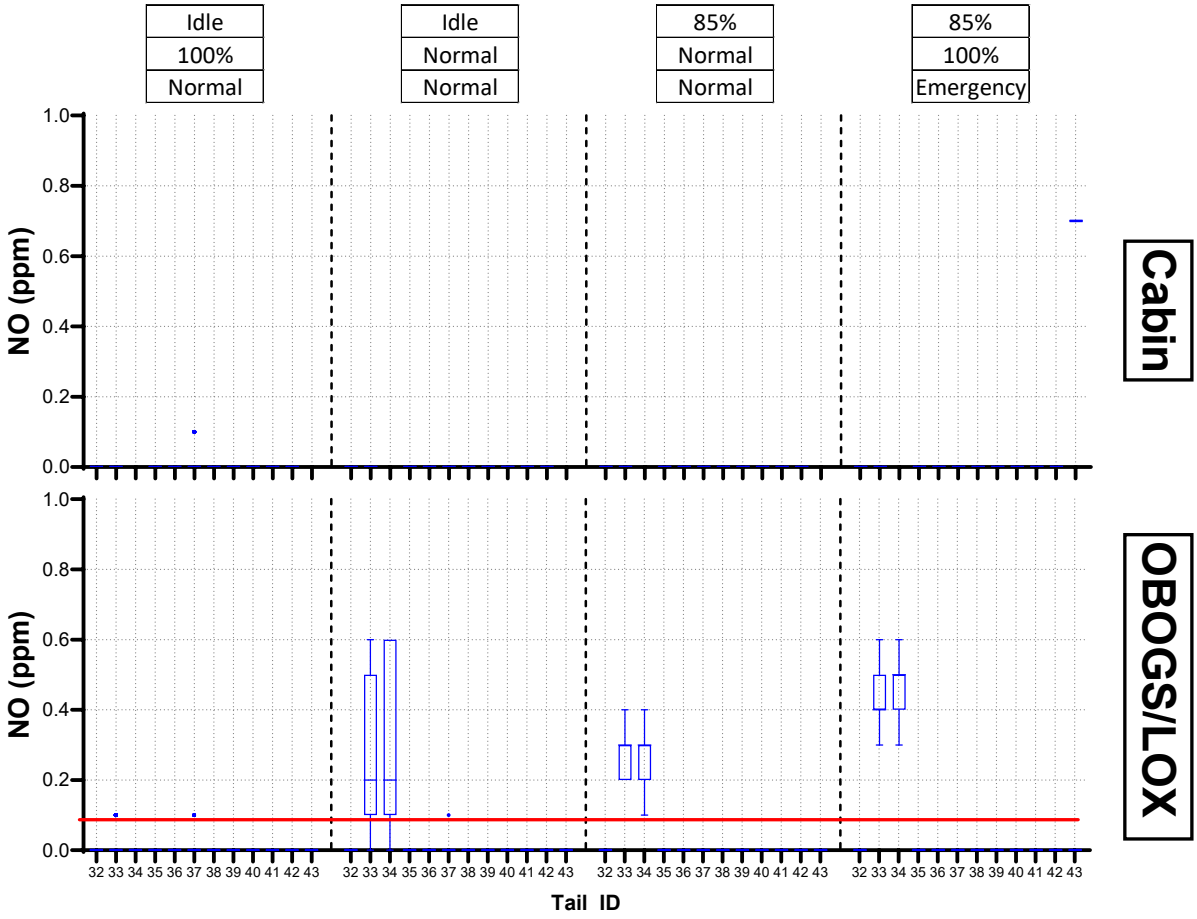

Figure 9. NO boxplot by aircraft, sampling location, throttle, regulator O_2, and regulator pressure settings. The red horizontal lines is the MIL-STD 3050 OEL of 0.1 ppm for OBOGS outlet for NO_x. The OEL of 5 ppm for cabin air is not shown. Aircraft 41 and 43 are LOX aircraft. Aircraft 35, 36 and 41 are incident aircraft.

SO_x concentrations rarely exceeded the OEL (Figure 10). The OEL for SOx was exceeded in pilot breathing air for aircraft 37 and 41 and in cockpit air in aircraft 41. Aircraft 41 is both a LOX and incident aircraft.

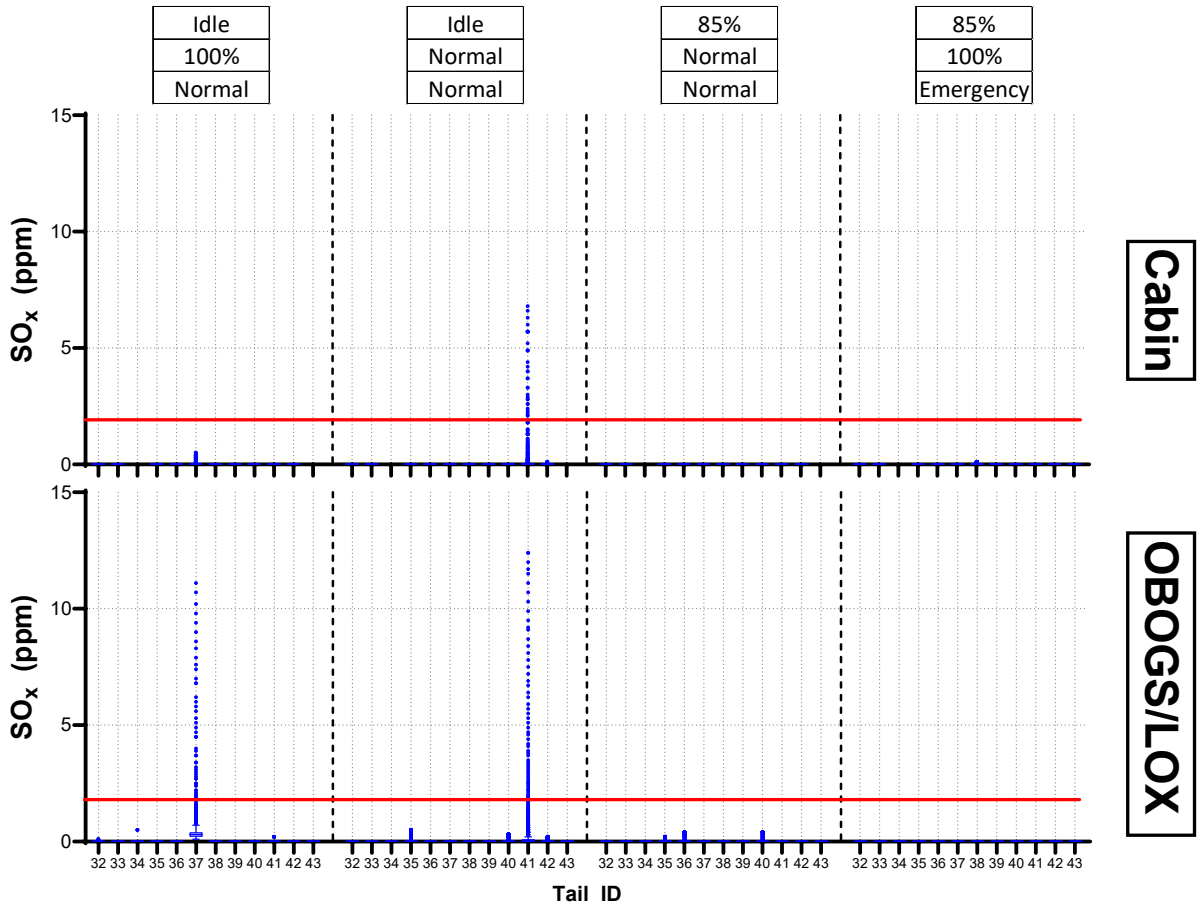

Figure 10. SO_x boxplot by aircraft, sampling location, throttle, regulator O_2, and regulator pressure settings. The red horizontal line is the NIOSH 8h-TWA of 2 ppm for SO_2. Aircraft 41 and 43 are LOX aircraft. Aircraft 35, 36 and 41 are incident aircraft.

Total VOCs exceeded the system control value of 1 ppm in only a few isolated readings (Figure 11).

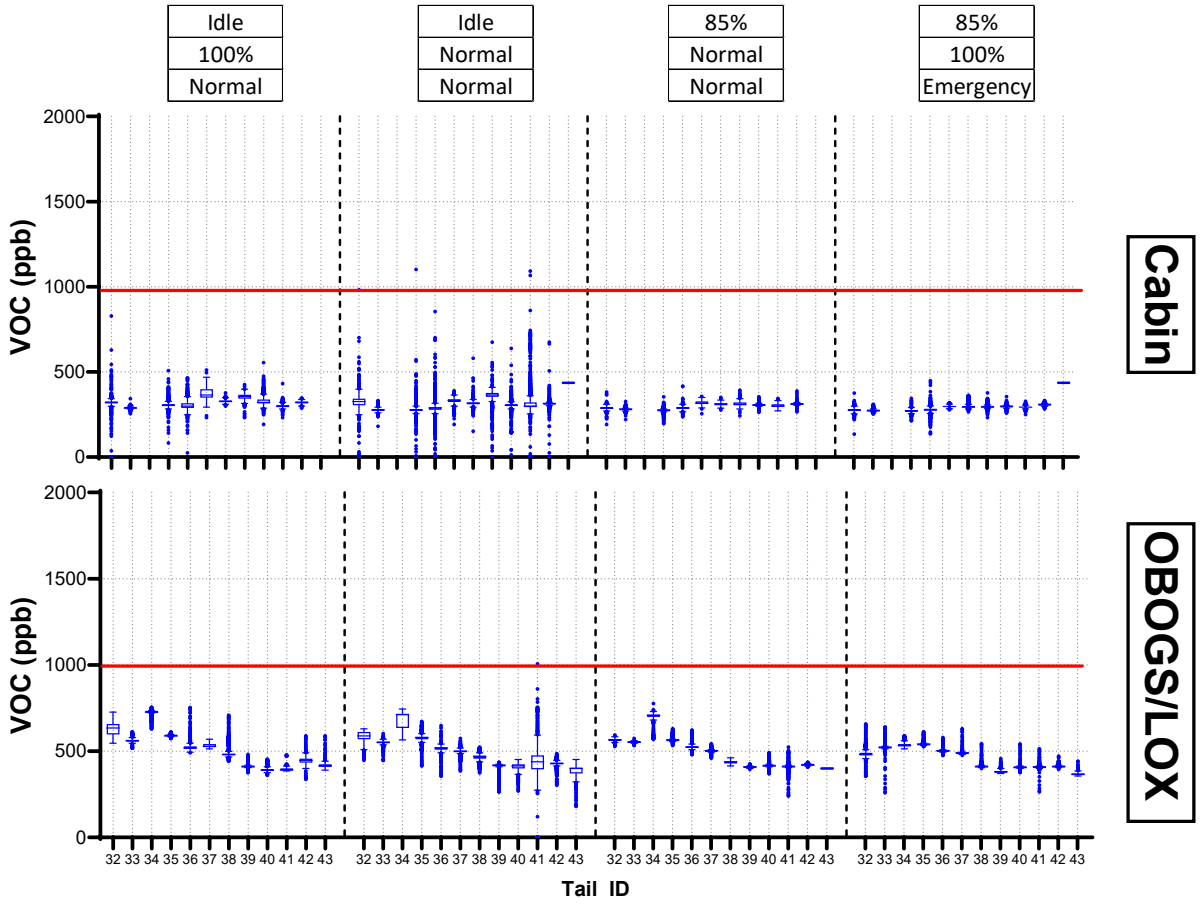

Figure 11. Total VOC boxplot by aircraft, sampling location, throttle, regulator O_2, and regulator pressure settings. The horizontal red line is the system control value of 1.0 ppm (1000 ppb) for total VOCs established by the 711th HPW. Aircraft 41 and 43 are LOX aircraft. Aircraft 35, 36 and 41 are incident aircraft.

The concentration of UFPs was measured as LDSA concentration (Figure 12). No OEL has been established for UFPs, and there was no clear difference in LDSA between incident and non-incident aircraft. The LDSA concentration was generally highest during test phases 1 and 2 but increased during test phases 3 and 4 for aircraft 38.

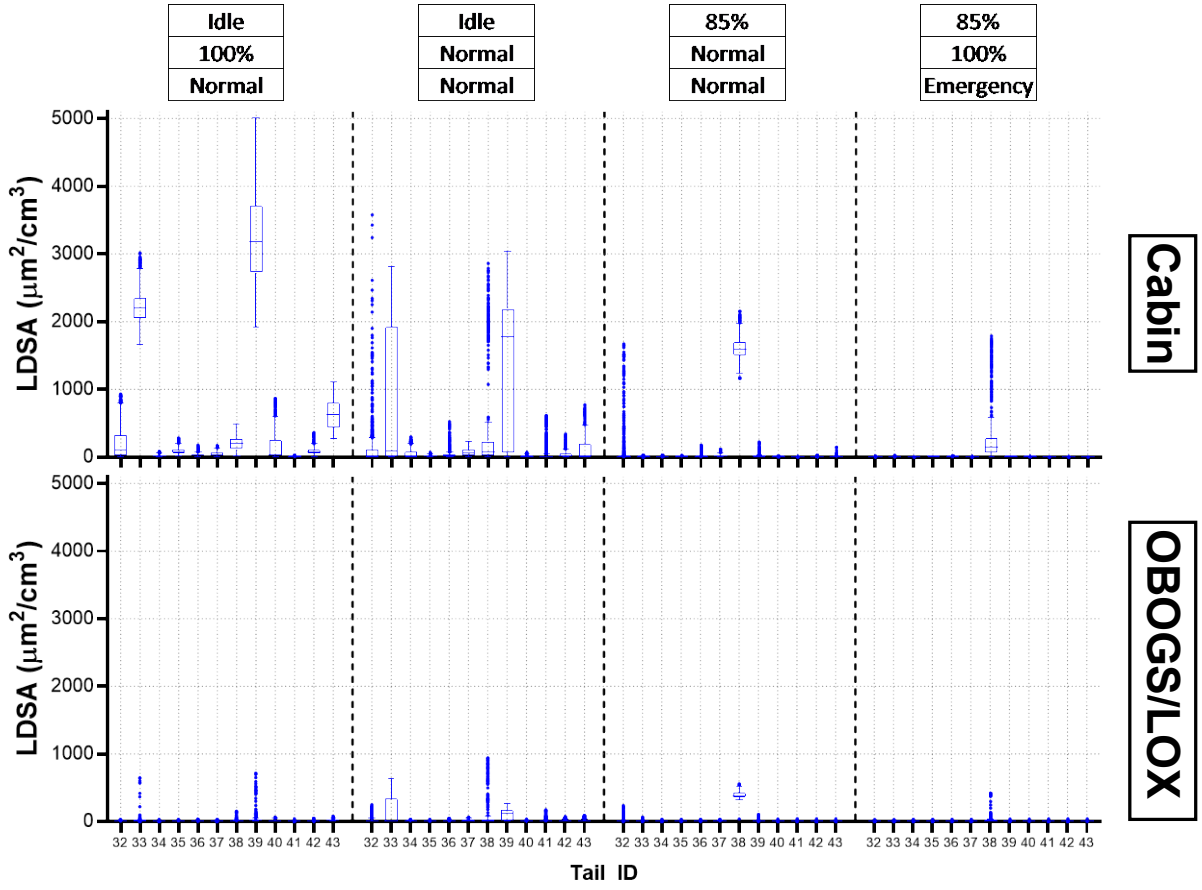

Figure 12. LDSA boxplot by aircraft, sampling location, throttle setting, and regulator O_2 and pressure settings. Aircraft 41 and 43 are LOX aircraft. Aircraft 35, 36 and 41 are incident aircraft.

Time series plots for each individual engine run further elucidate trends in CO_2, CO, NO_2, NO, total VOCs, and UFPs (see APPENDIX D). Real-time plots elucidate that increases in CO_2, CO, and NO_2 typically manifested as short spikes during the engine run. NO sensor creep can be observed for runs with aircraft 33 and 34 (Figure D2 and Figure D3). Total VOC concentrations tended to remain more consistent throughout individual engine runs.

Chemical Contaminants Analyzed Offline

All samples for aldehydes and metals were below the respective limits of detection of approximately 0.1 ppb and 0.2 – 69.3 (dependent on element).

Out of 51 specific VOCs tested for using TO-17 method, 15 were detected in at least one sample (Table 6). One sample of one compound, propene, saturated the GC/MS. None of the detected VOCs exceeded an explicit OEL based on MIL-STD 3050, ACGIH, NIOSH or OSHA (see APPENDIX B). Figures 12-18 further break down the eight most detected VOC contaminants by location and engine/regulator setting. APPENDIX E lists VOCs analyzed for but not detected in the ground engine runs. In Table 6 and Figures 12-18, a value of 50% the lower detection limit was substituted for the non-detects.

Table 6. Detected VOCs

Compound	Lower Detection Limit (ppb)	Mean (ppb)	Standard Deviation (ppb)	Minimum (ppb)	Maximum (ppb)	Times Detected
Acetone	4	9.30	7.39	2	47.89	60
Ethanol	2	3.52	6.60	1	53.96	46
Toluene	2	3.31	3.99	1	19.41	34
1,3-Butadiene	2	1.87	1.35	1	8.78	29
Methylene chloride	2	1.98	1.48	1	6.91	26
Propene[1]	7	8.10	15.41	3.5	100.00	19
Isopropyl Alcohol	2	1.98	2.50	1	11.92	14
Methyl Ethyl Ketone	2	1.23	0.55	1	3.19	11
Acrolein (2-Propenal)	2	1.29	1.23	1	10.38	7
Benzene	3	2.75	3.94	1.5	19.92	3
n-Hexane[2]	2 or 8	4.59	9.75	1	37.76	3
1,4-Dioxane	2	1.06	0.29	1	2.37	1
4-Ethyltoluene	2	1.02	0.19	1	2.61	1
Cyclohexane	2	1.03	0.23	1	2.96	1
Styrene	2	1.02	0.17	1	2.45	1

[1]One of the 19 samples in which propene was detected exceeded the upper detection limit of 100 ppb and saturated the detector. The mean, standard deviation, minimum, and maximum values were calculated after using a value of 100 ppb for that sample.

[2]Depending on the sample, the lower detection limit for n-hexane was reported as 2 or 8 ppb.

Acetone was the most frequently detected compound. The highest values detected occurred in OBOGS aircraft during engine run test phase 2; however, the average value for this phase remained similar to other phases and locations (Figure 13).

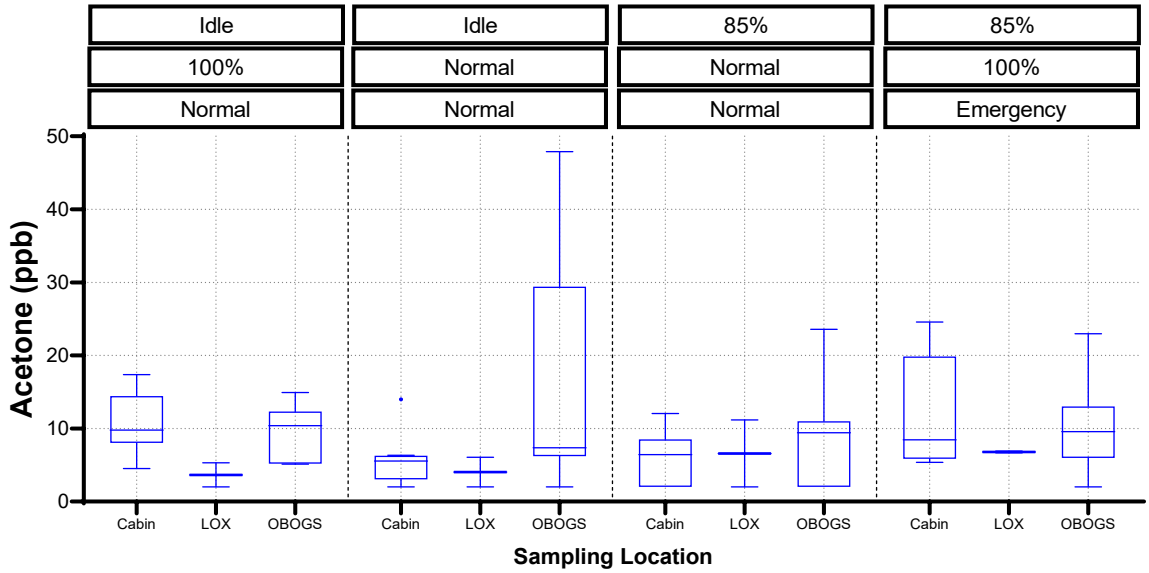

Figure 13. Acetone boxplot by sampling location and engine run test phase

Ethanol displayed similar patterns to acetone but was detected at lower concentrations (Figure 14). Notably, the highest concentrations were again observed in OBOGS aircraft during the Idle/Normal/Normal setting (engine run test phase 2).

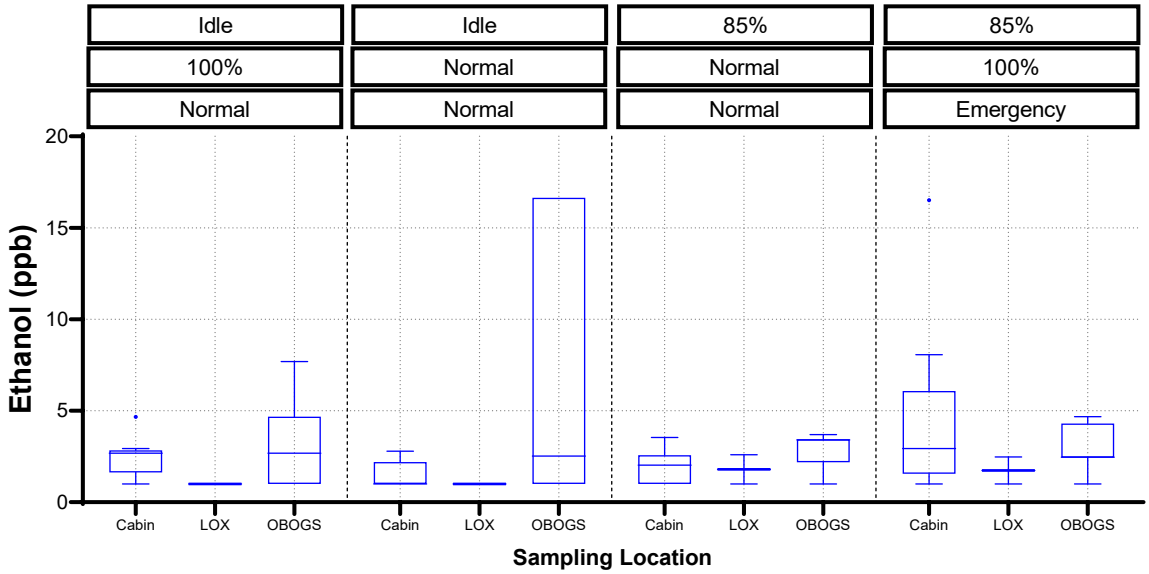

Figure 14. Ethanol boxplot by sampling location and engine run test phase

Toluene concentrations were more variable and displayed different patterns than the other detected compounds (Figure 15). Higher concentrations were observed in the cockpit than OBOGS during Idle/100%/Normal and 85%/100%/Emergency (test phases 1 and 4).

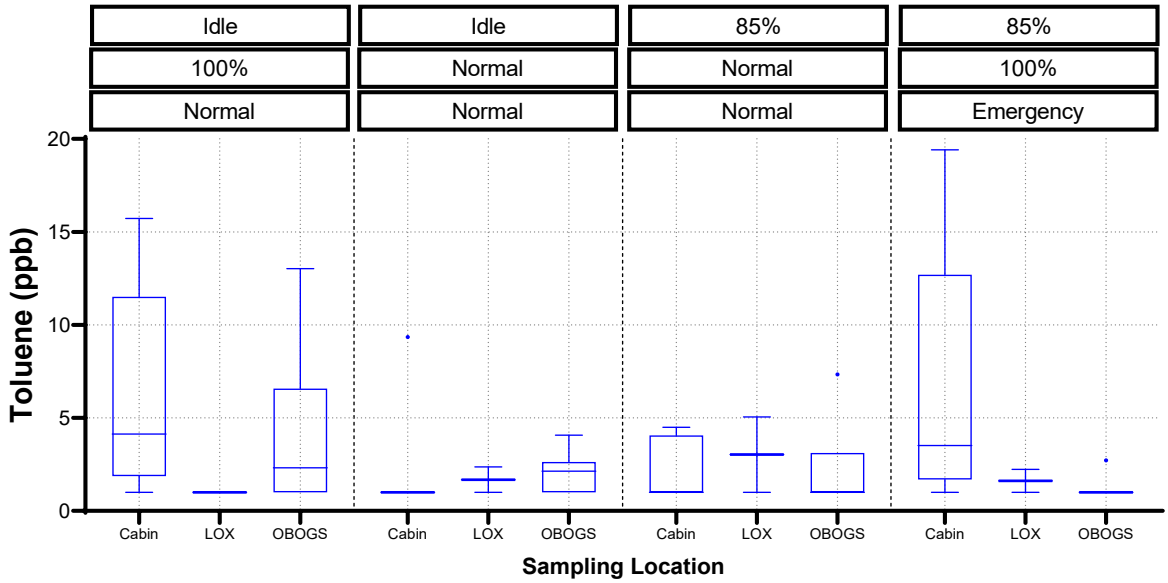

Figure 15. Toluene boxplot by sampling location and engine run test phase

Figure 16 shows higher levels of 1,3-Butadiene detected in the OBOGS than the LOX or cockpit of the A-10 aircraft. In LOX aircraft, this compound was only detected during one test phase (Idle/Normal/Normal).

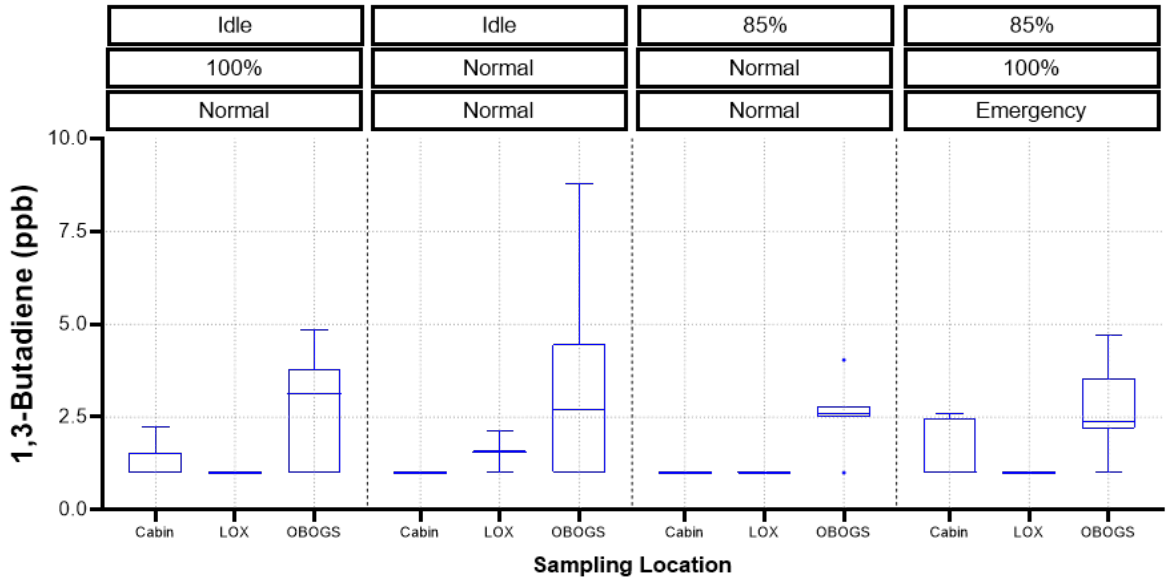

Figure 16. 1.3-Butadiene boxplot by sampling location and engine run test phase

Methylene chloride was present at higher concentrations in the OBOGS systems, with lower concentrations observed in the LOX systems (Figure 17). Methylene chloride was not detected in the cockpit of any aircraft.

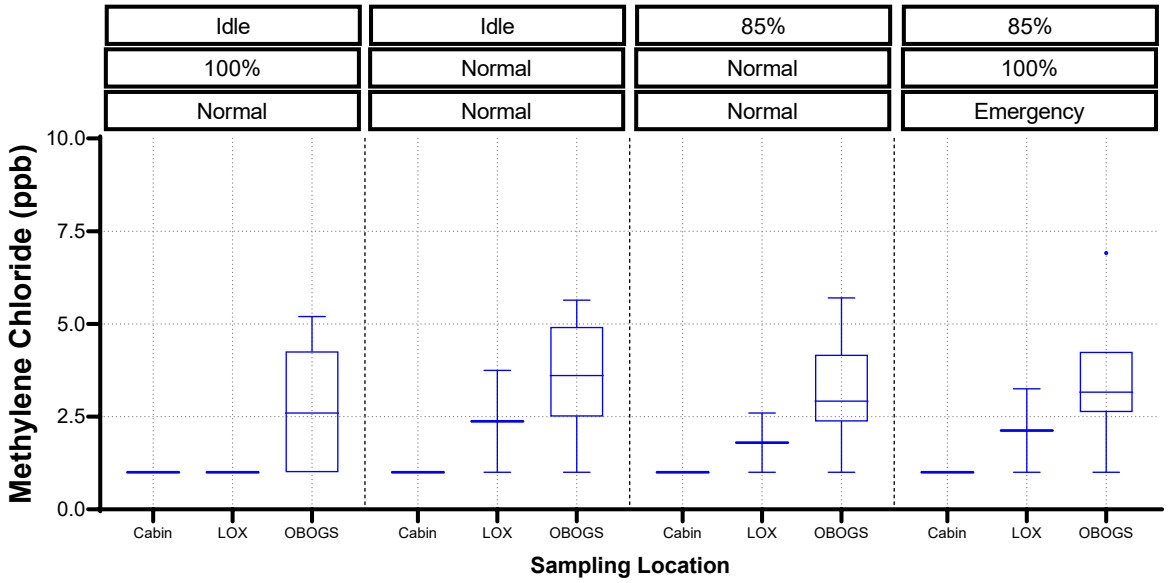

Figure 17. Methylene chloride boxplot by sampling location and engine run test phase

Propene was frequently detected in the OBOGS but rarely in the LOX system or cockpit (Figure 18). The highest concentrations occurred during the Idle/100%/Normal settings (test phase 1).

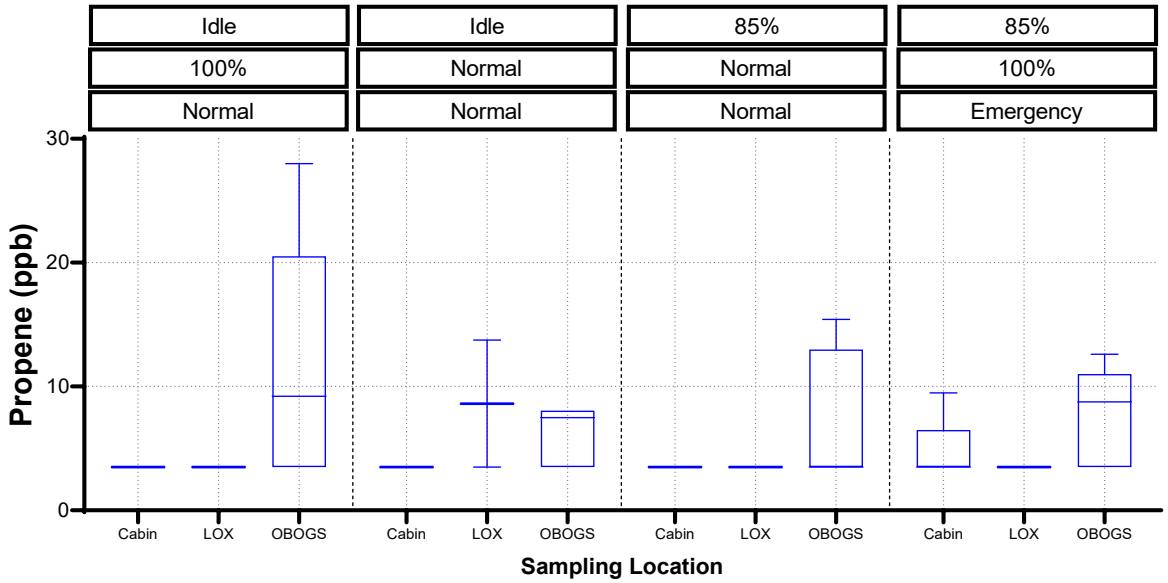

Figure 18. Propene boxplot by sampling location and engine run test phase

Opposing the patterns of most of the VOCs, isopropyl alcohol was never detected in the OBOGS but was detected both in the cockpit and LOX (Figure 19). The highest detected concentrations occurred in the cockpit.

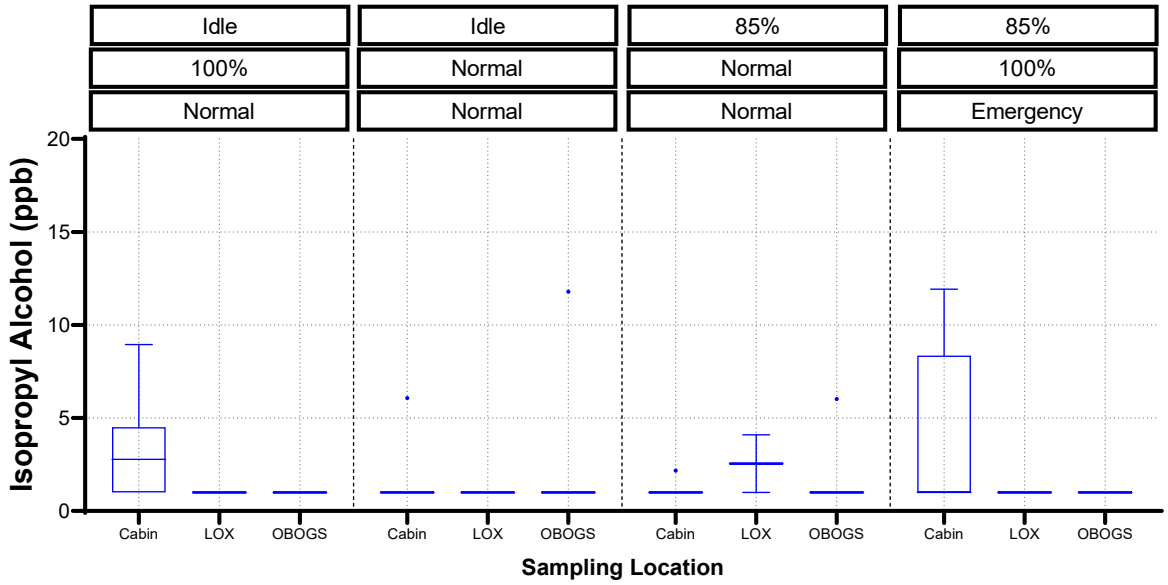

Figure 19. Isopropyl alcohol boxplot by sampling location and engine run test phase

Methyl ethyl ketone was detected only during test phases 1 and 4 (Figure 20). It was never detected in LOX systems.

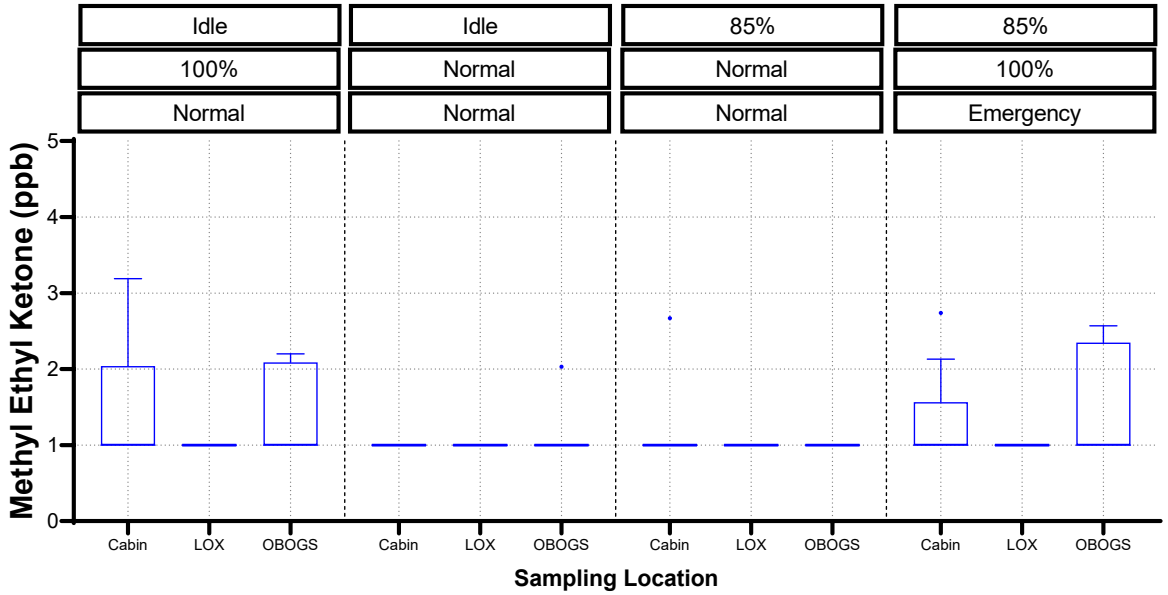

Figure 20. Methyl ethyl ketone boxplot by sampling location and engine run test phase

3.5 Discussion

The goal of this study was to measure the levels of O_2, airflow conditions, and chemical contaminants in cockpit and pilot breathing air of A-10 aircraft during ground engine runs. Engine runs were completed for twelve different aircraft over the course of three days. During each engine run, there were four test phases, each using a different combination of engine thrust and regulator settings to mimic different scenarios that could potentially lead to unexpected changes in O_2 or the introduction of chemical contaminants into breathing air (see Table 1 for description of test phases). Two of the twelve aircraft were equipped with LOX systems, while the remaining were equipped with OBOGS. Three of the twelve aircraft had recently been involved in a PE. The list of aircraft sampled is included in Table 2.

The OAGr system built to conduct these measurements was designed to sample simultaneously from two locations (see Figure 1 and Table 3). For the present study, these two locations were the cockpit (labelled Cabin in boxplots) and pilot breathing air system (OBOGS or LOX). It was important to characterize cockpit air since pilots may drop their mask when the pilot breathing air system faults or does not seem trustworthy. Further, cockpit air is representative of the air introduced into the OBOGS. The OAGr sampling flow path connected to the pilot breathing air system was connected at the regulator where the pilot would normally connect his or her mask.

O_2 concentrations remained near ambient in the cockpit during all engine run test phases and were strongly affected by regulator settings in the pilot breathing air system (see Table 4 and Table C1; Figure 2 and Figures D1-D12). According to MIL-STD-3050, the O_2 concentration should vary between 40 and 90% depending on the specific operating parameters, such as inlet air pressure, cabin altitude and demand flow (Department of Defense, 2015). Generally, the results indicate that the pilot breathing systems operated as expected. Across all engine runs, the mean O_2 concentration was 57% at idle thrust / 100% O_2 / normal pressure (test phase 1) and 76% at 85% thrust / 100% O_2 / emergency pressure (test phase 4). O_2 averaged 47% and 46% for test phases 2 and 3, respectively, when the regulator was set to normal O_2 (see Table C1). The O_2 concentration in the two aircraft with LOX systems approached the upper limit of the sensor range of around 92% at 85% thrust / 100% O_2 / emergency pressure (test phase 4).

The volumetric flow rate of air drawn into the OAGr sampling system from the pilot breathing air flow path was measured in real-time. Flow rate was not monitored in the second flow path that was open to the cockpit. The flow rate of air sampled from the pilot breathing air system averaged 4.7 $L*min^{-1}$ and reached a maximum of 7.2 $L*min^{-1}$ (see Table 4 and Figure 3). According to the MIL-STD-3050, the OBOGS may not be expected to operate as expected when demand flow is less than 7 $L*min^{-1}$ (Department of Defense, 2015). During engine runs with aircraft 34 and 35, volumetric flow rates were about 1 and 3 $L*min^{-1}$, respectively. These low flow rates appeared to correlate with lower peak O_2 readings of < 75% during the 100% O_2 emergency pressure setting (test phase 4). However, this trend was not consistent for all engine runs. For example, during engine runs with aircraft 39, O_2 concentrations reached over 80% during test phase 4, while volumetric flow rate hovered between 3 and 4 $L*min^{-1}$.

An additional concern related to the relatively low flowrate drawn by the OAGr system compared to the inspiratory flow rate of a pilot is that it likely results in an underestimation of contaminant exposures. According to measurements made by Gorge in 1993, the mean inspiratory peak flow of Navy aircrew was 78 $L*min^{-1}$ during routine flight operations. This indicates that exposures during real world operations could be on the order of ten times higher

during flight operations than what was reported in the present study. Future studies should focus on putting a demand on the OBOGS during ground engine runs that is more representative of a pilot breathing. In the present study, drawing higher flow rates posed an engineering challenge when using sampling pumps designed for exposure assessments. However, vacuum pump technologies designed for high flow applications could be adapted and integrated into future versions of the OAGr system.

The temperature and RH of air was also measured in real-time since these parameters can play a role in the comfort level of breathing air, as well as on sensor performance. Further, water build-up in the OBOGS can degrade performance, which has been hypothesized to be related to the release of chemical contaminants absorbed in the zeolite bed (Department of Defense, 2015). Temperature increased steadily over the duration of each engine run by 4-5°C, which is likely associated with thermal build-up in the OAGr system (see Table 4, APPENDIX C, APPENDIX D). Future iterations of the OAGr should thermally isolate thermocouples to get a true measurement of air temperature. Regardless, the temperatures did not vary more than what is allowable per MIL-STD-3050, which is within +10°F and -20°F (~+6°C and -11°C) of the ambient aircraft cabin temperature (Department of Defense, 2015).

The RH of cockpit air averaged 14.5%, and the RH of pilot breathing air averaged 4.7% (see Table 4 and Figure 5). RH showed an inverse relationship with O_2 concentration in the breathing air, reaching a value of zero or close to zero during test phase 4 during most engine runs (see Figure 5 and Figures D1-D12). The RH of cockpit air trended inversely with temperature, which is expected, since RH is a measure of the amount of water vapor relative to the amount required for saturation at a given temperature expressed as a percentage.

Chemical contaminants measured in real-time included CO_2, CO, NO_2, NO, SO_x, total VOCs, and UFPs expressed as LDSA. Concentrations were monitored in each aircraft as a function of test phase, and values were compared to OELs based on MIL-STD-3050 (for CO_2, CO, NO_2, and NO), NIOSH recommendations (for SO_x), and a system control value established in the 711th HPW (for total VOCs). The list of OELs referenced are listed in APPENDIX B, Table B1.

Across all twelve engine runs, most contaminants were well below referenced OELs (see Table 5). Concentrations of CO_2 and CO were well below OELs based on MIL-STD 3050. Sampling location played a significant role for both CO_2 and CO, where concentrations in cockpit air were much higher and more variable than those found in the pilot breathing air (see Figure 6 and Figure 7). This is likely due to a leak in the canopy seal resulting in exhaust from the aircraft entering through the leak versus through engine bleed air.

NO_2 and NO exceeded OELs more consistently than any of the other contaminants measured. Across all twelve engine runs, 67.5% of NO_2 readings and 13.0% of NO readings in pilot breathing air were at or above the maximum allowable concentration of 0.1 ppm for NO_x based on MIL-STD-3050 when measured in pilot breathing air (see Table 5). For both NO_2 and NO, the OEL was exceeded during all test phases. For NO_2, the percentage of readings above the OEL was highest during test phase 4, and for NO, the percentage of readings above the OEL was highest during test phases 2-4 (see Table C2). The maximum allowable concentration of 5 ppm for NO_x was never exceeded in cockpit air using either sensor.

Across all twelve engine runs, SO_x concentrations exceeded the 8h-TWA NIOSH recommended value of 0.2 ppm for SO_2 in 0.1% of the observations in pilot breathing air and 0% of the observations in cockpit air (see Table 5 and Figure 10). Total VOC concentrations rarely

exceeded the 1 ppm system control value established by the 711th HPW (see Table 5 and Figure 11). UFPs averaged 274.5 $\mu m^2/cm^3$ in the cabin and 23.5 $\mu m^2/cm^3$ in the breathing air. Although there is no standard OEL for evaluating the significance of these measurements, the cabin air values are higher than typical urban environment values for LDSA (12 - 94 $\mu m^2/cm^3$) (Kuuluvainen, 2016). According to MIL-STD-3050, the OBOGS should have an outlet particulate filter, but it is only required to capture particles with a size of 0.4 micron or greater (Department of Defense, 2016).

Chemical contaminants were also measured in air samples collected for offline analysis. All samples for aldehydes and metals were below the respective limits of detection of approximately 0.1 ppb and 0.2 – 69.3 (dependent on element). Samples analyzed for TO-15 compounds contained several VOCs above the detection limit, including acetone, ethanol, toluene, 1,3-butadiene, methylene chloride, propene, isopropyl alcohol, methyl ethyl ketone, and others (see Table 6). However, all of these VOCs were detected at ppb levels and were well below relevant OELs from MIL-STD 3050, OSHA, NIOSH, or ACGIH (see APPENDIX B).

Based on the above results, NO_2 is the most likely exposure concern in pilot breathing air, although further studies should confirm this result. NO_x has also been detected in commercial aircraft cabins. In a study aboard a commercial aircraft cabin, Waters et al. (2002) found an average concentration for total NO_x of 0.57 ppm during 36 commercial flights. However, two other studies found lower cabin concentrations. The highest average total NO_x concentration reported by Lee et al. (1999) during five Cathay Pacific Airlines flights was 0.05 ppm if one excludes one flight segment where there were smoke fumes at the airport. Spengler et al. (1997) measured average NO_2 levels of 0.036 ppm during Boeing 777 flights. Acute exposure to NO_2 can cause respiratory irritation, and longer-term exposure may contribute to asthma or respiratory infection (US EPA, 2016).

It is important to note that in the present study, the resolution of both the NO_2 and NO sensors is 0.1 ppm, so any signal read by these sensors would register as meeting the maximum allowable concentration. Further, NO values showed a positive increase with increasing temperature during two of the engine runs, which may have led to erroneously high values in engine runs 2 and 3 where NO reached peaks of 0.5 and 0.6 ppm, respectively (see APPENDIX D, Figures D2 and D3). Electrochemical sensors are known to be sensitive to temperature, and according to the manufacturer, the NO_2 and NO sensors zero current starts to drift to positive values at 35°C. Further, electrochemical sensors can dry out and stop responding at low RH. (Thongplang, 2018). The lower RH limit is reported to be 15% for the NO_2 and NO sensors used in the present study. Therefore, there is a potential for under-reported results for all contaminants measured using electrochemical sensors (CO, NO_x, SO_x) in pilot breathing air where RH was < 15%.

4.0 TOXICOKINETIC SIMULATION

4.1 Background

CO is a gaseous contaminant found in air nearly ubiquitously across the world. Typical ambient air concentrations of CO range from 0.03-0.20 parts per million (ppm) in rural areas, but this can be elevated to closer to 0.5-5 ppm in large cities and areas with significant combustion engine exhaust, sources for CO release (EPA, 2010). While there are low levels of endogenous CO concentrations expected in the body (CDC, 2018), significant exposures to CO can be dangerous, and even lethal to humans.

The symptoms of severe CO poisoning have been well documented (EPA 2010). CO binds to hemoglobin in the body about 200 times more readily than oxygen, and the displacement of oxygen from hemoglobin is the major mechanism by which CO exerts its toxic effects. As such, the extent of CO exposure is typically determined by the percentage of hemoglobin bound by CO (%COHb). Prior research has indicated that %COHb ≥ 20% is highly correlated with the development of neurological symptoms, including headache, disorientation, and confusion, while %COHb > 40% frequently leads to severe adverse effects and death (EPA 2010). However, what remains controversial is the presence of negative effects, if any, to CO leading to %COHb < 20%, and particularly %COHb ≤ 5%.

Adverse effects of low levels of CO exposure have largely focused on two major sets of symptoms: cardiovascular function and neuropsychological effects. Sheps *et al*. have demonstrated an increase in frequency of ventricular arrhythmias in coronary artery disease patients with %COHb of 5.3%, but not 3.7% (Sheps, 1990; Sheps, 1991). A later study was unable to corroborate these findings, however, with neither 3% nor 5% %COHb leading to an increase in the incidence of ventricular arrhythmia (Dahms 1993). Additionally, it was shown that in healthy young adults there was no impairment in submaximal exercise capacity at %COHb levels up to 20% (Kizakevich, 2000). The neuropsychological outcomes at low CO exposures have been equally challenging to characterize as there is such a wide range of detrimental effects that, in contrast to the neurological symptoms described above, are often difficult to differentiate from normal behavior. These subtle cognitive effects of interest include minor detriments in visual perception, motor and sensorimotor performance, judgment, and vigilance among others.

Evidence for presence of subtle cognitive effects of low-level CO exposure started accumulating decades ago, including one study by Beard *et al*. demonstrating a negative effect of inhaling 50-250 ppm CO for 20-90 minutes (~3-5% COHb) on the ability to judge the passage of short amounts of time (Beard, 1967). The accumulation of this evidence led both the World Health Organization and the Environmental Protection Agency (EPA) to issue warnings about the subtle, “nonadverse” cognitive effects of exposures leading to ~5% COHb (Levels, 2010). However, during the same time period there was evidence indicating that some of the effects seen at low CO studies, such as time impairment, could not be replicated in other studies (Stewart 1970, Stewart 1975). A review written by Raub *et al*. covers the extent of the disagreement in the literature more completely (Raub 2002). Nonetheless, the preponderance of evidence points to the likely presence of at least some subtle cognitive effects of 3-5% COHb, which has caused many health safety agencies to suggest standards that keep daily human exposures to levels that will not increase past 2% COHb (Hawkins 2017, Barn 2018).

A large part of what makes these subtle cognitive effects so challenging to understand is that they may not affect the day-to-day life of an average individual. For example, an individual working at a desk all day to write a paper may not even notice mild impairment to visual light threshold. However, these subtle cognitive effects become much more of a concern in cases where snap judgments and precisely coordinated movements based on rapidly changing information are required. For example, Archsmith *et al*. showed that a 1 ppm increase in 3-hour CO exposure over ambient levels (ranges investigated 0.5-2.5 ppm) increased the propensity of Major League Baseball umpires to make incorrect calls by 11.5% (Archsmith, 2017). The present study investigates the potential for similar effects of low to medium CO environment levels (10-500 ppm) on fighter pilots in the USAF while operating their aircraft.

Several models exist for connecting the %COHb seen in the body to inhaled air concentrations of CO. The first and most well-known model is the Coburn-Foster-Kane (CFK) model. This model utilizes a system of equations to describe the major physiological variables that determine blood COHb concentration (Coburn 1965). Most subsequent models have built upon the CFK model to accomplish understanding of other aspects of CO inhalation including arterial versus venous levels of COHb (Benignus, 1994; Smith, 1994), the effects of exercise on CO inhalation and COHb levels (Peterson 1975), the distribution of CO to the skeletal muscle (Bruce 2003), and even exposure of a fetus to CO after maternal CO inhalation (Hill, 1977). A relatively recent model from Gosselin *et al*. adds an extravascular space compartment to understand the amounts of CO bound to hemeproteins and additionally allows for incorporation of several different individual factors including exercise level, sex, weight, and height (Gosselin 2009). This model was specifically validated for humans exposed to low levels of CO. As such, this model was ideal for modification and used for this investigation.

4.2 Approach

The intent of this investigation was to determine the potential for short term exposures of USAF pilots waiting in a flight line to be exposed to CO from aircraft exhaust that will result in %COHb high enough to potentially cause subtle cognitive deficits. These deficits would clearly be detrimental to the pilots' ability to fly these complex airframes, and therefore understanding the potential for CO-based toxicity is of utmost importance.

4.3 Methods

Model Replication

The model developed by Gosselin *et al*. was replicated and modified slightly for use in this investigation (Gosselin 2009). The model was generated using acslX version 3.0.2.1. The *csl* model file is available in APPENDIX F. One difference implemented in the present model included an increase in the partial pressure of oxygen (PO2) from the value indicated in the Gosselin model ((-0.24 * Age) + 104.7), to 500 mmHg during flight to represent the theoretical pressurized, hyperoxic air provided to the pilots through the flight mask (Bruce 2003). Additionally, an empirical formula ((502.24 * REndo) – 2.381) was used to generate an initial COHb concentration based on the endogenous production rate (REndo = endogenous regressors). Variations in initial concentrations ultimately have little effect on COHb pharmacokinetics, but the empirical formula helps relate those initial concentrations to the endogenous production

(Gosselin 2009). Because model validation was already performed in the Gosselin paper, it was not pursued further in the present paper.

Simulations

The model was used to perform simulations relevant to pilots waiting for takeoff on the flightline, who may have been exposed to aircraft exhaust. The conditions that are unknown or are expected to change between individual exposures include the air concentration of CO, the time that an individual may be exposed while waiting in the flight line, and the work load that the pilot is under (e.g. at ease and breathing lightly versus active and breathing more heavily). Simulations were first performed to understand the impact of variations in these conditions individually. In these simulations, all factors and covariates were held constant (or calculated the same way) except for the factor of interest in that simulation. The first set of simulations varied inhaled CO between concentrations of 10, 30, 50, 100, 130, 195, 300, and 500 ppm. The next set of simulations examined exposure times of 15, 30, 45, and 60 minutes. Finally, workloads of 12%, 32%, and 64% were simulated, representing rest, light workload, and heavy workload, respectively. In each of these simulations, pilots were assumed to take off (and put on their mask) at the end of the exposure period and perform a 60-minute flight, after which they landed (taking their mask off).

Following the individual simulations, MC simulations (n = 1000 iterations) were performed allowing these and other anthropomorphic and physiologic factors to vary. In particular, age, body weight, sex, height, exposure time, and workload were varied according to distributions discussed more in the Results section. Following MC simulation, the number of simulations attaining a max %COHb > 3% and > 5% was ascertained.

4.4 Results

A slightly modified version of the CO model published by Gosselin *et al*. was used for this investigation (Gosselin 2009). The main differences between the original model and modified version were in the definition of certain parameters, noted in Table 7. Given that this model was previously validated, no further validation was pursued for this investigation.

Table 7. Toxicokinetic Model Parameters

Parameter Name	Variable	Value or Equation	Units	Source
Bodyweight	BW	Varied (75.0)	Kg	-
Height	HT	Varied (174.4)	Cm	-
Sex	G	Varied (1)	0 = female, 1 = male	-
Age	A	Varied (20.0)	Y	-
Body temperature	Temp_K	310.15	K	-

Volume of extravascular space	Vtis	2.2	L	Valentin 2002
Haldane affinity ratio for Hb	MHb	240	Unitless	Gosselin 2009
Gas constant	R	2.55	mmHg*mL air/K * mL CO	Gosselin 2009
Concentration of inhaled CO	CO_Inh	Varied (50.0)	ppm	-
Concentration of inhaled CO	COExt	CO_Inh/1x10^6	mL/mL	
Length of inhalation exposure	TChng	Varied (30.0)	min	-
Time oxygen mask is applied	MaskOn	TChng	min	-
Time oxygen mask is removed	MaskOff	TChng + 60	min	-
Workload	Pwl	Varied (32.0)	watts	-
Time to experiment end	Tstop	180	min	-
Scaled endogenous CO amount	ACO_Init	(502.24 * REndo) – 2.381	mL	Empirical equation to set initial = endogenous
Alveolar volume	VAlv	Vt - Vd	mL	Gosselin 2009
Alveolar air flow	QAlv	fR * VAlv	mL/min	Gosselin 2009
Energy consumption over baseline	Wtot	Wcon - Wrest	watts	Gosselin 2009
STPD to BTPS conversion factor	Beta	1.21	Unitless	Gosselin 2009
Lung diffusion capacity of CO at given workload	DLCO	DLCO_Rest + 0.06*Wtot	ml/min/mmHg	Gosselin 2009
Max amount of CO that can bind to 1 g of Hb	bMax	Beta * 1.389	mL/g	Gosselin 2009
Volume of blood	VBld	0.079 * BW	L	Gosselin 2009
Max volume of Hb that can be bound by CO	CHbMax	bMax * CHb* VBld	mL	Gosselin 2009
Partial pressure of oxygen	PO2	(-0.24 * A) + 104.7	mmHg	Gosselin 2009
Partial pressure of oxygen (Mask On)	PO2	500	mmHg	Bruce 2003
Endogenous production rate of CO (STPD)	Rendostp	0.007 * (BW / 69.5)	mL/min	Gosselin 2009

Endogenous production rate of CO (BTPS)	Rendo	Beta * Rendostp	mL/min	Gosselin 2009
Oxidizing rate of carbon monoxide	kCO2	3.33x10^-5	/min	Gosselin 2009, Luomanmäki 1969
Capture rate of CO	kSf	0.01	/min	Gosselin 2009
Release rate of CO	kHS	0.2 * kSf	/min	Gosselin 2009
Sex-dependent Quantities				
Concentration of Hb in whole blood	CHb	M: 165.0 F: 145.0	g/L	Valentin 2002
Tidal volume	Vt	M: 613.49*log(PWL)-732.45 F: 465.81*log(PWL)-603.44	mL	Empiric equation based on Valentin 2002 values
Respiratory frequency	fR	M: 7.0994*log(PWL)-4.1335 F: 9.7555*log(PWL)-9.7275	breaths/min	Empiric equation based on Valentin 2002 values
Total dead space volume	Vd	M: 111.96*log(PWL)-102.67 F: 84.977*log(PWL)-51.944	mL	Empiric equation based on Valentin 2002 values
Resting energy consumption	Wrest	M: 30.0 F: 21.7	watts	Gosselin 2009
Resting lung diffusion capacity of CO	DLCO_rest	M: 46.332*exp(-0.005*A) F: 30.247*exp(-0.002*A)	ml/min/mmHg	Empiric equation based on Valentin 2002 values
Energy consumption at given workload	Wcon	M: 65.741*log(PWL)-127.83 F:60.833*log(PWL)-123.72	watts	Empiric equation based on Valentin 2002 values

Simulations

Three major factors with the potential to vary CO exposure were considered: air concentration, length of exposure time, and breathing conditions. The parameters that were varied and the values at which they were held constant are shown in Table 8.

Table 8. Values for Toxicokinetic Model Variables

Parameter	Conditions Tested	Max %COHb	Time > 3% COHb (min)
Inhaled CO Concentration (ppm)	10	0.3	0
	30	0.8	0
	50	1.2	0
	100	2.3	0
	130	2.9	0
	195	4.3	25.4
	300	6.5	51.5
	500	10.7	79.1
Inhalation Time (min)	15	0.7	0
	30	1.2	0
	45	1.7	0
	60	2.1	0
Percent of Maximal Workload (%)	12	0.6	0
	32	1.2	0
	64	1.7	0

Varying Dose

The most obvious variation on the scenario of a pilot being exposed to CO from an aircraft engine in front of him/her while idling on a runway would be a change in the concentration of CO in the air. Unfortunately, at this time, there is very little information available to indicate even a rough estimate of what those concentrations may be. A previous study indicated that air concentrations of CO from aircraft engines at the point of exit were in the range of 130-195 ppm (Lozano 1968). As such, air CO concentrations from 10-500 ppm were simulated, while dose time was held at 30 minutes and 32% workload were held constant (Figure 21. The results of these simulations indicated that concentrations above 50 ppm were required to achieve at least 3% COHb at the indicated conditions, while concentrations greater than 200 ppm were required to achieve at least 5% COHb. Peak COHb percentage was 0.3% for 10 ppm exposures and 10.7% for 500 ppm exposures.

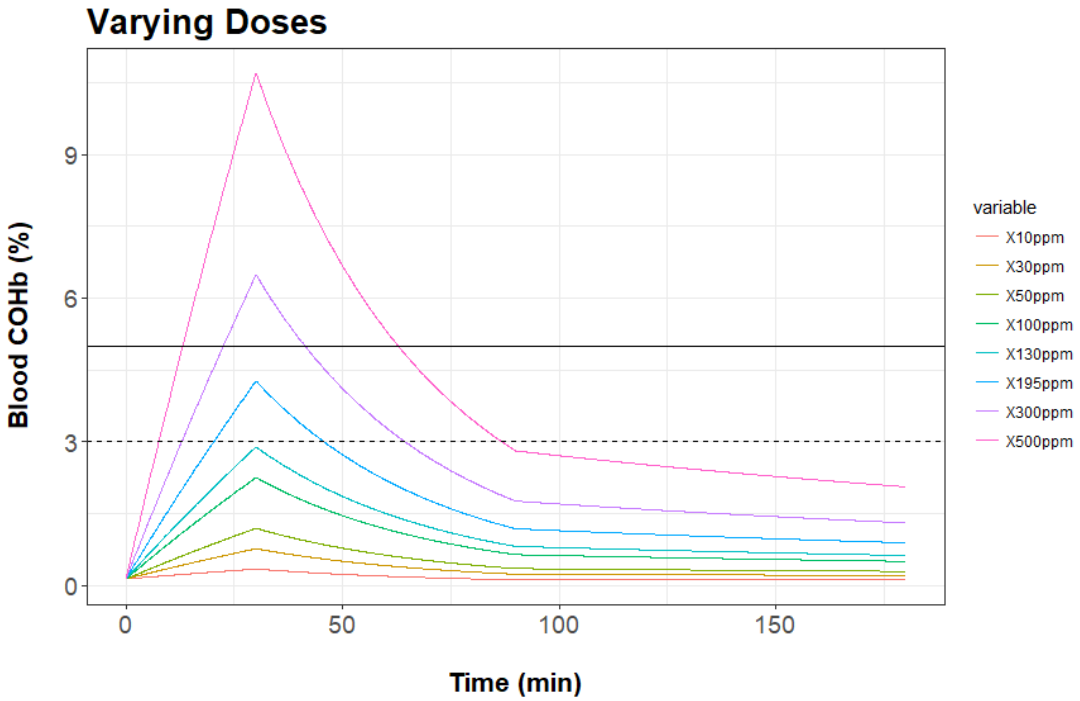

Figure 21. %COHb versus time for varying CO concentrations. Exposure time of 30 minutes and workload of 32%

Varying Exposure Times

Another consideration in this analysis is the potential for pilots to be exposed to CO from aircraft exhaust for varying amounts of time dependent on how long they are idling while waiting to launch. As shown in Figure 22, this set of simulations explored exposures of 15-60 minutes in length. At 50 ppm and 32% workload, not even 60-minute exposures approach %COHb > 3%.

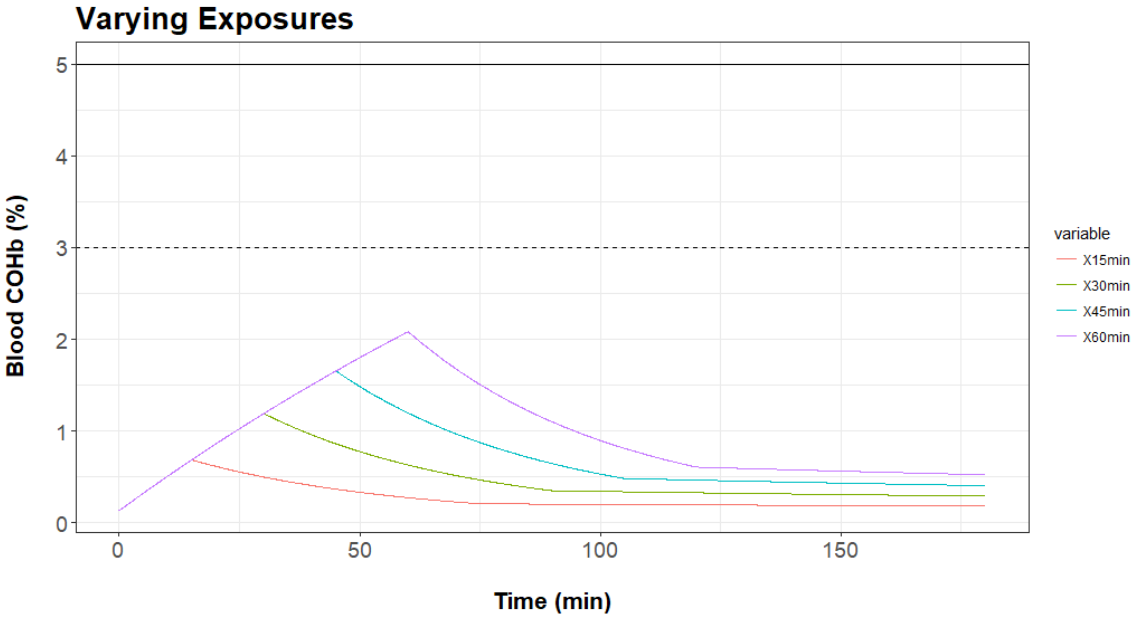

Figure 22. %COHb versus time for varying exposure times. CO concentration of 50 ppm and workload of 32%

Varying Workload

Additionally, simulations were run by varying the workload of a virtual individual exposed to CO. In this investigation (Figure 23), individuals were simulated at rest, at the equivalent of light work, and at the equivalent of heavy work, representing 12%, 32% and 64% of maximal workload respectively. For each different workload level, the tidal volume, physiological dead space, respiratory rate, workload, and diffusing capacity of the lungs for CO were modified according to Table 8 to simulate lung physiology under those levels of work. For 30-minute exposure to 50 ppm CO, even a simulated heavy workload did not reach 2% COHb.

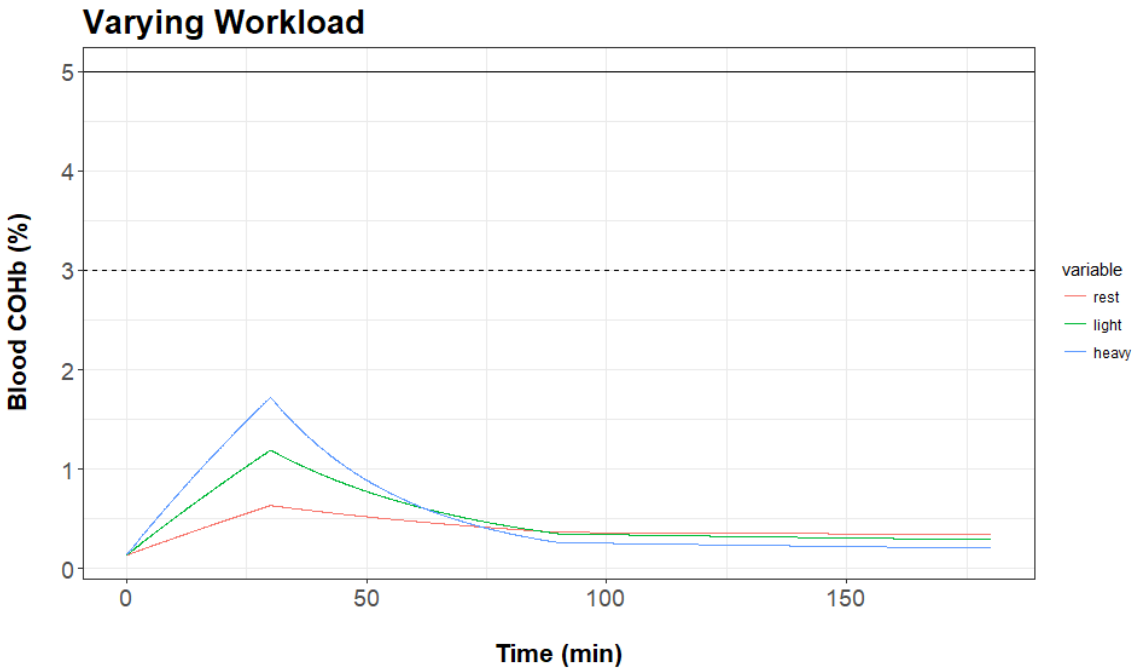

Figure 23. %COHb versus time for varying pilot workload. CO concentration of 50 ppm and exposure time of 30 minutes

Monte Carlo (MC) Simulations

Finally, MC simulations were performed to understand what percentage of a population of 1000 virtual pilots with exposures to CO at 50 or 100 ppm would reach the %COHb thresholds of 3% or 5% after those exposures. The parameters varied and their distributions are summarized in Table 9. Ultimately, of the 1000 simulated exposures, none resulted in %COHb > 3% (max: 1.77%). Figure 24 shows the mean and 95% confidence interval of the concentration-time profiles of the simulated individuals.

Table 9. Monte Carlo Simulation Parameters

		Prior				Simulated (n = 1000)			
Parameter	Distribution	Mean	SD	Min	Max	Mean	SD	Min	Max
Age (y)	Normal	25	5	18	34	25.6	3.9	18	34
Bodyweight (kg)	Normal	75	10	50	120	74.8	9.9	51.5	103.8
Height (cm)	Normal	174.4	10	156	192	174.2	8.1	156.2	191.9
Workload (% max)	Normal	32	5	8	64	31.9	5	16.2	47.9
Inhalation time (min)	Uniform	-	-	15	60	37.2	1.3	15	59
Sex (M/F)	Binomial	-	-	-	-	-	-	-	-

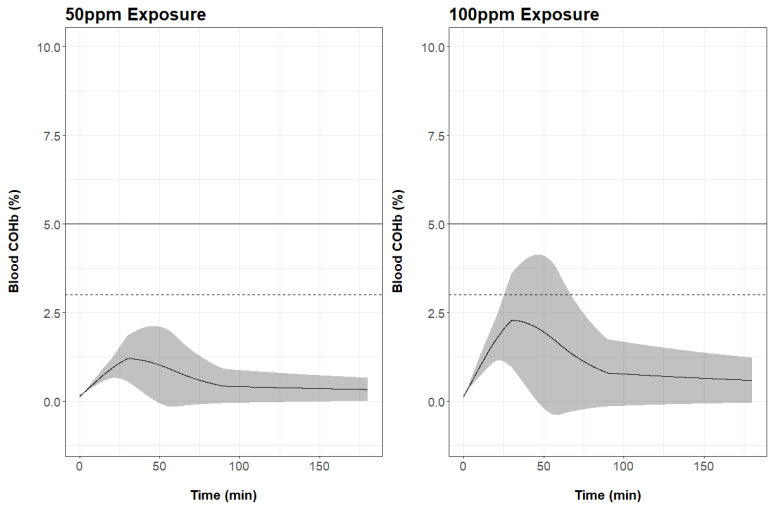

Figure 24. Monte Carlo simulations of a virtual population of 1000 pilots exposed to CO. CO exposure concentration include 50, 100. Mean %COHb is represented by the black curve, while the grey shaded area represents the mean ± (3 * SD) in each simulation. Horizontal dotted lines demarcate the theoretical subtle cognitive effect threshold (%COHb = 3%) while horizontal solid lines indicate the demonstrated subtle cognitive effect threshold (%COHb = 5%).

4.5 Discussion

The toxicokinetic model utilized in this analysis was heavily adapted from that of Gosselin *et al*. 2009. Because only minor numerical changes were made to this model which had been previously validated, this investigation does not include any additional validation. Instead, the intent of this investigation was to utilize this model to simulate a number of situations of interest. In particular, there was a desire to understand the extent to which a pilot idling on a runway waiting for takeoff may be exposed to CO, and to anticipate if and how those exposures could affect a pilot's performance during the subsequent flight.

The first consideration in this scenario is the exposure to CO from engines of a plane positioned anterior to the pilot in a flight line. Lozano *et al*. measured a mean CO concentration of 130 and 195 ppm from air ejected from two types of older, idling aircraft engines (J-57 and TF-33 respectively) with JP-4 aircraft fuel. However, preliminary readings collected from more recent engines (data not shown) indicate that the content of CO in air that reaches pilots waiting in flight lines may be closer to 30-50 ppm. Additionally, there was little information available regarding the amount of time that pilots were waiting on the runway prior to takeoff. Finally, it seems likely that there would be some variation in the workload experienced by a pilot waiting for launch (Grassmann 2016). In their paper, Gosselin *et al*. use a workload of 12% of maximal to indicate an individual at rest while 64% of maximal was used for an individual doing heavy exercise. A workload of 32% maximal is used for light exercise and generally where most pilots awaiting takeoff may be expected to fall. Therefore, this investigation focused on how increased air concentration, length of exposure, and workload affects the %COHb in the human body.

In particular, the focus was on determining whether variations in those and other factors could reasonably result in %COHb > 3% or 5%, in turn manifesting subtle cognitive deficits. As mentioned previously, these chosen %COHb thresholds for subtle cognitive effects are still under some debate. Nonetheless, there is expert opinion that the conservative estimate of 3%

COHb may be sufficient to result in small deficits in cognitive ability and reasoning while there is some equivocal evidence supporting 5% COHb leading to these subtle effects (Hawkins 2017). As such, these cutoffs were selected for consideration in this analysis. Particularly, while %COHb less than those thresholds can be reasonably ruled out for leading to subtle cognitive deficits, %COHb greater than those thresholds simply suggest that cognitive deficits cannot be ruled out.

In simulations with discretely varied quantities, it was demonstrated that exposures to CO with air concentrations < 100 ppm were exceptionally unlikely to reach the 3% COHb threshold for potential subtle cognitive effects, even when exposures lasted 60 minutes or the pilot was under heavy workload conditions. Indeed, air concentrations of about 150 ppm (130-195 ppm) were required to result in %COHb levels transiently achieving the 3% threshold, and even 30-minute exposures to 500 ppm CO air would be expected to return to below the 3% threshold before the end of a 60-minute flight (Peak = 10.7%).

MC simulations demonstrated similar trends. Specifically, two MC simulations (n = 1000 replicates) were performed, one with an air CO concentration of 50 ppm and one with a concentration of 100 ppm. The MC simulation at 50 ppm indicated that, at that air concentration, no %COHb > 3% would be expected. Thus, if the air concentrations that pilots are exposed to is ≤ 50 ppm, then no subtle cognitive effects would be expected. Conversely, if pilots are actually exposed to 100 ppm, MC simulations indicated that ~15% of scenarios would result in individuals reaching peak %COHb > 3% (though still none with peaks > 5%).

Ultimately, it can be concluded at exposures of ≤ 50 ppm, it is exceptionally unlikely that CO is leading to any subtle cognitive effects in pilots. However, if air concentrations are closer to 100 ppm, then the influence of CO exposure on cognition cannot be entirely ruled out.

5.0 CONCLUSION

Direct measurements of pilot breathing air during ground engine runs revealed that most chemicals rarely or never exceeded an OEL; however, NO_2 and NO frequently exceeded the MIL-STD 3050 maximum allowable concentrations in pilot breathing air in both incident and non-incident aircraft. Pilot breathing air was dryer than cockpit air, trending inversely with increases in O_2. The O_2 concentration was heavily dependent on the engine run phase for breathing air, but the cockpit air was unaffected by the engine run phase. Total VOCs rarely exceeded the OEL, and the most frequently detected VOCs included acetone, ethanol, and toluene. CO at concentrations observed in the cockpit and pilot breathing air were not present at concentrations likely to result in cognitive deficits due to CO binding to hemoglobin based on a toxicokinetic simulation.

There are several limitations to these studies. First, they were focused on ground-based exposures, which may not be representative of contaminants present during flight. Second, the flowrates of air drawn from the O_2 system by the OAGr were much lower than would be drawn by a pilot breathing on the system. Third, electrochemical sensors used for combustion gases are sensitive to temperature and RH, producing false positive response at temperatures > 35°C and potentially false negatives at RH < 15% if they dry out during the test. Further, chemicals can produce toxicity through synergistic and additive effects, and OELs developed to protect the typical workforce may not be applicable during high performance flight operations. Therefore, future research will focus on drawing larger volumes during ground-based measurements, measuring chemical contaminants during flight operations, as well as on developing and applying more advanced toxicokinetic simulations that evaluate the impact of chemical contaminant mixtures on pilot performance characteristics using physiological parameters representative of high-performance flight.

6.0 REFERENCES

ACGIH® (2019*) TLVs® and BEIs® Based on the Documentation of the Threshold Limit Values for Chemical Substances and Physical Agents & Biological Exposure Indices*. Cincinnati, Ohio: American Conference of Governmental Industrial Hygienists.

Air Education and Training Command (2018a) *19th Air Force Commander Directs T-6 Operational Pause*. Joint Base San Antonio-Randolph. Available at: https://www.aetc.af.mil/News/Article/1429270/19th-air-force-commander-directs-t-6-operational-pause/

Air Education and Training Command (2018b) *T-6 Operational Pause Lifted Today*. Joint Base San Antonio, Texas. Available at: https://www.aetc.af.mil/News/Article/1452516/t-6-operational-pause-lifted-today/

Archsmith, J., Heyes, A., & Saberian, S. (2017). *Air quality and error quantity: Pollution and performance in a high-skilled, quality-focused occupation* (SSRN Scholarly Paper ID 2683656). Social Science Research Network. https://papers.ssrn.com/abstract=2683656

Barn, P., Giles, L., Héroux, M.-E., & Kosatsky, T. (2018a). A review of the experimental evidence on the toxicokinetics of carbon monoxide: The potential role of pathophysiology among susceptible groups. *Environmental Health: A Global Access Science Source*, *17*(1), 13. https://doi.org/10.1186/s12940-018-0357-2

Beard, R. R., & Wertheim, G. A. (1967a). Behavioral impairment associated with small doses of carbon monoxide. *American Journal of Public Health and the Nation's Health*, *57*(11), 2012–2022. https://doi.org/10.2105/ajph.57.11.2012

Benignus, V. A., Hazucha, M. J., Smith, M. V., & Bromberg, P. A. (1994). Prediction of carboxyhemoglobin formation due to transient exposure to carbon monoxide. *Journal of Applied Physiology (Bethesda, Md.: 1985)*, *76*(4), 1739–1745. https://doi.org/10.1152/jappl.1994.76.4.1739

Bruce, E. N., & Bruce, M. C. (2003a). A multicompartment model of carboxyhemoglobin and carboxymyoglobin responses to inhalation of carbon monoxide. *Journal of Applied Physiology (Bethesda, Md.: 1985)*, *95*(3), 1235–1247. https://doi.org/10.1152/japplphysiol.00217.2003

CDC (2018). *Immediately dangerous to life or health concentrations (IDLH): Carbon monoxide—NIOSH publications and products*. https://www.cdc.gov/niosh/idlh/630080.html

Coburn, R. F., Forster, R. E., & Kane, P. B. (1965a). Considerations of the physiological variables that determine the blood carboxyhemoglobin concentration in man. *The Journal of Clinical Investigation*, *44*(11), 1899–1910. https://doi.org/10.1172/JCI105296

Coburn, R. F., Forster, R. E., & Kane, P. B. (1965b). Considerations of the physiological variables that determine the blood carboxyhemoglobin concentration in man. *The Journal of Clinical Investigation*, *44*(11), 1899–1910. https://doi.org/10.1172/JCI105296

Dahms, T. E., Younis, L. T., Wiens, R. D., Zarnegar, S., Byers, S. L., & Chaitman, B. R. (1993a). Effects of carbon monoxide exposure in patients with documented cardiac arrhythmias. *Journal of the American College of Cardiology*, *21*(2), 442–450. https://doi.org/10.1016/0735-1097(93)90687-v

Denola, G., Hanhela, P., and Mazurek, W. (2011) 'Determination of Tricreysl Phosphate Air Contamination in Aircraft', *Ann. Occup. Hyg.* 55 (7) pp. 710-722. https://doi.org/10.1093/annhyg/mer040

Department of Defense (2015) *Department of Defense Design Criteria Standard: Aircraft Crew Breathing Systems Using On-Board Oxygen Generating System (OBOGS)*. MIL-STD-3050.

Lt Col Elliott, J.J. & Maj Schmitt, D.R. (2019). Unexplained Physiological Episodes A Pilot's Perspective. *AIR & SPACE POWER JOURNAL*, 15–32. Available from: https://www.airuniversity.af.edu/Portals/10/ASPJ/journals/Volume-33_Issue-3/F-Elliott_Schmitt.pdf

Everstine, B.W. (2018). *Investigation into Root Cause of A-10 Physiological Incident Ongoing.* Air Force Magazine. Available from: https://www.airforcemag.com/investigation-into-root-cause-of-a-10-physiological-incident-ongoing/. Updated Jan 22, 2018, Accessed May 31, 2020.

Gordge, D. N. (1993) *In-Flight Measurement of Aircrew Breathing in Navy Aircraft*. AD-A271 811.

Gosselin, N. H., Brunet, R. C., & Carrier, G. (2009a). Determination of carboxyhaemoglobin in humans following low-level exposures to carbon monoxide. *Inhalation Toxicology*, *21*(13), 1077–1091. https://doi.org/10.3109/08958370902744848

Grassmann, M., Vlemincx, E., von Leupoldt, A., Mittelstädt, J. M., & Van den Bergh, O. (2016). Respiratory changes in response to cognitive load: A systematic review. *Neural Plasticity*, *2016*, 8146809. https://doi.org/10.1155/2016/8146809

Hanhela, P., Kibby, J., DeNola, G., and Mazurek, W. (2005) *Organophosphate and Amine Contamination of cockpit Air the Hawk, F-111, and Hercules C-130*. Defence Science and Technology Organization (DTSO): Fishermans Bend, Victoria, Australia. https://apps.dtic.mil/sti/pdfs/ADA448000.pdf

Hawkins, F. H., & Orlady, H. W. (2006). *Human factors in flight* (2. ed., reprint). Ashgate.

Hill, E. P., Hill, J. R., Power, G. G., & Longo, L. D. (1977). Carbon monoxide exchanges between the human fetus and mother: A mathematical model. *The American Journal of Physiology*, *232*(3), H311-323. https://doi.org/10.1152/ajpheart.1977.232.3.H311

Honeywell International Inc. (2008) On-Board Oxygen Generation Systems (OBOGS). http://www.f-16.net/forum/download/file.php?id=24831

Kizakevich, P. N., McCartney, M. L., Hazucha, M. J., Sleet, L. H., Jochem, W. J., Hackney, A. C., & Bolick, K. (2000a). Noninvasive ambulatory assessment of cardiac function in healthy men exposed to carbon monoxide during upper and lower body exercise. *European Journal of Applied Physiology*, *83*(1), 7–16. https://doi.org/10.1007/s004210000256

Kuuluvainen, H., Rönkkö, T., Järvinen, A., Saari, S., Karjalainen, P., Lähde, T., Pirjola, L., Niemi, J. V., Hillamo, R., & Keskinen, J. (2016). Lung deposited surface area size distributions of particulate matter in different urban areas. *Atmospheric Environment*, *136*, 105–113. https://doi.org/10.1016/j.atmosenv.2016.04.019

Lee, S., Poon, C., Li, X., and Luk, F. (1999) 'Indoor Air Quality Investigation on Commercial Aircraft', *Indoor Air* 9 pp. 180-187. https://doi.org/10.1111/j.1600-0668.1999.t01-1-00004.x

Levels, N. R. C. (US) C. on A. E. G. (2010). *Carbon monoxide acute exposure guideline levels*. National Academies Press (US). https://www.ncbi.nlm.nih.gov/books/NBK220007/

Lozano, E. R., Melvin, W. W., & Hochheiser, S. (1968). Air pollution emissions from aircraft engines. *Journal of the Air Pollution Control Association*, *18*(6), 392–394. https://doi.org/10.1080/00022470.1968.10469144

Luomanmäki, K., & Coburn, R. F. (1969). Effects of metabolism and distribution of carbon monoxide on blood and body stores. *The American Journal of Physiology*, *217*(2), 354–363. https://doi.org/10.1152/ajplegacy.1969.217.2.354

Michaelis, S. (2016) 'Oil Bearing Seals and Aircraft Cabin Air Contamination', *Sealing Technology*, April 2016, pp. 7-10. https://doi.org/10.1016/S1350-4789%2818%2930144-2

National Research Council. 2002. *The Airliner Cabin Environment and the Health of Passengers and Crew*. Washington, DC: The National Academies Press. https://doi.org/10.17226/10238.

Peterson, J. E., & Stewart, R. D. (1975). Predicting the carboxyhemoglobin levels resulting from carbon monoxide exposures. *Journal of Applied Physiology*, *39*(4), 633–638. https://doi.org/10.1152/jappl.1975.39.4.633

Raub, J. A., & Benignus, V. A. (2002a). Carbon monoxide and the nervous system. *Neuroscience and Biobehavioral Reviews*, *26*(8), 925–940. https://doi.org/10.1016/s0149-7634(03)00002-2

Rosenberger, W. (2018) 'Effect of charcoal equipped HEPA filters on cabin air quality in aircraft. A case study including smell event related in-flight measurements', *Building and Environment* 143 pp. 358-365. https://doi.org/10.1016/B978-0-323-54696-6.00047-1

Sheps, D. S., Herbst, M. C., Hinderliter, A. L., Adams, K. F., Ekelund, L. G., O'Neil, J. J., Goldstein, G. M., Bromberg, P. A., Ballenger, M., & Davis, S. M. (1991a). Effects of 4 percent and 6 percent carboxyhemoglobin on arrhythmia production in patients with coronary artery disease. *Research Report (Health Effects Institute)*, *41*, 1–46; discussion 47-58. https://doi.org/10.1056/NEJM198911233212102

Sheps, D. S., Herbst, M. C., Hinderliter, A. L., Adams, K. F., Ekelund, L. G., O'Neil, J. J., Goldstein, G. M., Bromberg, P. A., Dalton, J. L., & Ballenger, M. N. (1990a). Production of arrhythmias by elevated carboxyhemoglobin in patients with coronary artery disease. *Annals of Internal Medicine*, *113*(5), 343–351. https://doi.org/10.7326/0003-4819-113-5-343

Smith, M. V., Hazucha, M. J., Benignus, V. A., & Bromberg, P. A. (1994). Effect of regional circulation patterns on observed HbCO levels. *Journal of Applied Physiology (Bethesda, Md.: 1985)*, *77*(4), 1659–1665. https://doi.org/10.1152/jappl.1994.77.4.1659

Stewart, R. D. (1975a). The effect of carbon monoxide on humans. *Annual Review of Pharmacology*, *15*, 409–423. https://doi.org/10.1146/annurev.pa.15.040175.002205

Stewart, R. D. (1975b). The effect of carbon monoxide on humans. *Annual Review of Pharmacology*, *15*, 409–423. https://doi.org/10.1146/annurev.pa.15.040175.002205

Stewart, R. D., Peterson, J. E., Baretta, E. D., Bachand, R. T., Hosko, M. J., & Herrmann, A. A. (1970a). Experimental human exposure to carbon monoxide. *Archives of Environmental Health*, *21*(2), 154–164. https://doi.org/10.1080/00039896.1970.10667214

Thongplang, J. (23 Jul 2018). The challenges with electrochemical NO_2 sensors in outdoor air monitoring. Available at: https://www.aeroqual.com/challenges-electrochemical-no2-sensors-outdoor-air-monitoring

U.S. Environmental Protection Agency. (2010). *Quantitative Risk and Exposure Assessment for Carbon Monoxide—Amended*.

United States Air Force (2015) 'A-10 Thunderbolt II' Available at: https://www.af.mil/About-Us/Fact-Sheets/Display/Article/104490/a-10-thunderbolt-ii/

United States Air Force Scientific Advisory Board (2012) *Aircraft Oxygen Generation* SAB-TR-11-04. Distribution Level: A.

United States Air Force Scientific Advisory Board. (2012). *Report on Aircraft Oxygen Generation* (SAB-TR-11-04). https://www.airforcemag.com/PDF/DocumentFile/Documents/2012/AFSAB_Oxygen_020112.pdf

US EPA, O. (2016, July 6). *Basic information about no2* [Overviews and Factsheets]. US EPA. https://www.epa.gov/no2-pollution/basic-information-about-no2

Valentin, J. (2002). Basic anatomical and physiological data for use in radiological protection: Reference values: ICRP Publication 89: Approved by the Commission in September 2001. *Annals of the ICRP*, *32*(3–4), 1–277. https://doi.org/10.1016/S0146-6453(03)00002-2

van Netten, C., and Leung, V. (2000) 'Comparison of the Constituents of Two Aircraft Engine Lubricating Oils and their Volatile Pyrolytic Degradation Products', *Applied Occupational and Environmental Hygiene* 15 pp. 277-283. https://doi.org/10.1080/104732200301593

Waters, M., Bloom, T., Grajewski, B., and Deddens, J. (2002) 'Measurements of Indoor Air Quality on Commercial Transport Aircraft', Proceedings I 9th *Conference on Indoor Air Quality and Climate*, Monterey, California, 30 June – 5 July, 2002, pp. 782-787. https://doi.org/10.1243/095440803322611688

APPENDIX A. A-10 PILOT BREATHING AIR SYSTEMS

The A-10 Thunderbird II, often called the Warthog, is a sub-sonic, single-seat ground attack aircraft with a range of 2580 miles that can loiter over a battlefield for long periods to provide support to ground forces (USAF, 2015). It is powered by two General Electric TF34-GF turbofan engines.

Most A-10s are equipped with the OBOGS to supply pilot breathing air. The OBOGS uses two zeolite beds to remove atmospheric molecular nitrogen gas (N_2) from bleed air taken from the aircraft engine's compressor. The bleed air passes through a 0.6 µm filter to remove particulates prior to reaching the OBOGS. Removal of the N_2 concentrates O_2 in the air supply. The other major component of the supplied breathing air is argon. The OBOGS contains two zeolite beds, so that as one bed becomes saturated with N_2, the system switches to the other bed while the first bed is purged of N_2 (Honeywell, 2008). In the A-10, the OBOGS regulator settings can be changed with respect to O_2 concentration (normal or 100%) and pressure (normal or maximum).

Some A-10s are equipped with a LOX system. Like the OBOGS regulator, the LOX regulator settings for LOX O_2 (normal or 100%) and pressure (normal or emergency) can be modified. The primary difference with the LOX system is the storage of liquid oxygen on the aircraft, rather than using a zeolite bed for generating oxygen.

APPENDIX B. OELS FOR COMPOUNDS MEASURED

Table B1. Occupational Exposure Limits for Partial Combustion Gases and Detected VOCs

	Concentration (ppm)									
	MIL-STD 3050[2]		NIOSH RELS		OSHA PELs		ACGIH TLVs		Explicit Ceiling Limits[6]	
Chemical	Outlet[3]	Inlet[4]	TWA[5]	STEL[6]	TWA[7]	STEL[6]	TWA[7]	STEL[6]	Value	Source
CO_2	500	5000	5000	30000	500	-	5000	30000	-	N/A
CO	10	50	35	200	50	-	25	-	200	NIOSH
NO_2	0.1[a]	5[a]	-	1	-	5	0.2	-	5	OSHA
NO	0.1[a]	5[a]	25	-	25	-	25	-	-	N/A
SO_2	-	-	2	5	5	-	-	0.25	-	N/A
Acetone	-	-	250	-	1000	-	250	500	-	N/A
Acrolein	-	-	0.1	0.3	0.1	-	-	0.1	0.1	ACGIH
Benzene	-	-	-	1	1	5	0.5	2.5	-	N/A
1,3-Butadiene	-	-	-	-	1	5	2	-	-	N/A
Cyclohexane	-	-	300	-	300	-	300	-	-	N/A
1,4-Dioxane	-	-	-	1[b]	100	-	20	-	1	NIOSH
Ethanol	500	1000	1000		1000	-	-	1000	-	N/A
4-Ethyltolune[1]	-	-	-	-	-	-	-	-	-	N/A
n-Hexane	-	-	50	-	500	-	50	-	-	N/A
Isopropyl alcohol	-	-	400	500	400	-	200	400	-	N/A
Methylene chloride	-	-	-	-	25	125	50	-	-	N/A
Methyl ethyl ketone	-	-	-	0.2	-	-	-	0.2	0.2	ACGIH
Propene	-	-	-	-	-	-	500	-	-	N/A
Styrene	-	-	50	100	100	200	20	40	200	OSHA
Toluene	-	-	100	150	200	300	20	-	300	OSHA

[1]No OELs were found for 4-ethyltoluene

[2]OELs from MIL-STD 3050 are maximum allowable concentrations (Department of Defense, 2015)

[3]Product gas from OBOGS

[4]Source gas to OBOGS, which is the same air introduced into the cockpit

[5]Time-Weighted Average for a 10-hour workday and 40-hour work week

[6]Short-Term Exposure Limit, usually for a 15-minute period; [b]In this instance the STEL is for a 30-minute period

[7]Time-Weighted Average for an 8-hour workday and 40-hour work week

[8]In the absence of an explicit ceiling limit, the ACGIH 8-hour TWA is multiplied by five (3/5 Rule, ACGIH, 2019)

[a]MIL-STD 3050 is for Nitrogen Oxides (NO_x)

APPENDIX C. ENGINE RUN REAL-TIME DATA SUMMARY

Table C1 contains summary statistics and, where relevant, percentage of observations exceeding OELs for the real-time data, subdivided by the air source (cabin or pilot breathing air) and engine/throttle settings. Data collected when there was a noted sensor malfunction was not included in the summary statistic calculations. Additionally, data was examined for physically unrealistic values such as negative flow in the breathing air system and O_2 or CO_2 values of 0. These values indicated a sensor reset and are usually followed by about a minute of inaccurate data. These values were excluded from the summary statistics.

Table C1. Summary Statistics for O_2 and Airflow Characteristics by Engine Run Phase

Endpoint	Air Source	Engine Setting [2]	Mean	Std. Dev.	Minimum-Maximum	Observations
O_2 (%)	Cockpit	I/100%/N	21.2	0.3	19.9 - 23.7	24569
		I/N/N	21.3	0.6	16.3 - 31.1	29434
		85%/N/N	21.3	0.4	20.3 - 22.9	19074
		85%/100%/E	21.6	0.7	20 - 25.4	21613
	OBOGS /LOX	I/100%/N	57.1	12.3	19.3 - 88.1	28564
		I/N/N	46.7	12.0	18.3 - 90.3	34088
		85%/N/N	46.4	9.1	27.6 - 72.4	22488
		85%/100%/E	76.3	10.2	33.3 - 92	23906
Volumetric Flow Rate (L/min) [1]	OBOGS /LOX	I/100%/N	4.7	1.9	0.4 - 7.2	19560
		I/N/N	4.4	2.2	0 - 7.5	42218
		85%/N/N	4.7	1.9	0.2 - 8.8	12455
		85%/100%/E	4.7	2.4	0.2 - 8.3	14740
Temperature (°C)	Cockpit	I/100%/N	25.7	5.0	16.5 - 34.1	24707
		I/N/N	29.1	4.6	0 - 36	29638
		85%/N/N	29.4	4.2	21.7 - 34.9	19074
		85%/100%/E	30.1	3.5	24.5 - 35.7	21613
	OBOGS /LOX	I/100%/N	26.2	4.8	16.5 - 33.8	28702
		I/N/N	29.9	4.6	0 - 37.2	34261
		85%/N/N	30.3	4.2	22.9 - 35.6	22488
		85%/100%/E	31.1	3.6	25.1 - 36.9	23906
RH (%)	Cockpit	I/100%/N	14.5	4.7	8 - 23	24707
		I/N/N	12.2	3.7	0 - 21	29638
		85%/N/N	12.1	3.6	8 - 19	19074
		85%/100%/E	11.1	3.0	7 - 17	21613
	OBOGS /LOX	I/100%/N	4.7	3.7	0 - 17	28702
		I/N/N	4.3	2.9	0 - 12	34261
		85%/N/N	5.4	2.9	1 - 11	22488
		85%/100%/E	1.5	1.9	0 - 10	23906

[1]Volumetric flow data was collected only from the pilot breathing air flow path

[2]Engine/Oxygen/Regulator Settings: I = Idle, N = Normal, E = Emergency

Table C2. Summary Statistics for Chemical Contaminants by Engine Run Test Phase

Endpoint	Air Source	Engine Setting [2]	Mean	Std. Dev.	Minimum-Maximum	Observations	% > OEL[3,4]
CO_2 (ppm)	Cockpit	I/100%/N	311.4	42.8	292 - 811	24707	0.0
		I/N/N	302.6	24.1	292 - 498	29220	0.0
		85%/N/N	302.3	27.9	292 - 553	19074	0.0
		85%/100%/E	308.0	40.3	292 - 646	21613	0.0
	OBOGS /LOX	I/100%/N	300.8	4.1	279 - 324	28702	0.0
		I/N/N	300.4	3.8	279 - 324	34235	0.0
		85%/N/N	300.0	4.2	276 - 319	22488	0.0
		85%/100%/E	300.7	3.0	281 - 319	23906	0.0
CO (ppm)	Cockpit	I/100%/N	0.7	0.7	0 - 5	24707	0.0
		I/N/N	0.3	0.4	0 - 7.7	29638	0.0
		85%/N/N	0.2	0.3	0 - 2.4	19074	0.0
		85%/100%/E	0.1	0.4	0 - 3	21613	0.0
	OBOGS /LOX	I/100%/N	0.0	0.0	0 - 0.8	28699	0.0
		I/N/N	0.0	0.0	0 - 0.3	34261	0.0
		85%/N/N	0.0	0.0	0 - 0	22488	0.0
		85%/100%/E	0.0	0.0	0 - 0	23906	0.0
NO_2 (ppm)	Cockpit	I/100%/N	0.0	0.0	0 - 0.2	24707	0.0
		I/N/N	0.0	0.0	0 - 0.3	29638	0.0
		85%/N/N	0.0	0.0	0 - 1.1	19074	0.0
		85%/100%/E	0.0	0.0	0 - 1.3	21613	0.0
	OBOGS /LOX	I/100%/N	0.1	0.1	0 - 0.5	28702	60.0
		I/N/N	0.1	0.1	0 - 0.5	34261	50.8
		85%/N/N	0.1	0.1	0 - 0.4	22488	69.6
		85%/100%/E	0.2	0.1	0 - 0.4	23906	98.6
NO (ppm)	Cockpit	I/100%/N	0.0	0.0	0 - 0.1	24569	0.0
		I/N/N	0.0	0.0	0 - 0	29557	0.0
		85%/N/N	0.0	0.0	0 - 0	19074	0.0
		85%/100%/E	0.0	0.1	0 - 0.7	21613	0.0
	OBOGS /LOX	I/100%/N	0.0	0.0	0 - 0.1	28564	0.4
		I/N/N	0.0	0.1	0 - 0.6	34202	16.7
		85%/N/N	0.0	0.1	0 - 0.4	22488	18.1
		85%/100%/E	0.1	0.2	0 - 0.6	23906	18.1

[1]Volumetric flow data was collected only from the pilot breathing air flow path.

[2]Engine/Oxygen/Regulator Settings: I = Idle, N = Normal, E = Emergency

[3]OELs for CO_2, CO, NO, NO_2 (CO_2: 500 ppm, CO: 10 ppm, NO and NO_2: 0.1 ppm) are ceiling values from MIL-STD 3050 (Department of Defense, 2015). The OEL for total VOCs is 1 ppm, which the system control value indicated by the 711th HPW. The OEL used for SO_x is the NIOSH TWA of 2 ppm for SO_2.

Table C2 continued. Summary Statistics for Chemical Contaminants by Engine Run Test Phase

Endpoint	Air Source	Engine Setting[2]	Mean	Std. Dev.	Minimum-Maximum	# of Observations	% > OEL[3,4]
SO_x (ppm)	Cockpit	I/100%/N	0.0	0.0	0 - 0.6	24707	0.0
		I/N/N	0.0	0.1	0 - 6.8	29638	0.1
		85%/N/N	0.0	0.0	0 - 0	19074	0.0
		85%/100%/E	0.0	0.0	0 - 0.1	21613	0.0
	OBOGS /LOX	I/100%/N	0.0	0.2	0 - 11.1	28702	0.2
		I/N/N	0.0	0.3	0 - 12.4	34261	0.2
		85%/N/N	0.0	0.0	0 - 0.4	22488	0.0
		85%/100%/E	0.0	0.0	0 - 0	23906	0.0
Total VOCs (ppb)	Cockpit	I/100%/N	320.5	26.4	0 - 828.5	24476	0.0
		I/N/N	311.9	49.3	0 - 1101.9	30421	0.0
		85%/N/N	299.8	17.6	191.9 - 415.4	19074	0.0
		85%/100%/E	296.0	33.7	134.8 - 448.6	21613	0.0
	OBOGS /LOX	I/100%/N	508.3	103.2	337.3 - 753.3	28345	0.0
		I/N/N	496.1	94.5	0 - 1005.6	34261	0.0
		85%/N/N	495.9	90.4	239.9 - 775.8	22488	0.0
		85%/100%/E	458.8	60.8	259.5 - 657.6	23906	0.0
LDSA ($\mu m^2/cm^2$)	Cockpit	I/100%/N	593.9	1063.7	1.44 - 5012.81	10320	NA
		I/N/N	240.1	591.5	0.12 - 3578.63	15575	NA
		85%/N/N	157.6	460.0	0.25 - 2156.52	7604	NA
		85%/100%/E	31.1	150.2	0.17 - 1786.78	7680	NA
	OBOGS /LOX	I/100%/N	10.9	33.4	0.02 - 716.9	10320	NA
		I/N/N	34.4	90.0	0.02 - 939.84	15769	NA
		85%/N/N	37.8	111.1	0.01 - 556.08	7633	NA
		85%/100%/E	4.1	21.4	0.01 - 421.49	7680	NA

[1]Volumetric flow data was collected only from the pilot breathing air flow path.

[2]Engine/Oxygen/Regulator Settings: I = Idle, N = Normal, E = Emergency

[3]OELs for CO_2, CO, NO, NO_2 (CO_2: 500 ppm, CO: 10 ppm, NO and NO_2: 0.1 ppm) are ceiling values from MIL-STD 3050 (Department of Defense, 2015). The OEL for total VOCs is 1 ppm, which the system control value indicated by the 711th HPW. The OEL used for SO_x is the NIOSH TWA of 2 ppm for SO_2.

[4]Percentages > OEL calculated exclude the cockpit data from aircraft #43 when Makel battery in cockpit flow path failed (first three test phases).

APPENDIX D. ENGINE RUN TIME SERIES PLOTS

Time series plots for each parameter measured in real-time are included below for each engine run (1-12). Parameters measured and plotted include volumetric flow rate, T, RH, O_2, CO_2, CO, NO_2, NO, total VOCs, and UFPs (expressed as LDSA). The volumetric flow rate was only measured in the flow path sampling from pilot breathing air (OBOGS or LOX system). The remaining parameters were measured in both flow paths (cockpit and pilot breathing air system). Time series plots for SO_x are not included because the sensor reading was zero for nearly all time points during the engine runs.

Time Series Plots for Engine Run 1, Aircraft ID 32

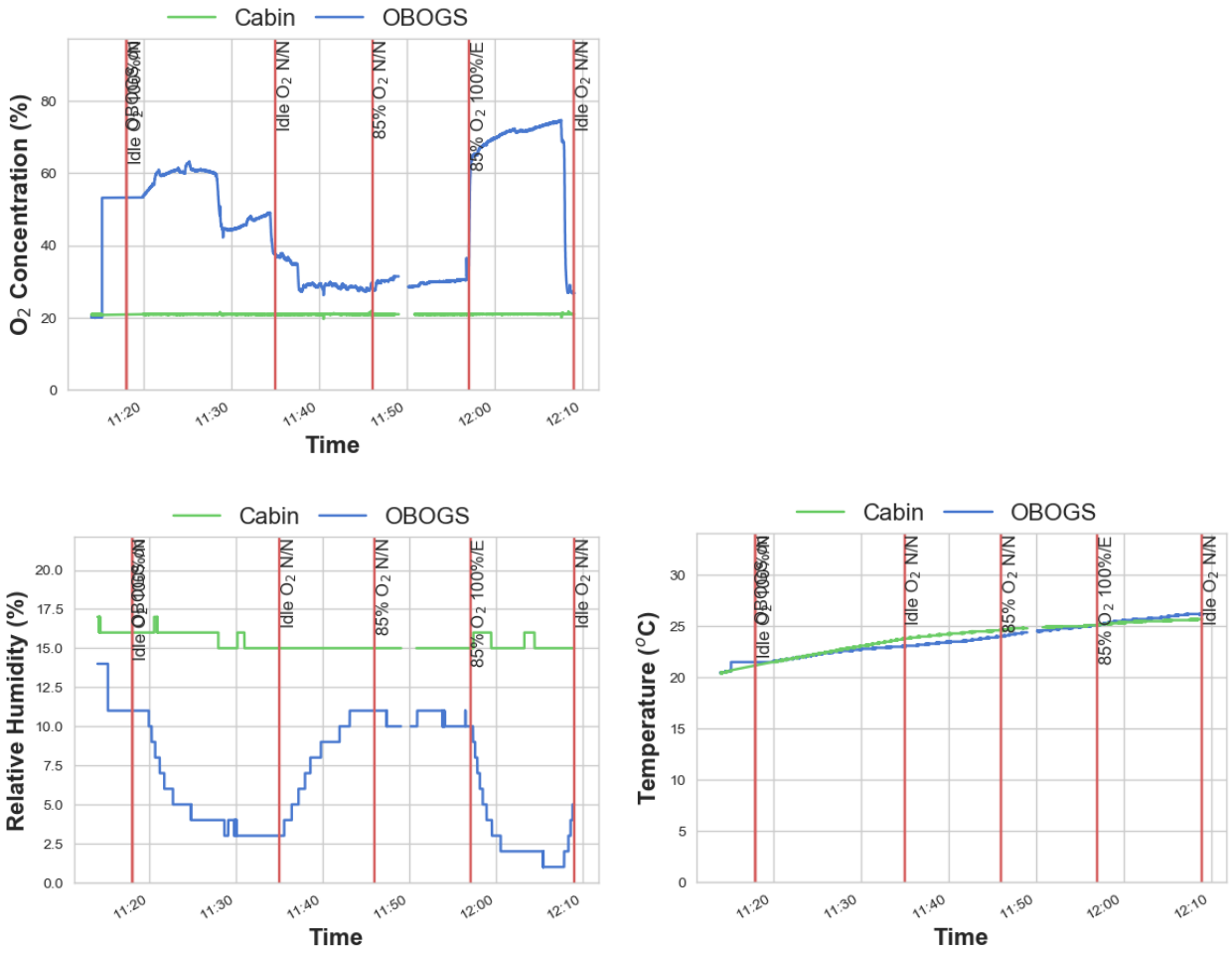

Figure D1. Time series plots for Engine Run 1, Aircraft ID 32: O_2 concentration, volumetric flowrate, relative humidity, and temperature

No volumetric flow data available for this engine run.

Time Series Plots for Engine Run 1, Aircraft ID 32 Continued

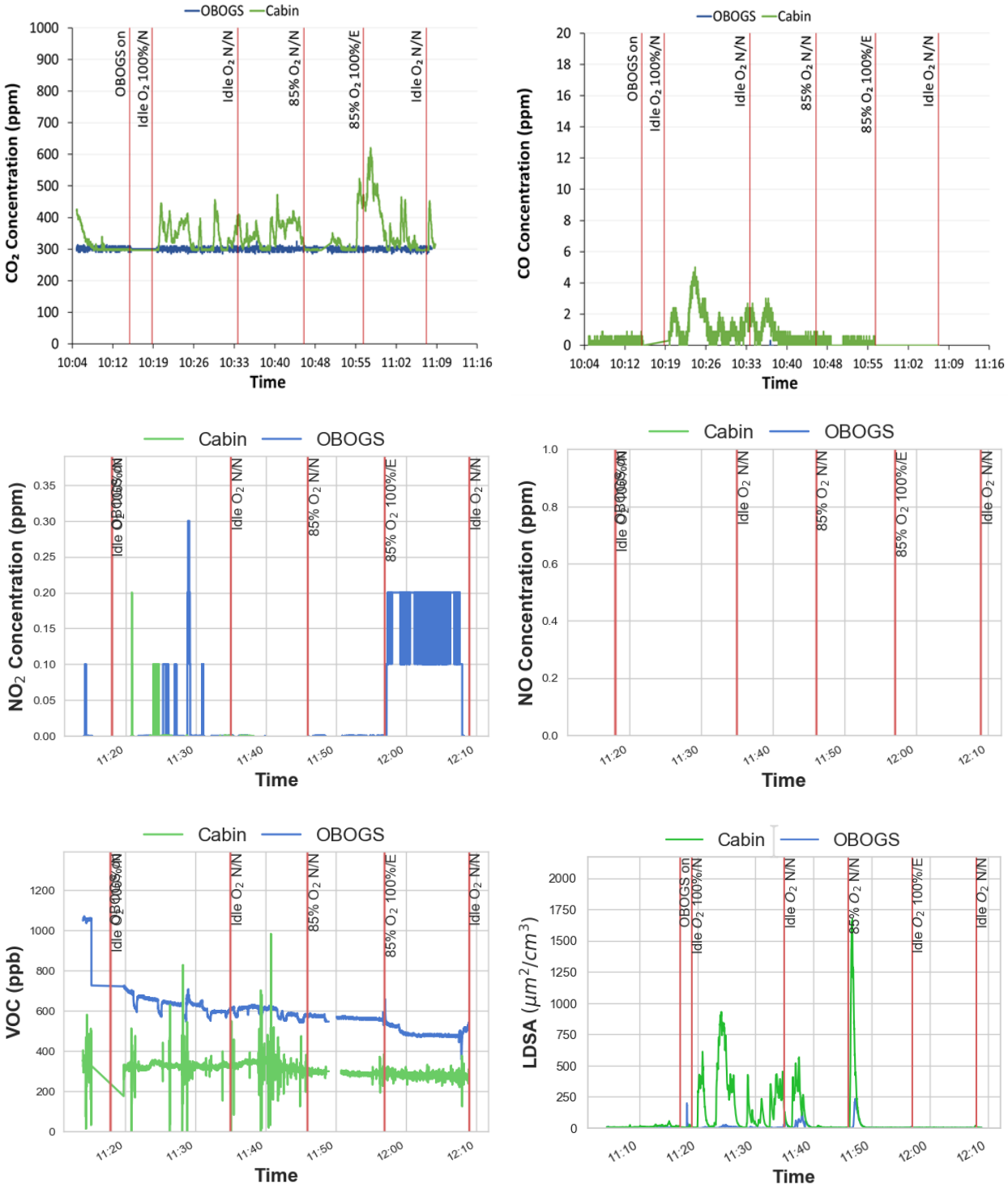

Figure D1 continued. Time series plots for Engine Run 1, Aircraft ID 32: Contaminants

Time Series Plots for Engine Run 2, Aircraft ID 33

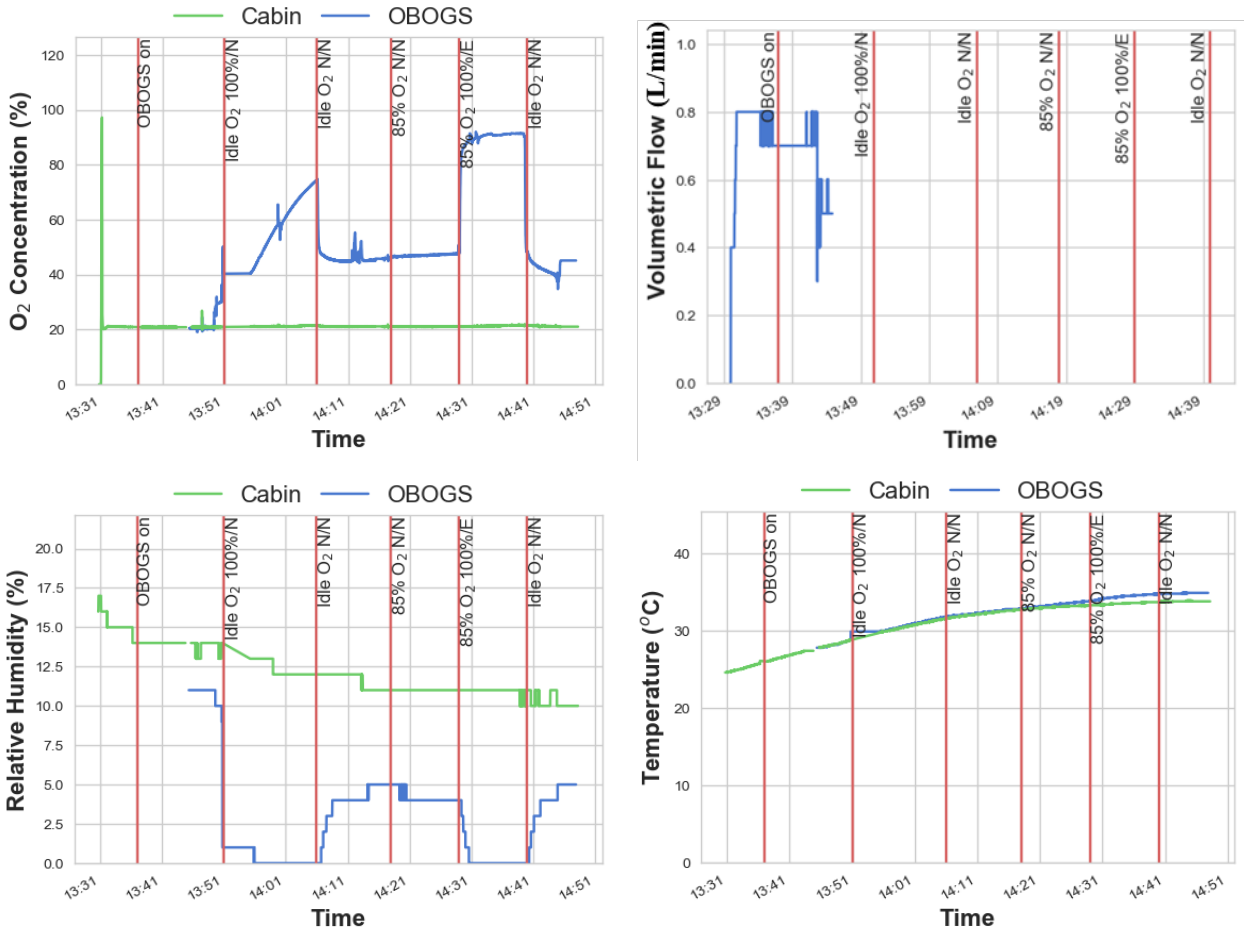

Figure D2. Time series plots for Engine Run 2, Aircraft ID 33: O_2 concentration, volumetric flowrate, relative humidity, and temperature

Time Series Plots for Engine Run 2, Aircraft ID 33 Continued

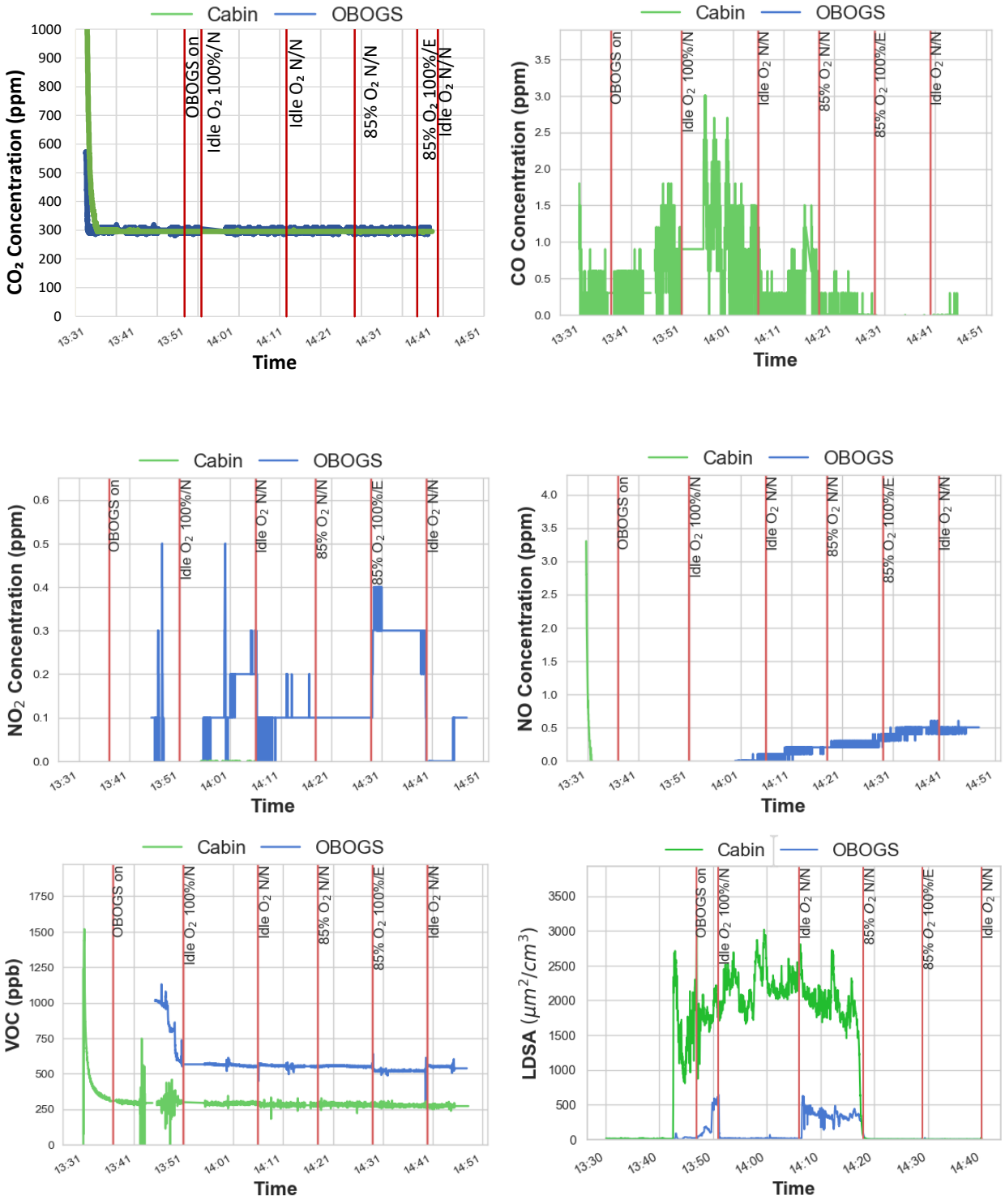

Figure D2 continued. Time series plots for Engine Run 2, Aircraft ID 33: Contaminants

Time Series Plots for Engine Run 3, Aircraft ID 34

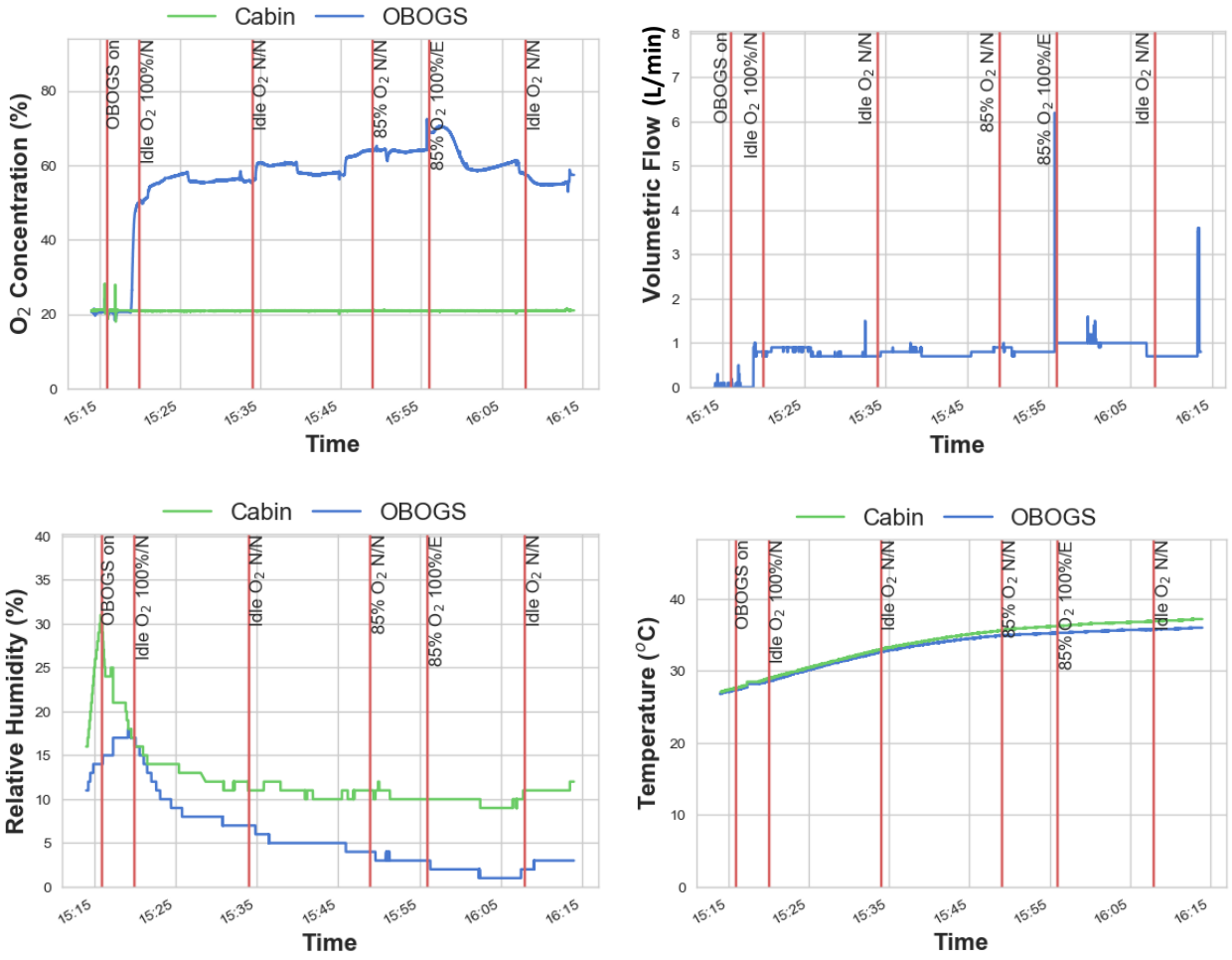

Figure D3. Time series plots for Engine Run 3, Aircraft ID 34: O_2 concentration, volumetric flowrate, relative humidity, and temperature

Time Series Plots for Engine Run 3, Aircraft ID 34 Continued

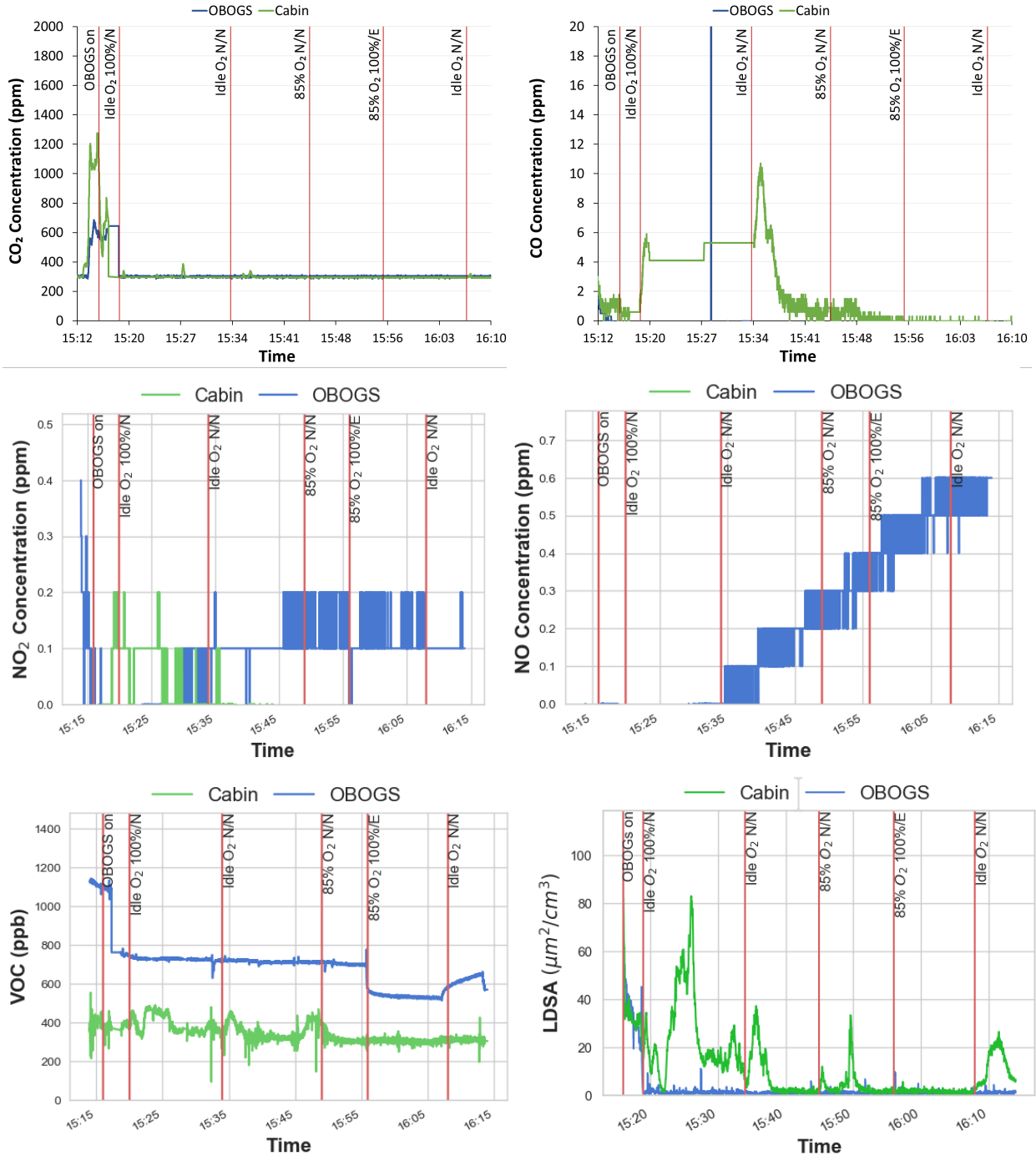

Figure D3 continued. Time series plots for Engine Run 3, Aircraft ID 34: Contaminants

Time Series Plots for Engine Run 4, Aircraft ID 35

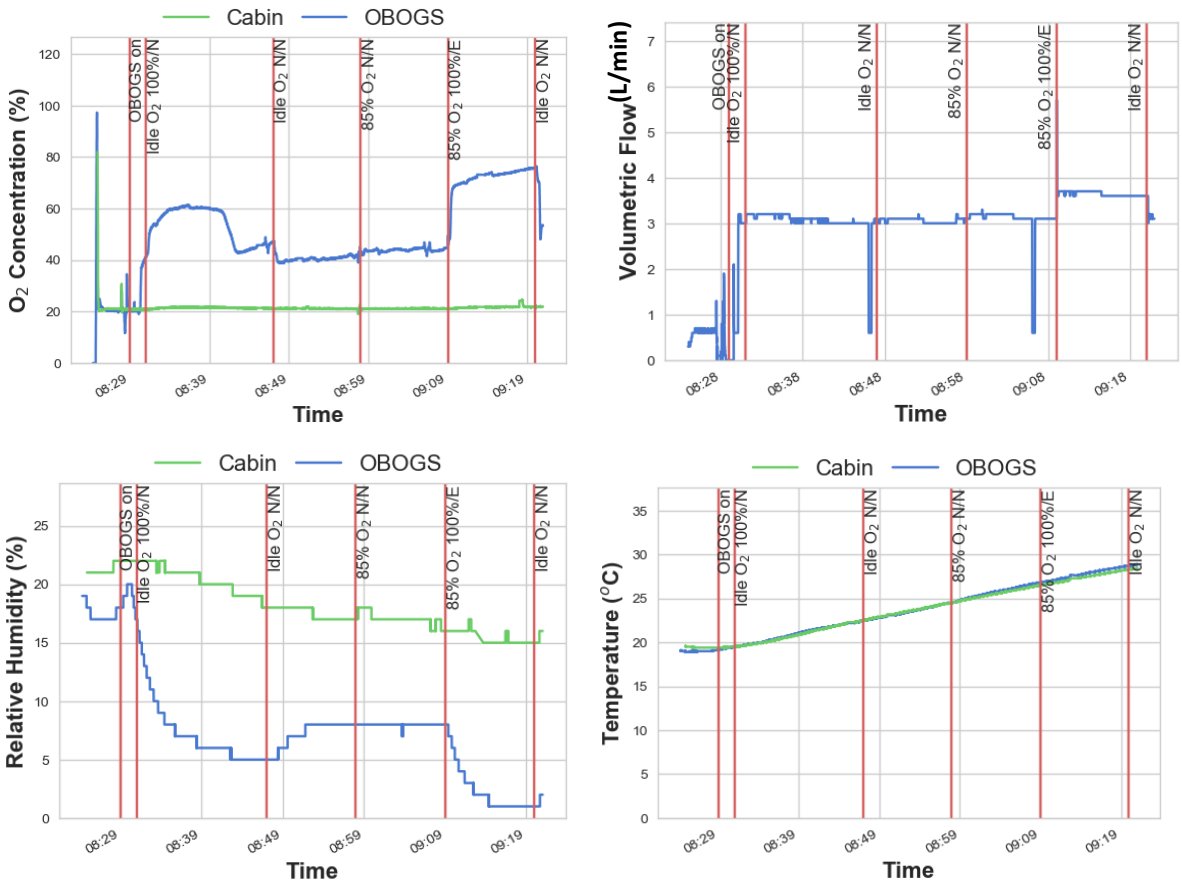

Figure D4. Time series plots for Engine Run 4, Aircraft ID 35: O_2 concentration, volumetric flowrate, relative humidity, and temperature

Time Series Plots for Engine Run 4, Aircraft ID 35 Continued

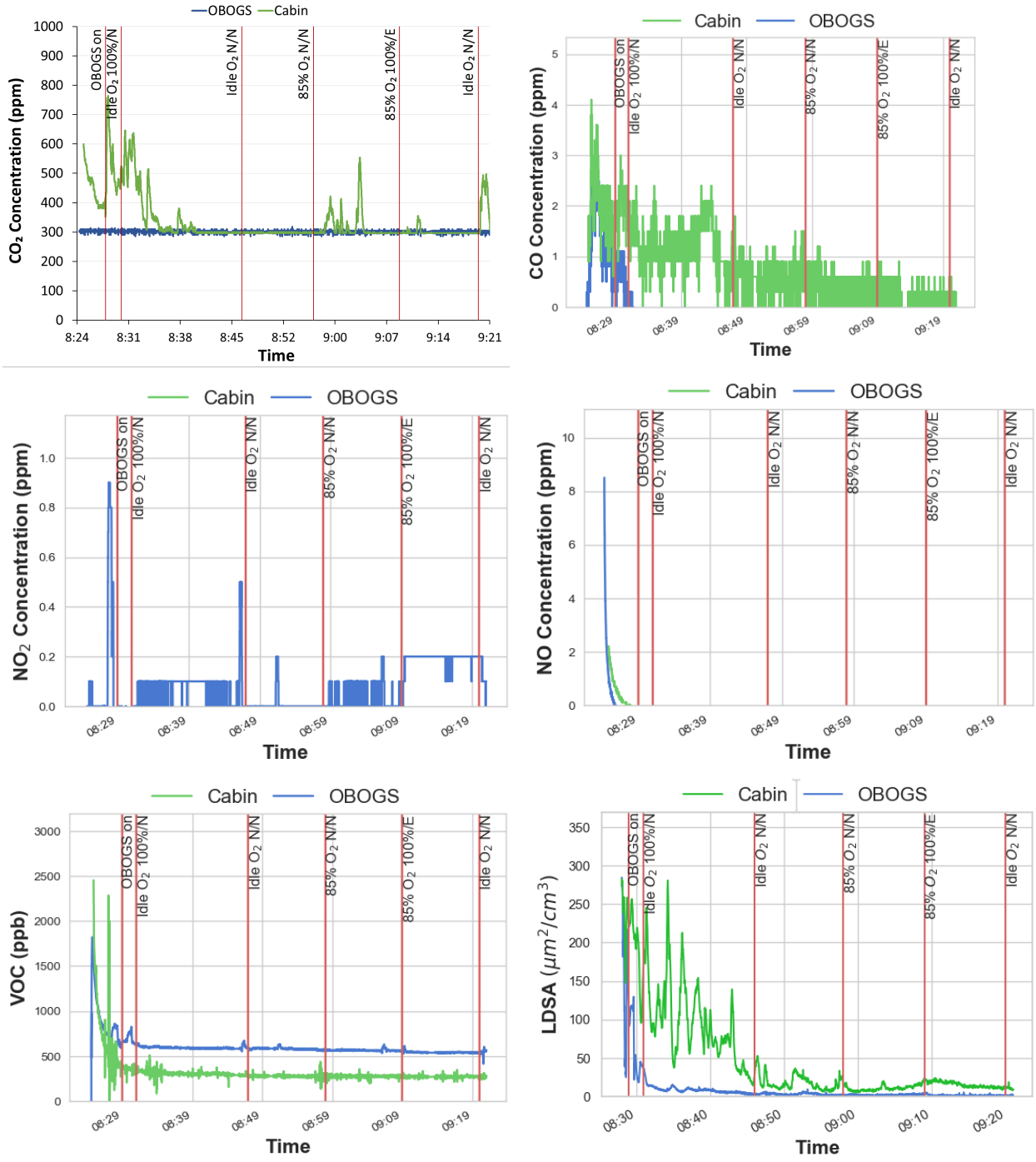

Figure D4 continued. Time series plots for Engine Run 4, Aircraft ID 35: Contaminants

Time Series Plots for Engine Run 5, Aircraft ID 36

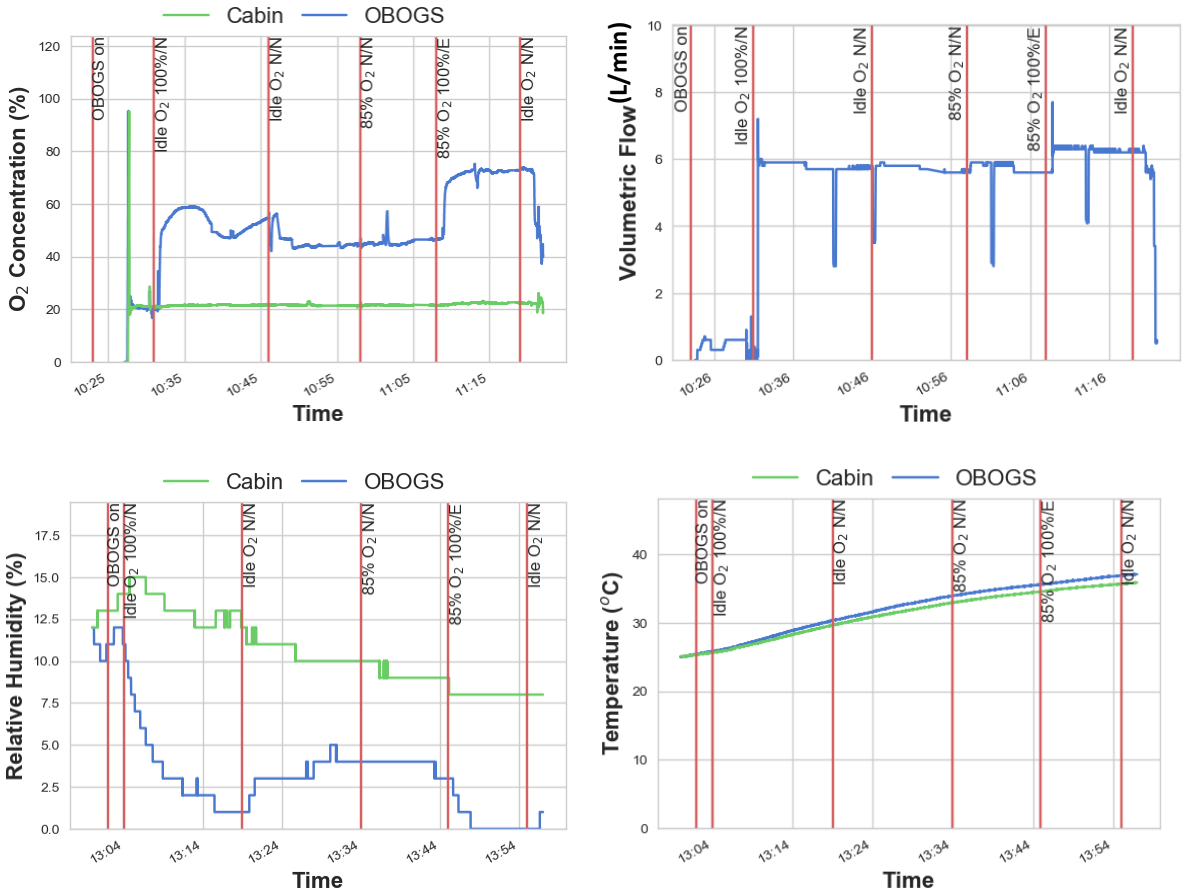

Figure D5. Time series plots for Engine Run 5, Aircraft ID 36: O_2 concentration, volumetric flowrate, relative humidity, and temperature

Time Series Plots for Engine Run 5, Aircraft ID 36 Continued

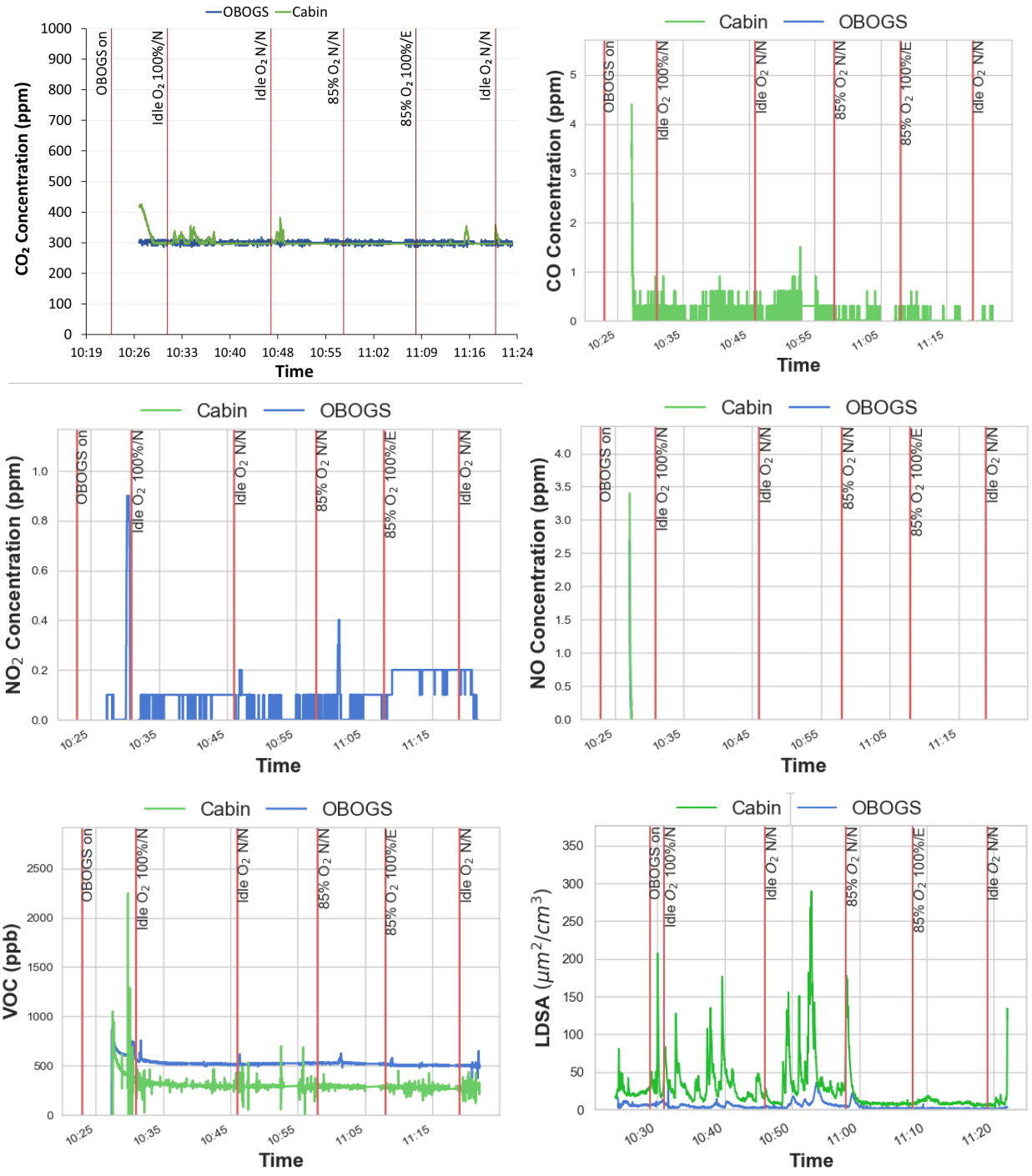

Figure D5 continued. Time series plots for Engine Run 5, Aircraft ID 36: Contaminants

Time Series Plots for Engine Run 6, Aircraft ID 37

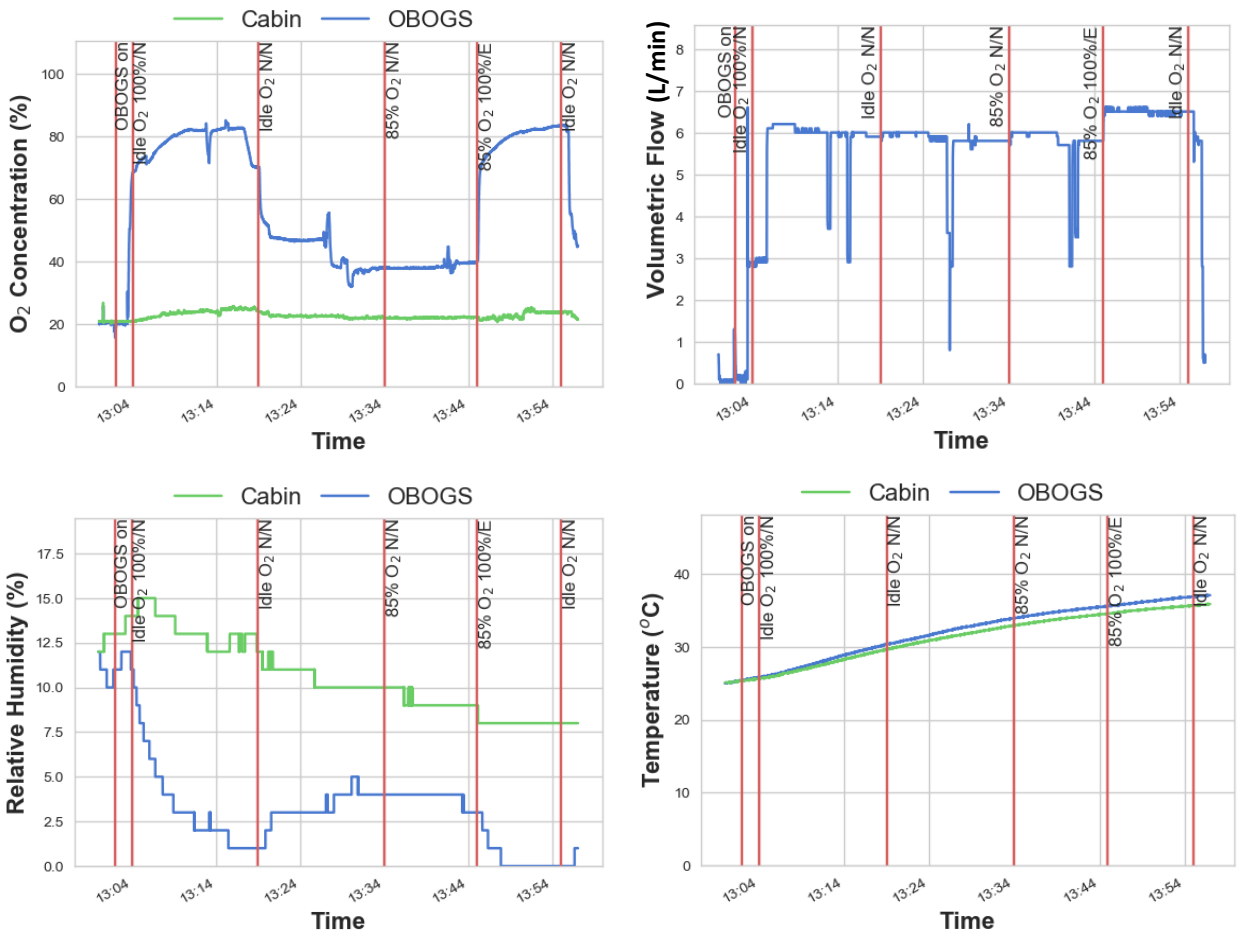

Figure D6. Time series plots for Engine Run 6, Aircraft ID 37: O_2 concentration, volumetric flowrate, relative humidity, and temperature

Time Series Plots for Engine Run 6, Aircraft ID 37 Continued

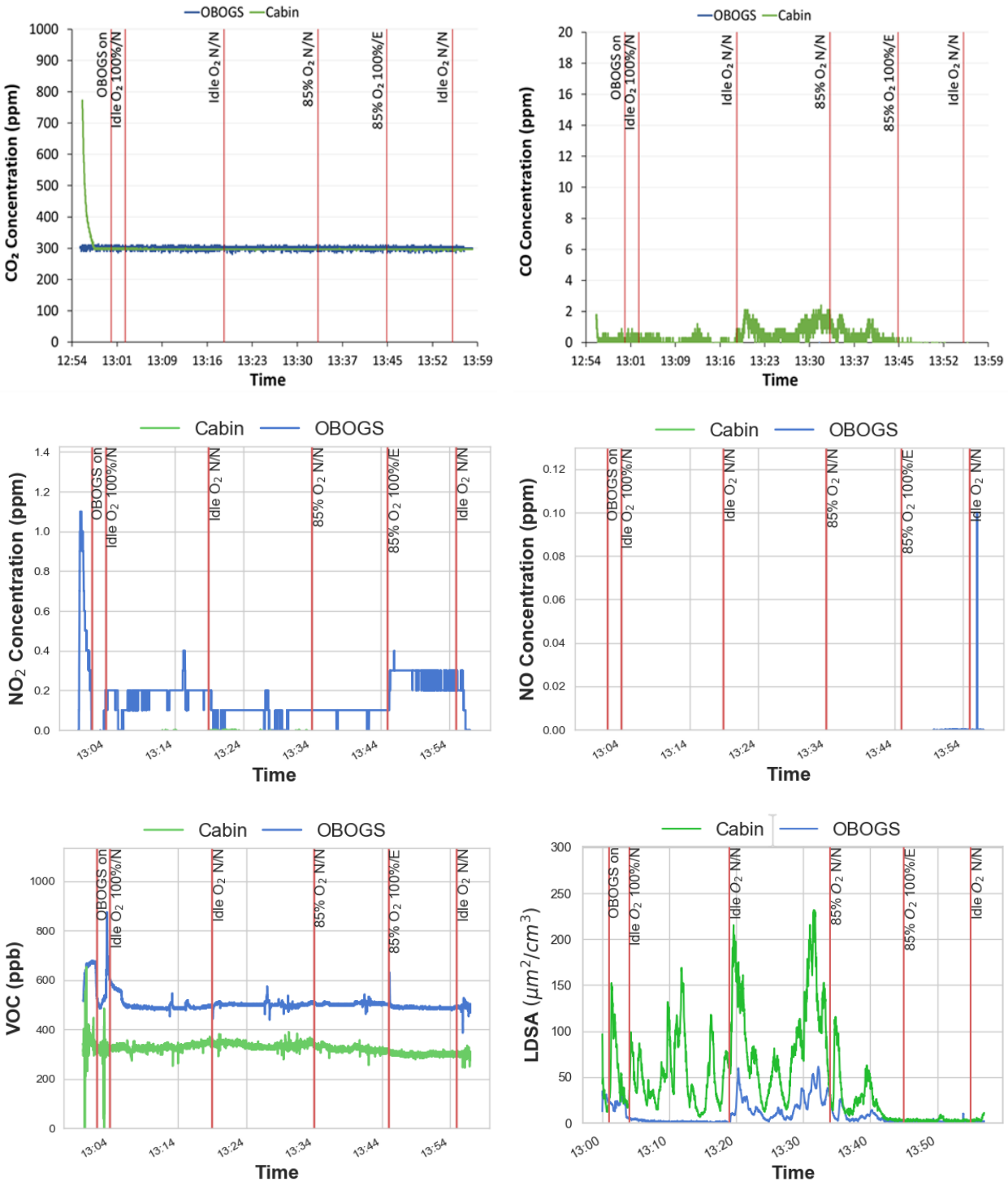

Figure D6 continued. Time series plots for Engine Run 6, Aircraft ID 37: Contaminants

Time Series Plots for Engine Run7, Aircraft ID 38

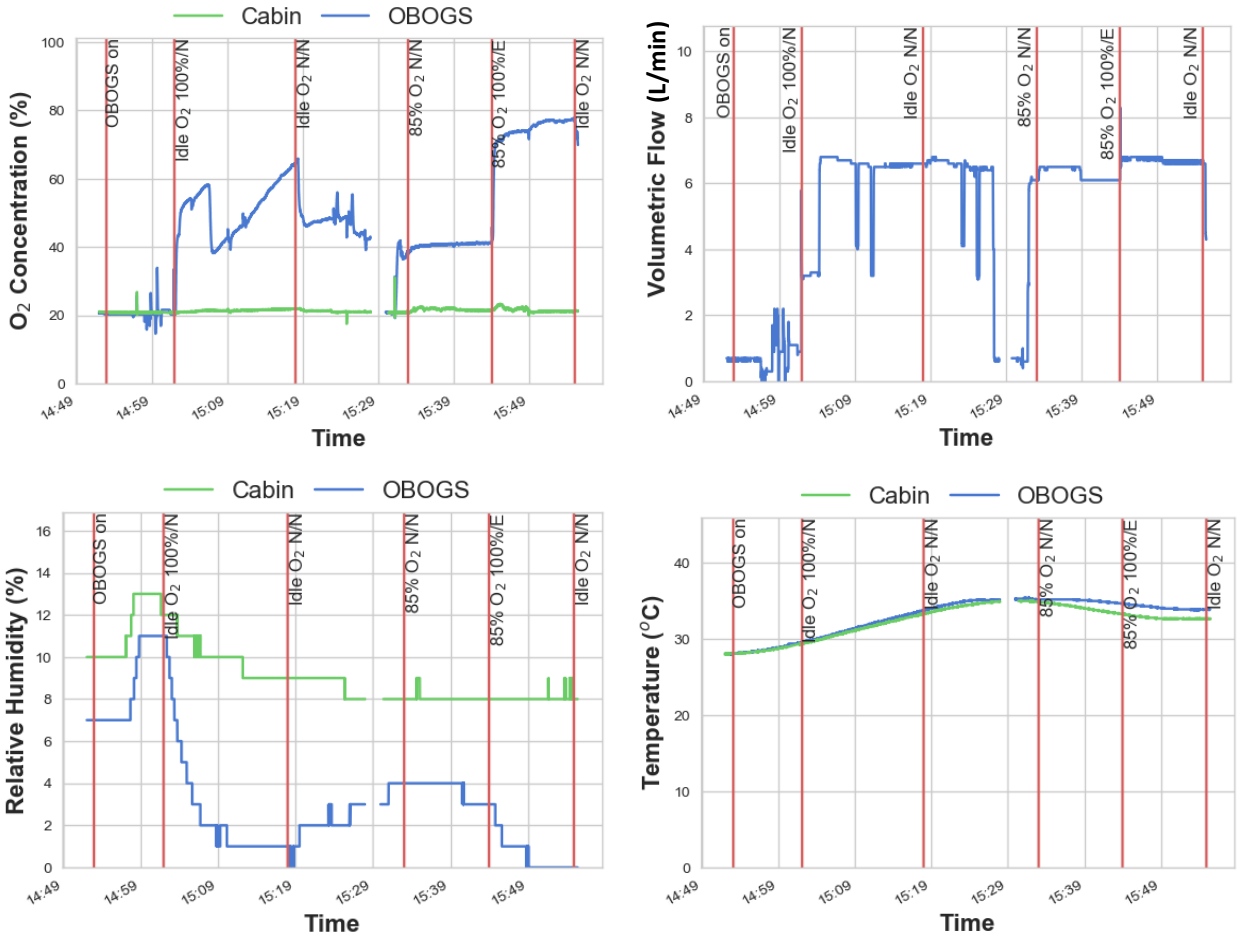

Figure D7. Time series plots for Engine Run 7, Aircraft ID 38: O_2 concentration, volumetric flowrate, relative humidity, and temperature

Time Series Plots for Engine Run 7, Aircraft ID 38 Continued

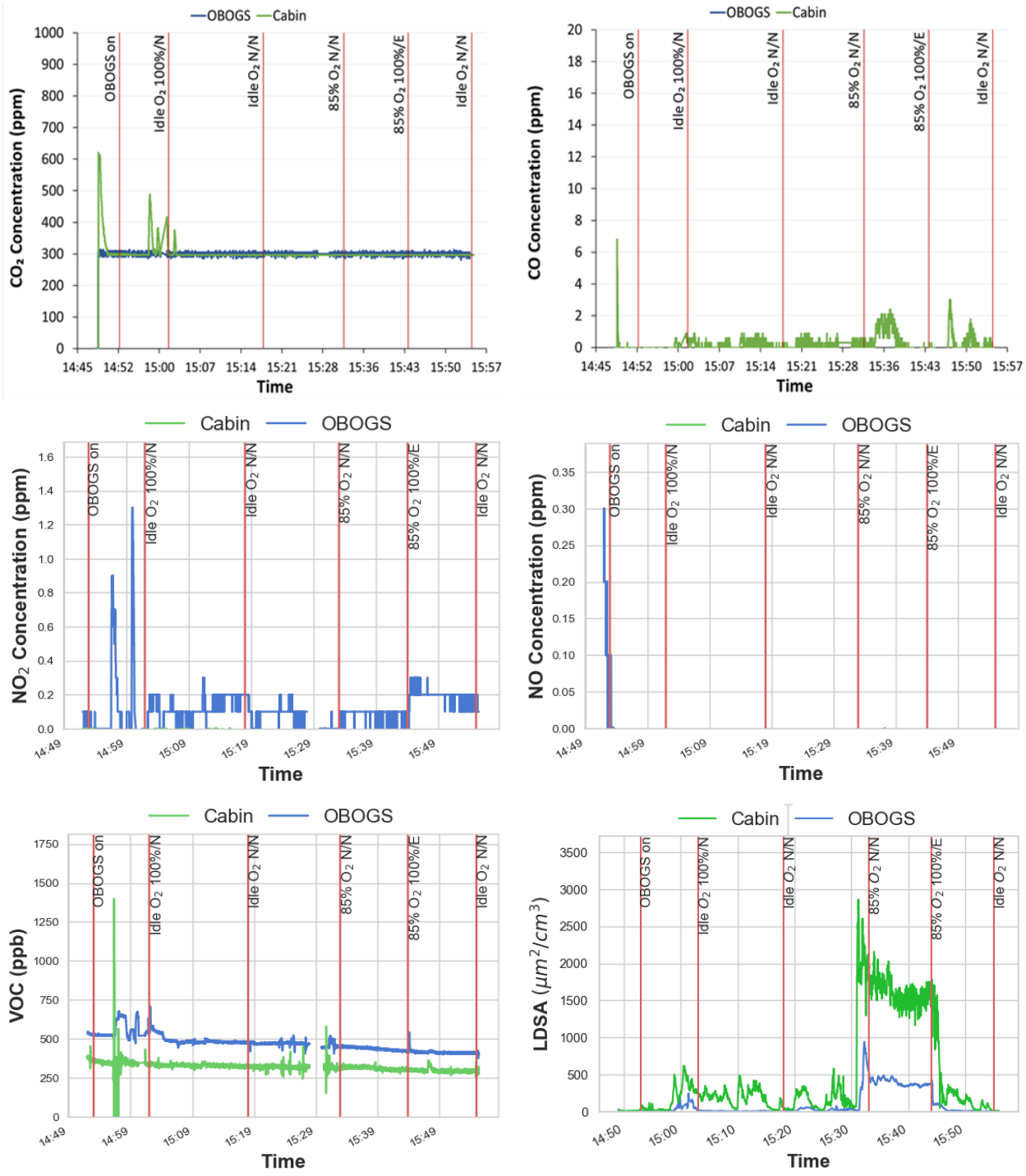

Figure D7 continued. Time series plots for Engine Run 7, Aircraft ID 38: Contaminants

Time Series Plots for Engine Run 8, Aircraft ID 39

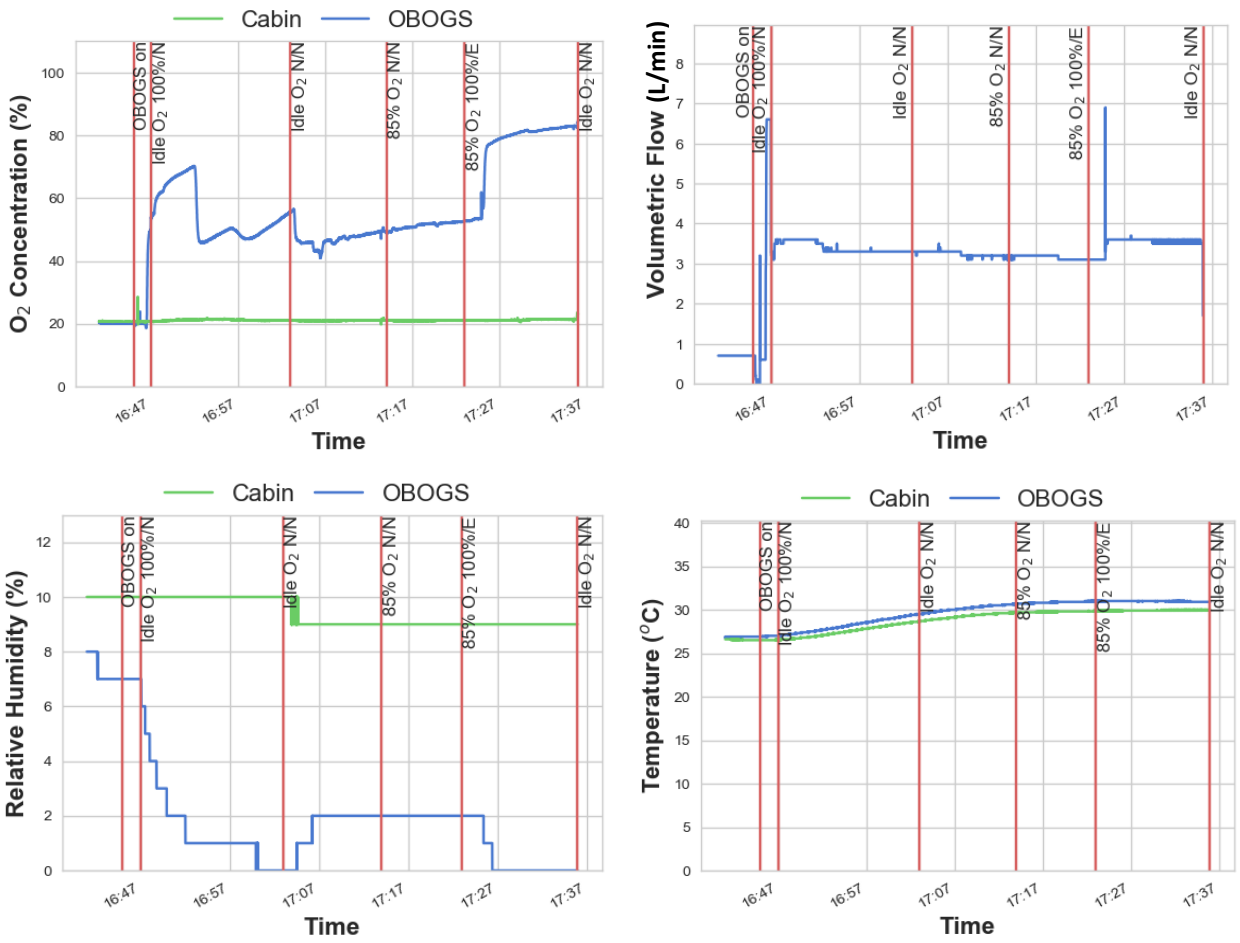

Figure D8. Time series plots for Engine Run 8, Aircraft ID 39: O_2 concentration, volumetric flowrate, relative humidity, and temperature

Time Series Plots for Engine Run 8, Aircraft ID 39 Continued

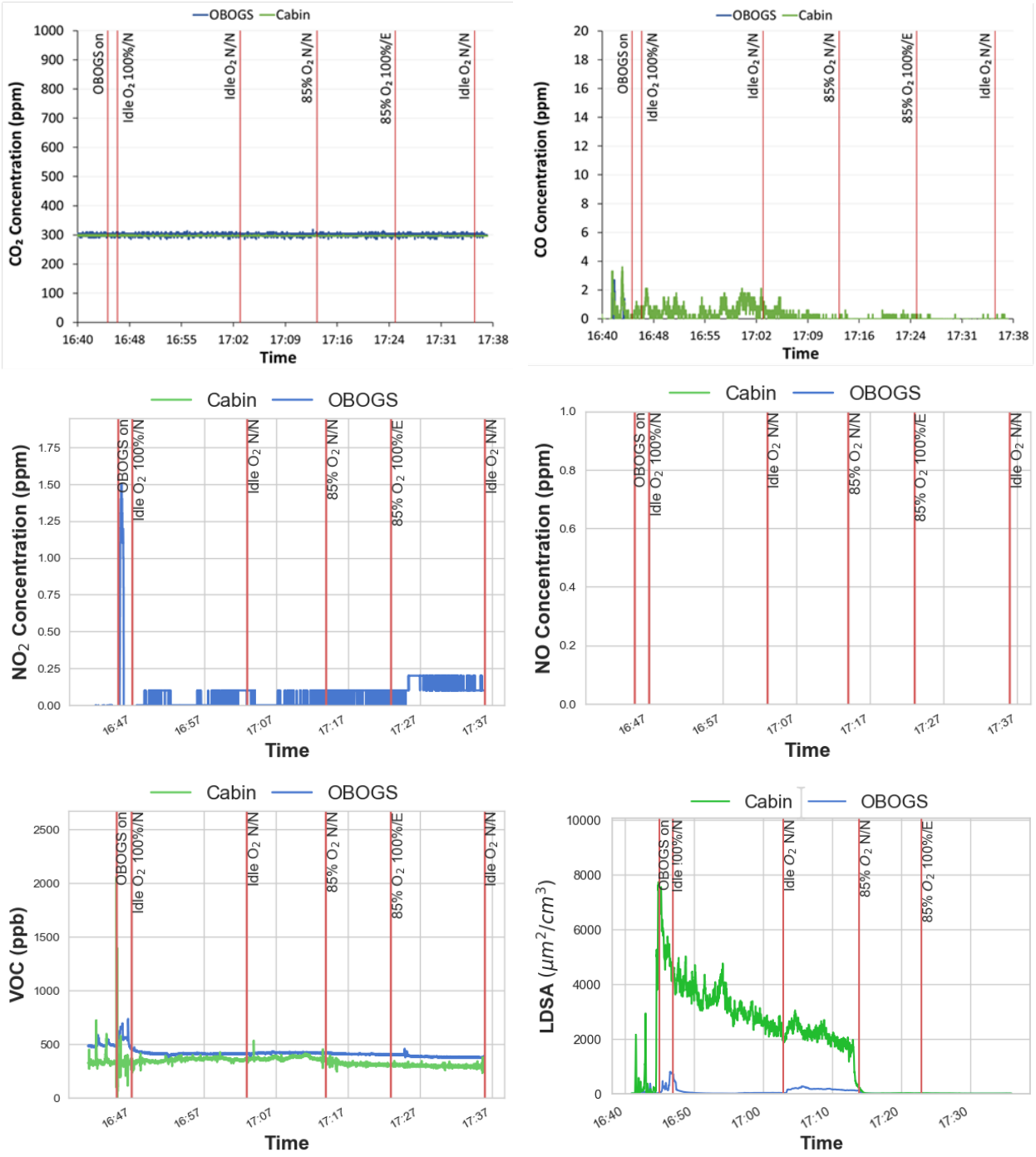

Figure D8 continued. Time series plots for Engine Run 8, Aircraft ID 39: Contaminants

Time Series Plots for Engine Run 9, Aircraft ID 40

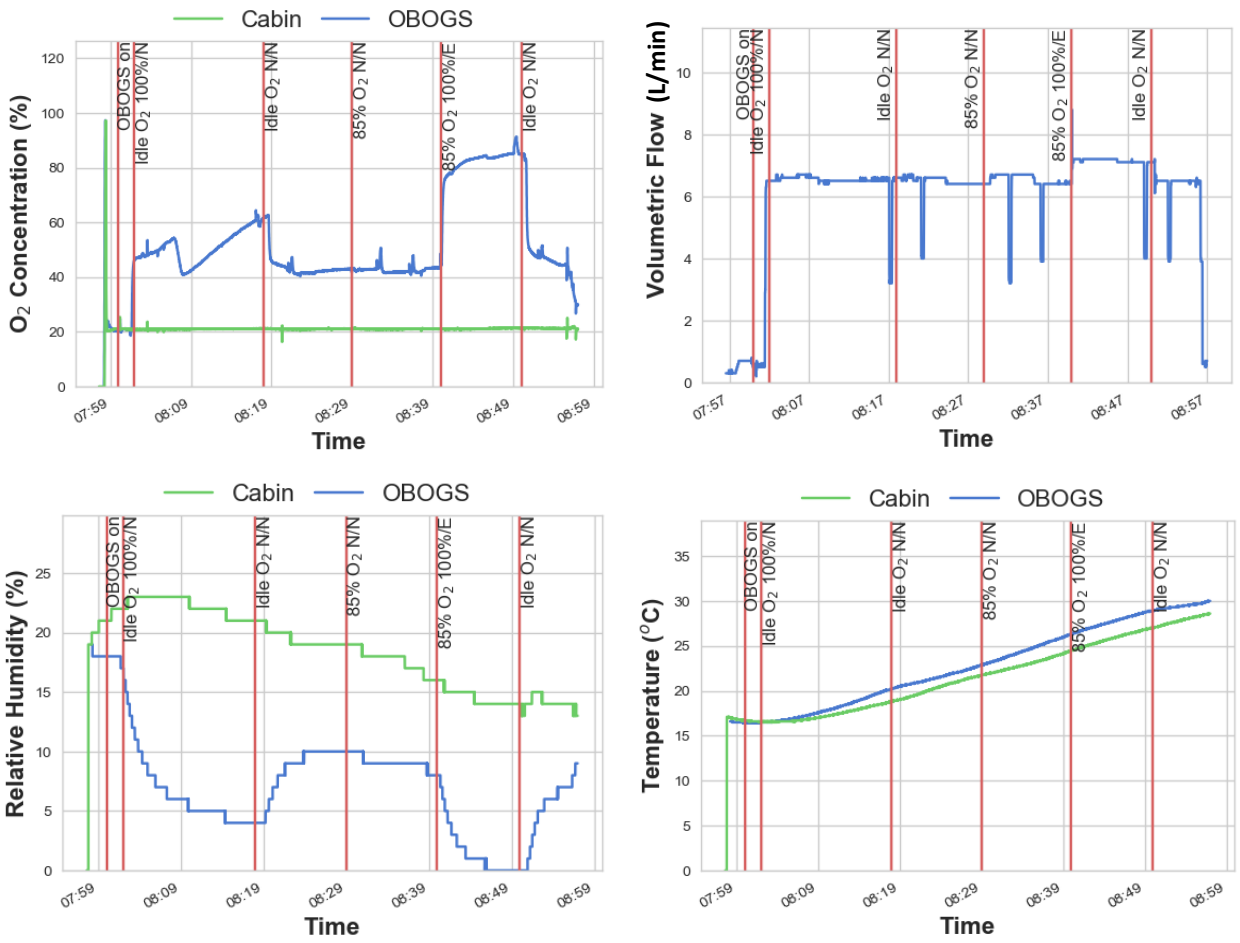

Figure D9. Time series plots for Engine Run 9, Aircraft ID 40: O_2 concentration, volumetric flowrate, relative humidity, and temperature

Time Series Plots for Engine Run 9, Aircraft ID 40 Continued

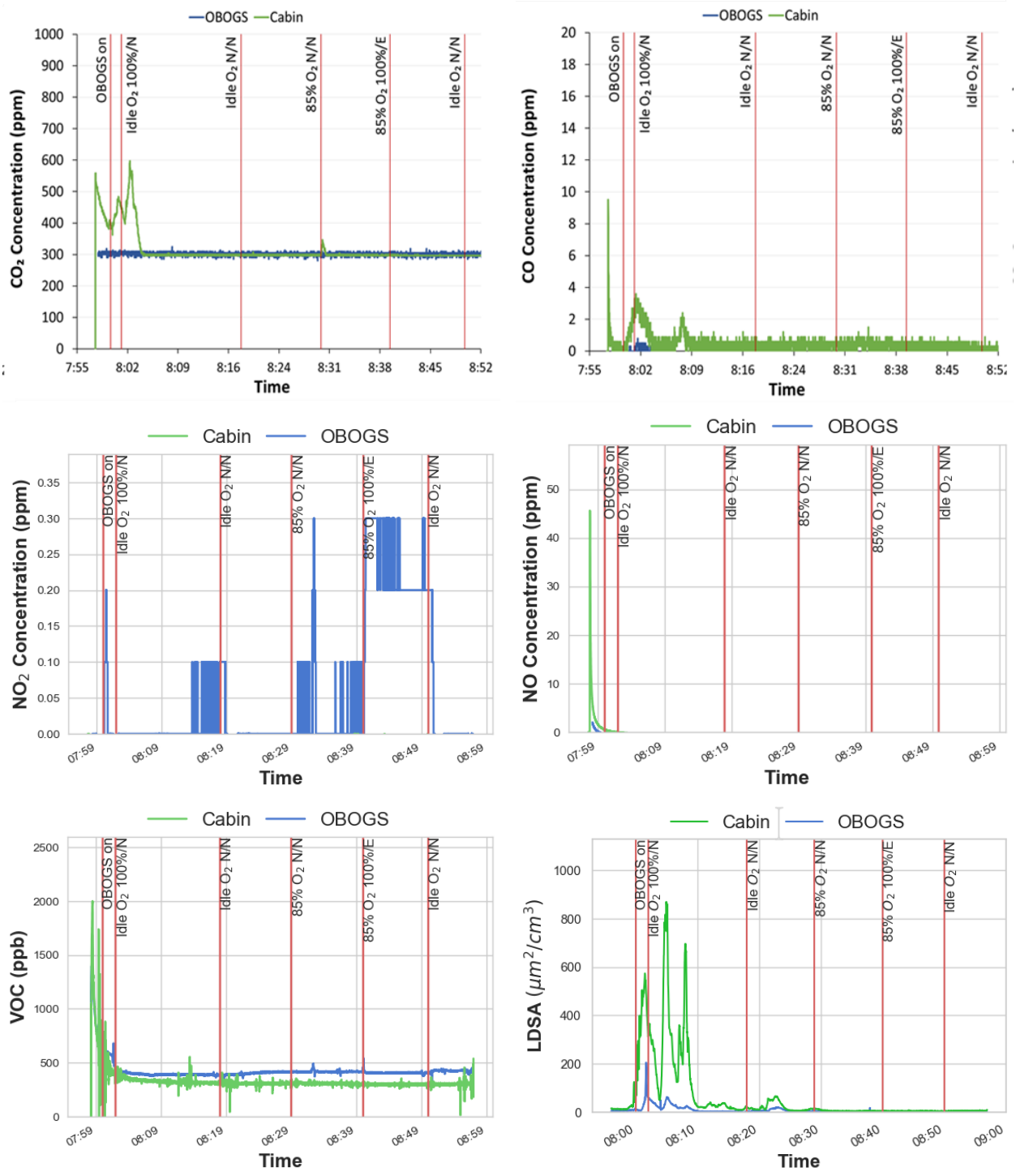

Figure D9 continued. Time series plots for Engine Run 9, Aircraft ID 40: Contaminants

Time Series Plots for Engine Run 10, Aircraft ID 41

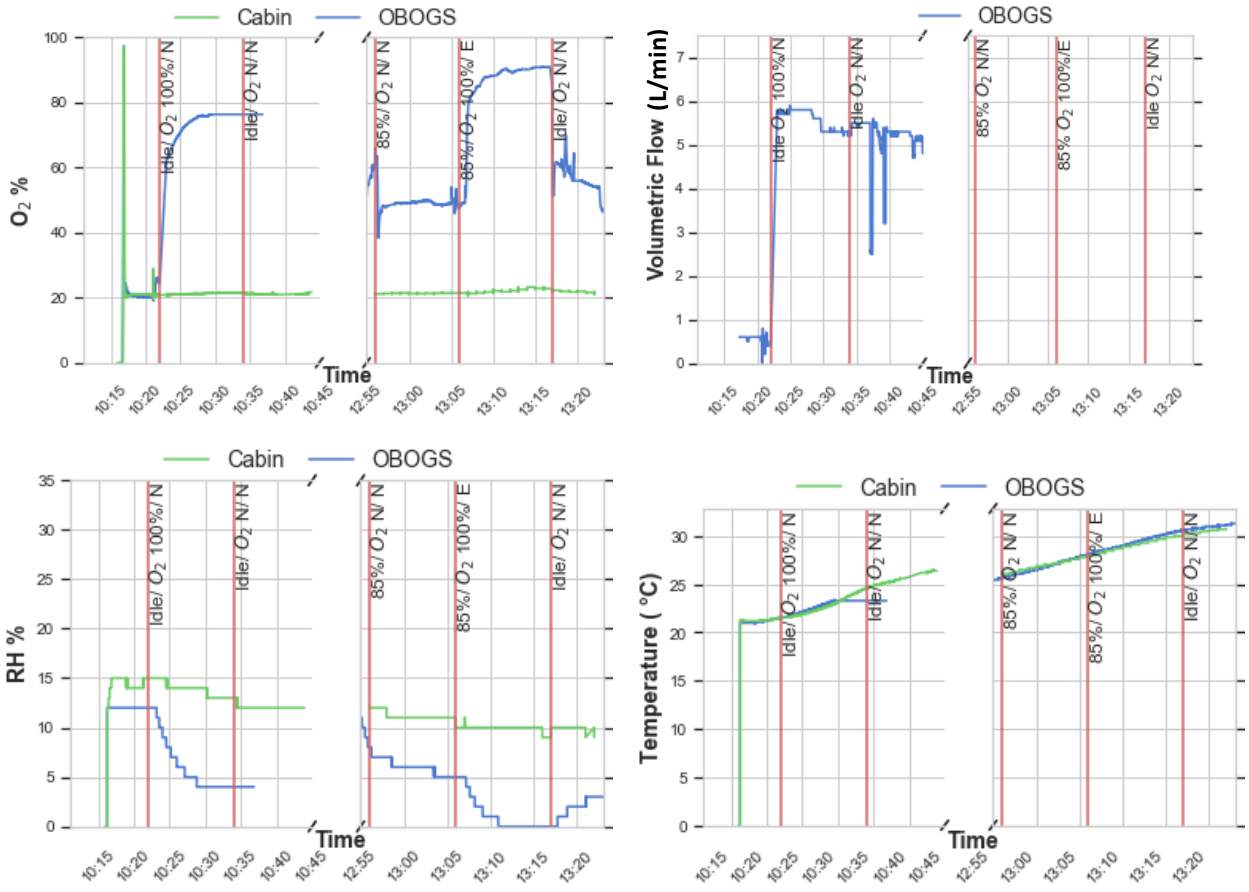

Figure D9. Time series plots for Engine Run 10, Aircraft ID 41: O_2 concentration, volumetric flowrate, relative humidity, and temperature

Time Series Plots for Engine Run 10, Aircraft ID 41 Continued

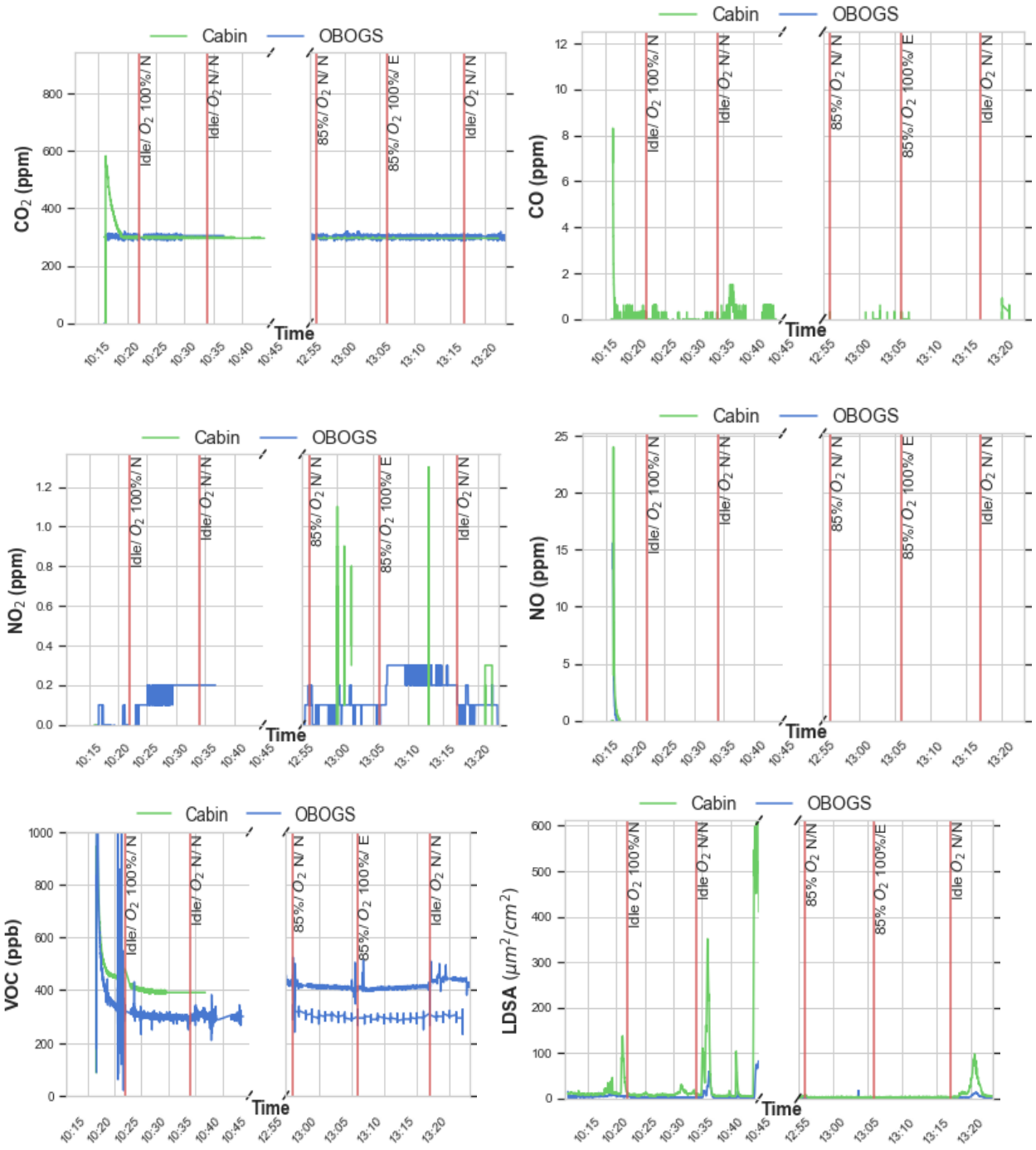

Figure D10 continued. Time series plots for Engine Run 10, Aircraft ID 41: Contaminants

Broken x-axis indicates interval during which no data was collected because of errors from Makel unit in pilot breathing air flow path. Engine was restarted at the end of the interval.

Time Series Plots for Engine Run 11, Aircraft ID 42

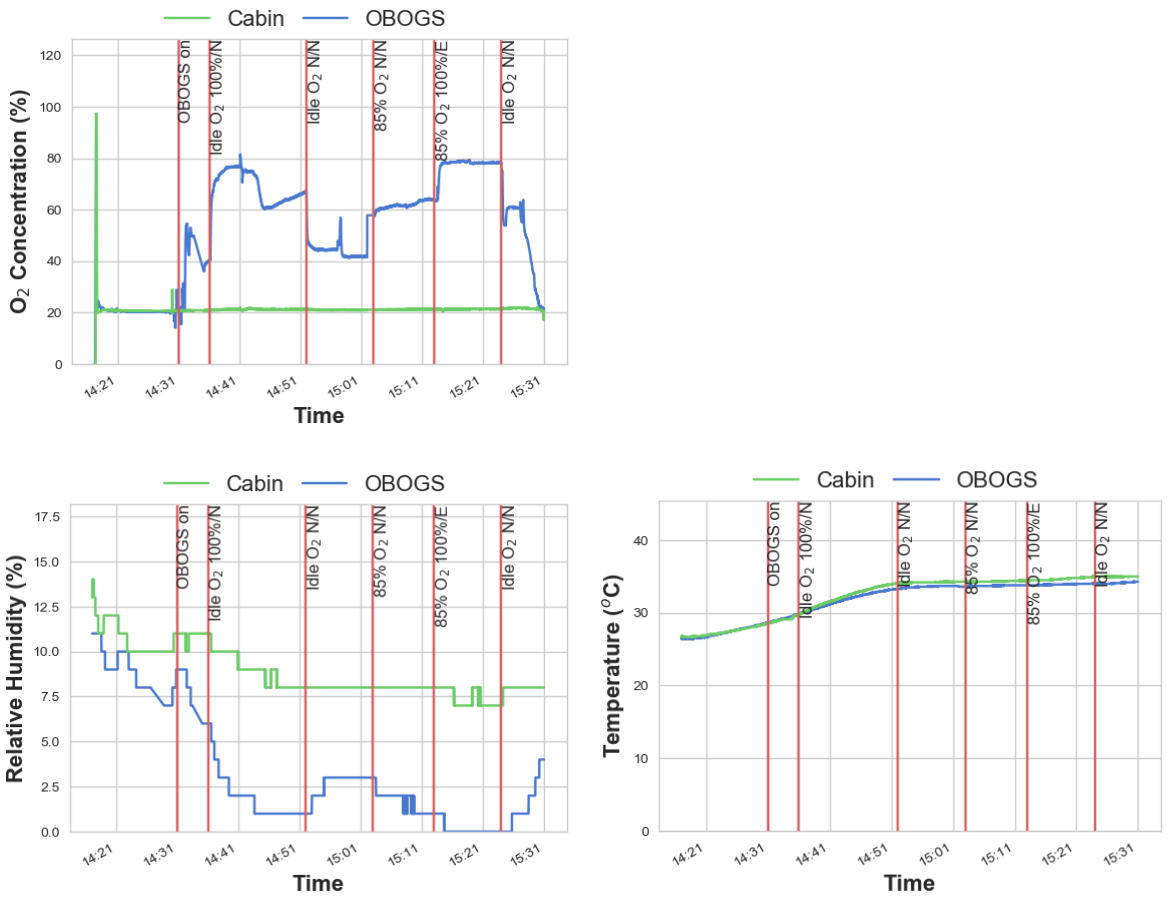

Figure D11. Time series plots for Engine Run 11, Aircraft ID 42: O_2 concentration, humidity, and temperature. No volumetric flow data available due to sensor malfunction.

Time Series Plots for Engine Run 11, Aircraft ID 42 Continued

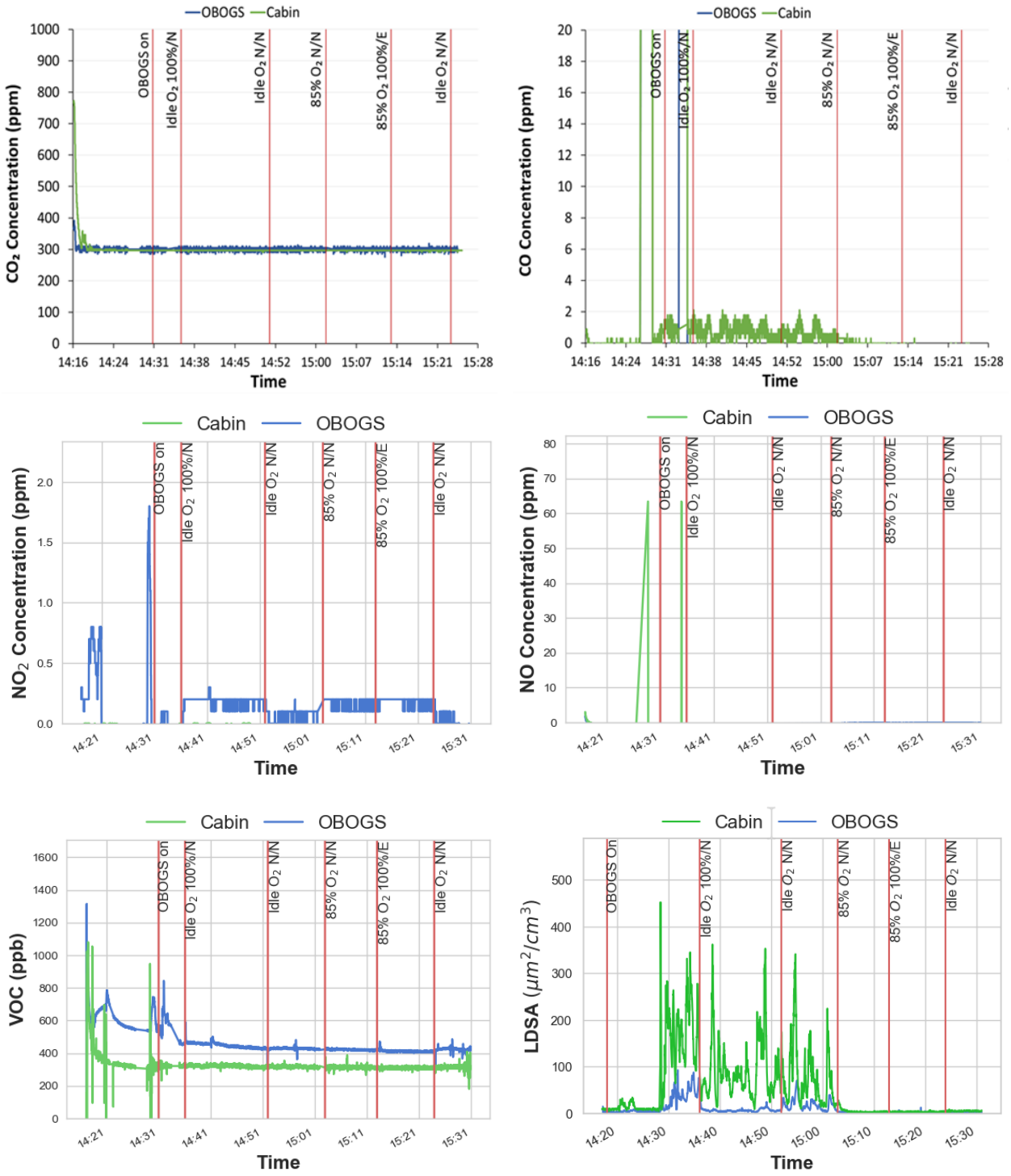

Figure D11 continued. Time series plots for Engine Run 11, Aircraft ID 42: Contaminants

Time Series Plots for Engine Run 12, Aircraft ID 43

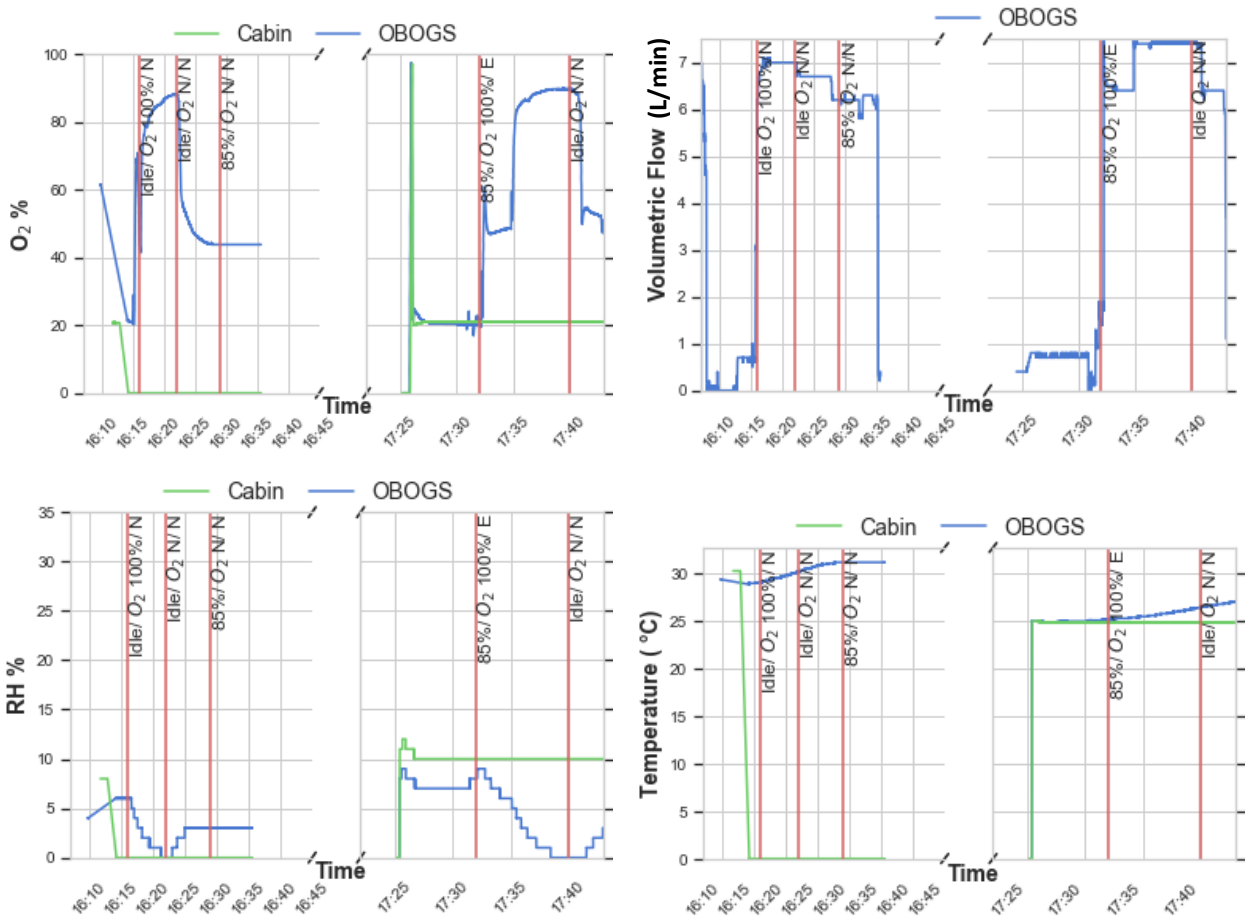

Figure D12. Time series plots for Engine Run 12, Aircraft ID 43: O_2 concentration, volumetric flowrate, relative humidity, and temperature

No real-time chemical compound cockpit data collected from the first three test phases, due to a failure of the battery for the Makel unit in the cockpit air flow path. Broken axes indicate interval when no data was collected in order to replace the battery for the cockpit Makel unit; at the end of the interval the engine was restarted.

Time Series Plots for Engine Run 12, Aircraft ID 43 Continued

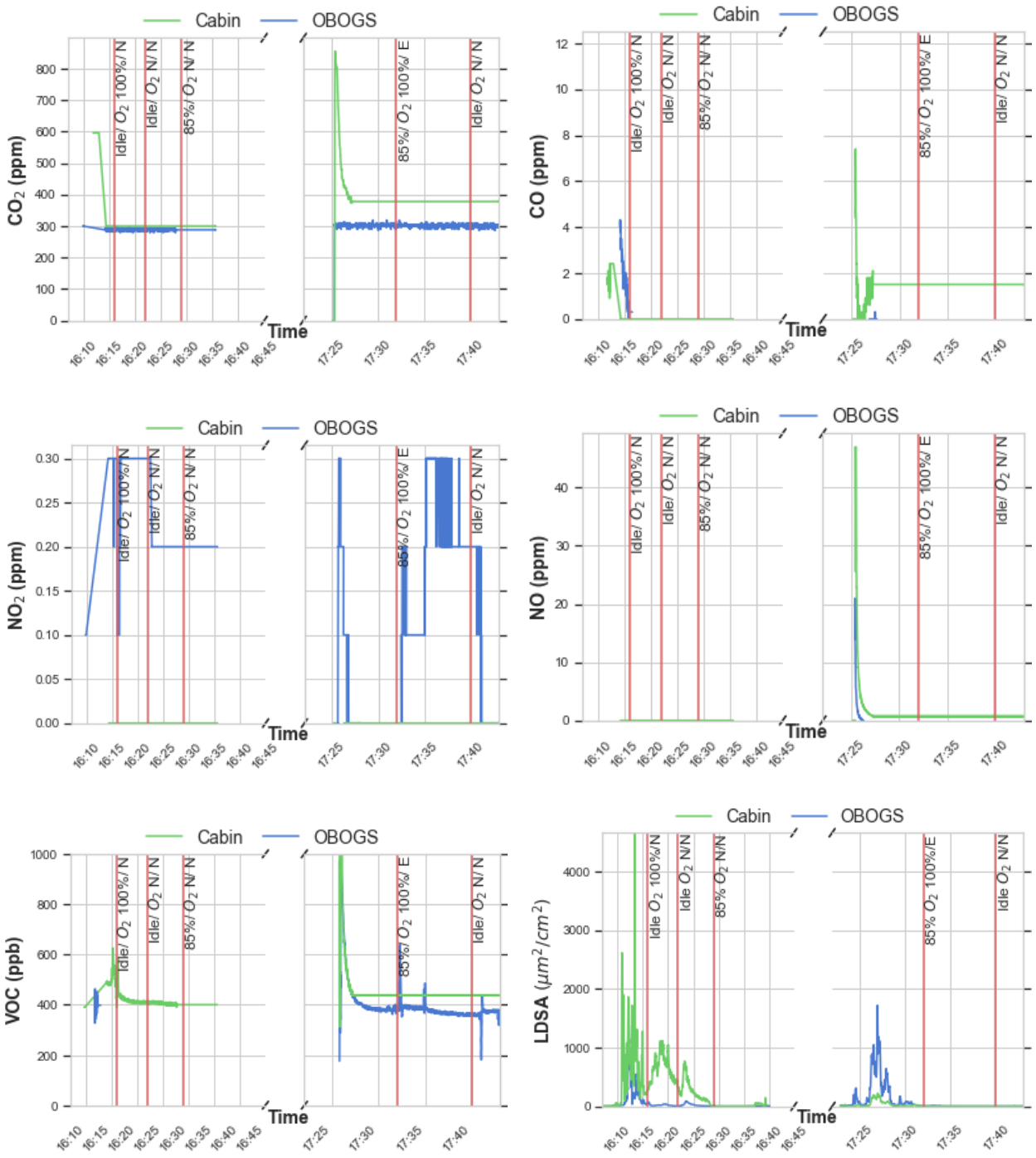

Figure D12 continued. Time series plots for Engine Run 12, Aircraft ID 43: Contaminants

No real-time chemical compound cockpit data collected from the first three test phases, due to a failure of the battery for the Makel unit in the cockpit air flow path. Broken axes indicate interval when no data was collected in order to replace the battery for the cockpit Makel unit; at the end of the interval the engine was restarted.

APPENDIX E. ENGINE RUN VOC LIMITS OF DETECTION

Table E1. VOCs tested for and not detected in any samples

Compound	Lower Detection Limit (ppb)
1,1,2,2-tetrachloro ethane	2
1,1,2-trichloro-1,2,2-trifluoroethane	2
1,1,2-Trichloroethane	2
1,1-Dichloroethane	2
1,2,4-Trichloro benzene,	2
1,2,4-Trimethyl benzene	2
1,2-dibromo ethane,	2
1,2-Dichloro benzene,	2
1,2-Dichloroethane	2
1,2-Dichlorotetrafluoroethane	2
1,3,5-Trimethyl benzene	2
1,3-Dichloro benzene	2
1,4-dichloro benzene,	2
Bromodichloromethane	2
Butyl Methyl Ketone (2-Hexanone)	2
Carbon disulfide	4
Carbon Tetrachloride	0
Chlorobenzene	2
Chloroform	2
cis 1,2-Dichloroethylene	2
Dibromochloro methane	2
Dichlorodifluoromethane	2
Ethene, 1,1-dichloro-	2
Ethylbenzene	2
Heptane	2
Hexachloro-1,3-butadiene	2
m,p-xylene	4
Methyl Isobutyl Ketone	2
Naphthalene	2
o-xylene	2
Tetrachloroethylene	2
Tetrahydrofuran	2
trans 1,2-dichloroethylene	2
Trichloroethylene	2
Trichloromonofluoromethane	2
Vinyl Chloride	2

APPENDIX F. CSL CODE

(intended to replicate Gosselin 2009 Figure 5, 30 ppm exposure)

```
PROGRAM: Gosselin_CO.CSL -- Inhalation Model for CO and COHb
! Based on Gosselin 2009 et al.
! Added code to shift start of exposure and changed code for determining dosing interval
! (added StrtExp and DoseInt parameters)
INITIAL
! Demographics
CONSTANT   BW = 70.0              ! Bodyweight (kg)
CONSTANT   HT = 174.4             ! Height (cm)
CONSTANT   G = 1                  ! Sex (0 = Female, 1 = Male)
CONSTANT   A = 40.0               ! Age (yrs)
! Physical Constants
 CONSTANT Temp_K = 310.15         ! Temperature (C) (37 C is 98.6 F and 310.15 K)
! Tissue Volumes (fraction of body weight for adult male)(from ICRP89)
CONSTANT    VTis = 2.2            ! Volume of extravascular space (L)
! Chemical-Specific Parameters (from Gosselin 2009)
CONSTANT   MHb = 240.0            ! Haldane affinity ratio for Hb (unitless)
CONSTANT   R = 2.55               ! Gas constant (mmHg*mLair/K*mLCO)
! Dosing Parameters
CONSTANT   CO_Inh = 30.0          ! Concentration of inhaled CO (ppm, uL/L)
CONSTANT   TChng = 1440.0         ! Length of inhalation exposure (min)
CONSTANT   DaysWk = 1.0           ! Number of exposure days per week
CONSTANT   StrtExp = 0.0          ! Time to start exposure (min)
CONSTANT   ExpEnd = 3600.0        ! Time to end exposure (min)
CONSTANT   MaskOn = 0             ! Time oxygen mask is applied (min)
CONSTANT   MaskOff = 0            ! Time oxygen mask is removed (min)
CONSTANT   Pwl = 32               ! Work level (watts)
COExt = CO_Inh/1000000            ! Concentration of inhaled CO (mL/mL)
! Calculation of QAlv and VAlv per Gosselin 2009 Appendix (Values from ICRP89)
CONSTANT Vdana = 150.0            ! Anatomical dead space (mL, adult male)
```

```
CONSTANT Vt = 1250.0            ! Tidal volume (mL, adult male)
CONSTANT fR = 20.0              ! respiration frequency (breaths per minute)
CONSTANT Vd = 259                       ! Man doing light exercise from Gosselin 2009
Vdalv = 0.16*Vdana              ! Volume of gas that reaches alveoli but has no
                                ! exchange with blood (Based on Baker 1987)

VAlv = Vt - Vd
QAlv = fR * VAlv
! Calculation of diffusing capacity of lungs for carbon monoxide (Gosselin 2009)
CONSTANT Wrest = 30.0           ! Energy consumption at rest (watts, ICRP 1994)
CONSTANT DLCO_rest = 37.8       ! DLCO at rest (ml/min/mmHg) for 40yo male
CONSTANT Wcon = 80              ! Energy consumption for selected workload (watts)
w = Wcon - Wrest                ! Workload over baseline/rest (watts)
DLCO = DLCO_rest + 0.06*w       ! Lung diffusion capacity for CO at BTPS
                                ! (mL/min/mmHg)
! Calculation of maximum hemoglobin capacity for CO
CONSTANT Beta = 1.21            ! Conversion for barometric pressure of 760
                                ! mmHg and water vapor pressure of 47 mmHg
CONSTANT CHb = 150.0            ! Avg. [Hb] in whole blood (g/L)
bMax = Beta * 1.389             ! Max CO that can bind to 1 g of Hb, BTPS (mL/g)
VBld = 0.079 * BW               ! Volume of blood (L)
CHbMax = bMax * CHb * VBld
! Partial Pressure of oxygen in lung capillaries
PO2 = (-0.24 * A) + 104.7       ! Partial pressure of O2 (mm Hg), (Cotes 1975)
! Endogenous production rate of carbon monoxoide
REndostp = 0.0070 * (BW / 69.5) ! Endogenous production at STPD (mL/min)
REndo = Beta * REndostp         ! Endogenous production at BTPS (mL/min)
ACO_Init = (502.24*REndo) - 2.381       ! Empirical CO volume from endogenous rate (mL)
! Oxidizing rate of carbon monoxide (/min) (Tobias 1945, Luomanmaki 1969)
CONSTANT kCO2 = 3.33E-5
! Capture and release rates (empirical values)
CONSTANT kSf = 0.01             ! Transfer rate (/min), estimated by least square fit
                                ! between model simulations and experimental data
                                ! from Tikuisis et al 1987a
```

```
kHbS = 0.2 * kSf                    ! Transfer rate (/min), estimated because median
                                    ! ratio of kHbS/kSf is 0.2 from IPCS 1999
! Initialization and Simulation Control Parameters
CONSTANT TStop = 3600.0
CINT = 0.1
CIZone = 0.0
DayExp = 1.0
SCHEDULE DoseOn .AT. StrtExp
END             ! End of Initial
DYNAMIC
ALGORITHM  IALG = 2          ! Gear stiff method
DISCRETE DoseOn
        INTERVAL DoseInt = 14400.0
        SCHEDULE Doseoff .AT. T + TChng
        IF (T.LT.ExpEnd) CIZone = 1.0
END
DISCRETE DoseOff
        CIZone = 0.0
END
IF((T > MaskOn) .AND. (T < MaskOff)) THEN
        PO2 = 500.0
ELSE
        PO2 = (-0.24 * A) + 104.7
ENDIF
DERIVATIVE
Hours = T / 60.0
Minutes = T
Days = T / (24.0 * 60.0)
! Amount in Alveoli (mL)
RAAlv = (QAlv * ((CIZone*COExt) - CAlv)) - (DLCO * ((CAlv * R * Temp_K) - ((ABldTot *
          PO2)/(MHb * (CHbMax - ABldTot)))))
AAlv = INTEG(RAAlv, 0.0)
CAlv = AAlv / VAlv
```

```
! Total amount in Arterial Blood (mL)
RABldTot = (DLCO * ((CAlv * R * Temp_K) - ((ABldTot * PO2)/(MHb * (CHbMax -
            ABldTot))))) - (kHbS * ABldTot) + (kSf * ATis) - (kCO2 * ABldTot) + REndo
ABldTot = INTEG(RABldTot, ACO_Init) !+ ACO_Init
CBldTot = ABldTot / VBld
HbCO_Per = ((CBldTot / (bMax * CHb)) * 100.0) !+ HbCOInitC
! Amount of CO bounded to heme proteins in EV space (mL)
RATis = (kHbS * ABldTot) - (kSf * ATis) - (kCO2 * ATis)
ATis = INTEG(RATis, 0.0)
CTis = ATis / VTis
TERMT(T.GT.TStop, 'Simulation Finished')
END             ! End of Derivative
END             ! End of Dynamic
END             ! End of Program
```

LIST OF SYMBOLS, ABBREVIATIONS AND ACRONYMS

°C	degrees Celsius
%	percent/percentage
711th HPW	711th Human Performance Wing
ACGIH	American Conference of Governmental Industrial Hygienists
AFB	Air Force Base
cm	centimeter
CO	Carbon monoxide
CO_2	Carbon dioxide
COHb	Carboxyhemoglobin
EPA	Environmental Protection Agency
GC/MS	Gas Chromatography Mass Spectroscopy
HEPA	High-Efficiency Particulate Air
Hz	Hertz (s^{-1})
LDSA	Lung-Deposited Surface Area
$L*min^{-1}$	Liters per minute
LOX	Liquid Oxygen
MEI	Makel Enginering, Inc.
MC	Monte Carlo
mm	millimeter
NDIR	Non-Dispersive Infrared
NIOSH	National Institute of Occupational Safety and Health
N_2	Nitrogen gas
NO	Nitric oxide
NO_2	Nitrogen dioxide
NO_x	Nitrogen oxides
O_2	Oxygen gas
OBOGS	On-Board Oxygen Generation System
OAGr	OBOGS Air Ground Run Sampling System
OEL	Over Exposure Limit
OSHA	Occupational Safety and Health Administration

ppb	Parts per billion
ppm	Parts per million
PE	Physiological Episode/Event
PID	Photo-Ionization Detector
pO_2	Partial pressure of Oxygen
ppm	Parts per million
ppb	Parts per billion
PSIA	Pounds per Square Inch Absolute
REL	Recommended Exposure Limit
RH	Relative Humidity
REndo	Endogenous Regressors
SO_x	Sulfur oxides
SO_2	Sulfur dioxide
STEL	Short-Term Exposure Limit, generally a 15-minute time-weighted average
SQL	Structured Query Language
SVI	Solid Vapor Intrusion
TD	Thermal Desorption
TO	Technical Order
TWA	Time-Weighted Average
UFP	Ultrafine Particles
USAF	United States Air Force
VOC	Volatile Organic Compound
µm	micrometer